Supporting Information

photophysical, thermal and electrochemical analysis of a series of phenothiazine cored conjugated aromatic unit appended D-π-A based high-solid state luminescence materials: their applications in reversible mechano-fluorochromism and volatile acid sensing

Bhaswati Sarkar, [†] *Edamana Prasad,* [*, †] *Ramesh. L. Gardas*[*, †]

†Department of Chemistry, Indian Institute of Technology Madras, Chennai, 600036, India

[*]Corresponding authors' email: pre@iitm.ac.in (EP) gardas@iitm.ac.in (RLG)

TABLE OF CONTENTS

No table of figures entries found.

Experimental details

Materials

All reagents were used as purchased from commercial sources. All reactions were carried out in oven-dried glassware under an atmosphere of nitrogen (N_2) gas and were magnetically stirred. Dichloromethane was distilled over CaH_2. Toluene was distilled over sodium. The reactions were monitored by thin-layer chromatography (TLC) analysis using Merck silica gel (60 F254) pre-coated plates (0.25 mm), and compounds were visualized under a UV chamber or using phosphomolybdic acid (PMA) solution. Column chromatography was performed on silica gel (100–200 mesh or 60–120 mesh).

Instrumentation

^{1}H (400 MHz) and ^{13}C (100 MHz) NMR spectra were obtained using a Bruker Avance 400 MHz FT-NMR spectrometer in deuterated chloroform ($CDCl_3$) with TMS as an internal reference unless otherwise stated. All chemical shifts are reported in parts per million (ppm, δ): ^{1}H NMR spectra are referenced to the residual proton solvent peak ($CDCl_3$, δ = 7.26 ppm); ^{13}C NMR spectra are referenced to the residual proton solvent peak ($CDCl_3$, δ = 77.16 ppm). The following abbreviations are used for the proton spectra multiplicities: s, singlet; d, doublet; t, triplet; q, quartet; qt, quintet; m, multiplet. Coupling constants (J) are reported in hertz (Hz). High-resolution mass spectra (HRMS) were recorded on a Q-Tofmicro micromass spectrometer. The infrared spectra of compounds were recorded on a JASCO FT/IR-4100 Fourier transform infrared spectrometer. Spectroscopic grade solvents (i.e., dichloromethane) purchased commercially were used for recording UV–vis absorption spectra (Shimadzu UV-3100 UV–vis–NIR absorption spectrophotometer). Fluorescence spectra were recorded using JASCO FP-6300 spectrofluorometer. Powder XRD (P-XRD) patterns have been performed on Bruker D8 Advance X-ray diffractometer using Cu K_α radiation (λ = 1.54178 Å). Thermogravimetric analyses (TGA) and Differential Scanning Calorimetry (DSC) studies were performed on SDT Q600 V20.9 Build 20 (Module- DSC TGA Standard and InstSerial 0600-1572) under nitrogen gas atmosphere at a heating rate of 10 °C/min. The voltammetric measurements were conducted using the electrochemical workstation (CH Instruments 660A) with the conventional three-electrode system. All DFT and TD-DFT calculations were performed using the Gaussian 09 program package.

Synthetic procedure and characterization of the fluorophore

Synthesis of 10-ethyl-10*H*-phenothiazine (8a) and 10-dodecyl-10*H*-phenothiazine (8b):

Alkylation reaction of phenothiazine was done according to the previous report.[1] A portion of 30 mL of 50% NaOH aqueous solution (30 mL) was added into a dried, two-neck, round-bottom flask furnished with a magnetic stir bar containing 10*H*-phenothiazine (10.0 g, 50.2 mmol) dissolved in toluene (30 mL). Afterward, tetrabutylammonium bromide (TBAB) (367 mg, 1.14 mmol) was added to the mixture. Then, 1-bromoalkane (4.46 mL, 60.2 mmol and 14.46 mL, 60.2 mmol for ethylbromide and dodecylbromide, respectively) was added very slowly in a dropwise manner into the final mixture and allowed to stir under reflux condition overnight. The reaction growth was checked by thin-layer chromatography (TLC). Immediately after the starting material was consumed fully (as verified by TLC), the reaction mixture was allowed to cool to room temperature. Then the organic compounds were extracted by ethyl acetate (30 × 7 mL). The combined organic layer was washed with brine, dried over anhydrous Na_2SO_4, filtered, and concentrated at the rotary evaporator. The crude product was then purified using hexane as the eluent to obtain the desired compound by silica gel column chromatography.

10-ethyl-10*H*-phenothiazine (8a):

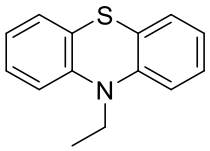

Time: 12 h. Yield: 11.07g, 97%. flexy greenish white solid. ^{1}H NMR (400 MHz, $CDCl_3$): δ 7.14 (t, J = 8.0 Hz, 2H) (PT-H), 7.12 (d, J = 7.6 Hz, 2H) (PT-H), 6.90 (t, J = 7.6 Hz, 2H) (PT-H), 6.86 (d, J = 8.4 Hz, 2H) (PT-H), 3.93 (q, J = 6.8 Hz, 2H)

(-CH_2-), 1.42 (t, *J* = 6.8 Hz, 3H) (-CH_3). ^{13}C NMR (100 MHz, $CDCl_3$): δ 145.1, 127.5, 127.3, 124.6, 122.4, 115.2, 41.9, 13.2.

10-dodecyl-10*H*-phenothiazine (8b):

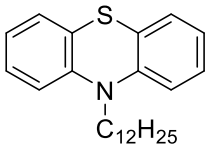

Time: 12 h. Yield: 17.52 g, 95%. waxy type yellowish-green liquid. ^{1}H NMR (400 MHz, $CDCl_3$): δ 7.14 (t, *J* = 8.0 Hz, 2H) (PT-H), 7.13 (d, *J* = 7.6 Hz, 2H) (PT-H), 6.90 (t, *J* =7.2 Hz, 2H) (PT-H), 6.86 (d, *J* = 8.0 Hz, 2H) (PT-H), 3.84 (q, *J* = 7.2 Hz, 2H) (-CH_2-), 1.80 (qt, *J* = 7.2 Hz, 2H) (-CH_2-), 1.42 (qt, *J* = 7.2 Hz, 2H) (-CH_2-), 1.34-1.22 (m, 16H) (8 ×-CH_2-), 0.89 (t, *J* = 6.8 Hz, 3H) (-CH_3). ^{13}C NMR (100 MHz, $CDCl_3$): δ 145.5, 127.5, 127.3, 125.0, 122.4, 115.5, 47.5, 32.1, 29.8 (× 2), 29.7 (× 2), 29.5, 29.4, 27.1, 27.0, 22.9, 14.3.

Synthesis of 10-ethyl-10*H*-phenothiazine-3-carbaldehyde (7a) and 10-dodecyl-10*H*-phenothiazine-3-carbaldehyde (7b):

The compound was synthesized according to previous literature with slight modifications.[2] In a two-neck, round-bottom flask, a freshly distilled dimethylformamide (DMF) solution was kept under an N_2 atmosphere and allowed to cool under an ice bath for 15 min. Then $POCl_3$ was added very slowly in a dropwise manner keeping under the ice for 30 min. Then the ice bath was removed and heated the Vilsmeier-Haack reagent at 45 ^{o}C for another 30 min. Afterward, the heating oil bath was removed, was allowed to cool to room temperature, and again kept under an ice bath. Then, after 10 min, the DCM solution of the N-alkyl-phenothiazine (4 g) was slowly added. Now, after 10 mins, the ice bath was removed and warmed to room temperature. Finally, the resulting mixture was heated at 80 ^{o}C for 3-4 hrs. The reaction progress was checked by thin-layer chromatography (TLC). After that, the reaction mixture was cooled to room temperature. Then, the reaction was quenched with 50-60 ml water, neutralized with a few drops of saturated Na_2CO_3 solution to remove $POCl_3$ altogether. Now, the reaction mixture was neutralized by 2N HCl, and the organic components were extracted by ethyl acetate (EtOAc). The combined organic layer was washed with ice-cold water and brine solution, then dried over anhydrous Na_2SO_4, filtered, and concentrated at the rotary evaporator. The crude product was then purified by silica gel column chromatography using hexane-ethyl acetate mixtures (5% ethyl acetate in hexanes) as the eluent to obtain the desired compound.

10-ethyl-10*H*-phenothiazine-3-carbaldehyde (7a):

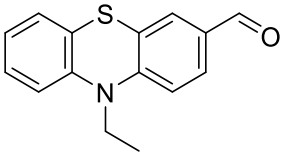

Time: 3 h. Yield: 2.92 g, 65%. Highly viscous yellowish-green liquid. ^{1}H NMR (400 MHz, $CDCl_3$): δ 9.79 (s, 1H) (-CH=O), 7.63 (dd, J_1 = 8.8 Hz and J_2 = 1.6 Hz, 1H) (PT-H), 7.57 (s, 1H) (PT-H), 7.16 (t, *J* = 8.0 Hz, 1H) (PT-H), 7.10 (d, *J* = 7.6 Hz, 1H) (PT-H), 6.96 (t, *J* = 7.6 Hz, 1H) (PT-H), 6.91 (d, *J* = 5.2 Hz, 1H) (PT-H), 6.89 (d, *J* = 5.2 Hz, 1H) (PT-H), 3.98 (q, *J* = 7.2 Hz, 1H) (-CH_2-), 1.45 (t, *J* = 7.2 Hz, 3H) (-CH_3). ^{13}C NMR (100 MHz, $CDCl_3$): δ 190.1, 150.4, 143.2, 131.1, 130.3, 128.3, 127.7, 127.6, 124.6, 123.7, 123.4, 115.7, 114.5, 42.6, 13.0.

10- dodecyl-10*H*-phenothiazine-3-carbaldehyde (7b):

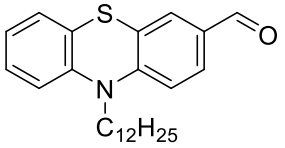

Time: 3 h. Yield: 2.58 g, 60%. Highly viscous yellowish-green liquid. ^{1}H NMR (400 MHz, $CDCl_3$): δ 9.79 (s, 1H) (-CH=O), 7.64 (dd, J_1 = 8.8 Hz and J_2 = 1.6 Hz, 1H) (PT-H), 7.58 (s, 1H) (PT-H), 7.16 (t, *J* = 7.6 Hz, 1H) (PT-H), 7.11 (d, *J* = 7.6 Hz, 1H) (PT-H), 6.96 (t, *J* = 7.6 Hz, 1H) (PT-H), 6.89 (t, *J* = 8.0 Hz, 1H) (PT-H), 6.89 (d, *J* = 7.6 Hz, 1H) (PT-H), 3.89 (q, *J* = 7.2 Hz, 2H) (-CH_2-), 1.81 (t, *J* = 7.2 Hz, 2H) (-CH_2-), 1.43 (qt, *J* = 7.2 Hz, 2H) (-CH_2-), 1.31-1.24 (m, 16H) (-CH_2-), 0.86 (t, *J*

= 7.2 Hz, 3H) (-CH_3). ^{13}C NMR (100 MHz, $CDCl_3$): δ 190.1, 150.8, 143.5, 131.1, 130.2, 128.4, 127.6, 125.1, 123.9, 123.6, 116.0, 114.9, 48.1, 32.01, 29.7, 29.6, 29.4, 29.3, 26.9, 26.8, 22.8, 14.2.

Synthesis of 3-(2,2-dibromovinyl)-10-ethyl-10*H*-phenothiazine (6a) and 3-(2,2-dibromovinyl)-10-dodecyl-10*H*-phenothiazine (6b)

In a two-neck, round-bottom flask, CBr_4 (10% 13C, 2.2 equiv.) was taken and dissolved in CH_2Cl_2 (30 mL). To this, PPh_3 (4 equiv.) was added and purged with nitrogen three minutes.[3] Then, the resulting solution was stirred for 10 minutes under ambient temperature. **7a/7b** (1 equiv.) in CH_2Cl_2 (3 mL) was added at 0 °C and slowly, the reaction mixture was warmed to room temperature, stirred for 1 h. The solvent was removed under reduced pressure, and the residue was purified by flash column chromatography to give the **6a/6b** (96%) as a highly viscous yellowish-green liquid which was used for the next step.

3-(2,2-dibromovinyl)-10-ethyl-10H-phenothiazine (6a):

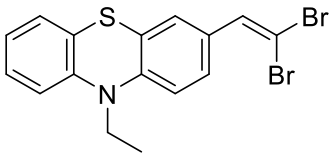

Time: 10 mins. Yield: 13.92 g, 96%. Highly viscous yellowish-green transparent liquid. ^{1}H NMR (400 MHz, $CDCl_3$): δ 7.36-7.29 (m, 2H) (PT-H), 7.31 (s, 1H) (-$CHBr_2$), 7.14 (t, *J* = 7.2 Hz, 1H) (PT-H), 7.10 (d, *J* = 7.6 Hz, 1H) (PT-H), 6.91 (t, *J* = 7.2 Hz, 1H) (PT-H), 6.85 (d, *J* = 8.4 Hz, 1H) (PT-H), 6.81 (d, *J* = 8.8 Hz, 1H) (PT-H), 3.92 (q, *J* = 7.2 Hz, 2H) (-CH_2-), 1.42 (t, *J* = 7.2 Hz, 3H) (-CH_3). ^{13}C NMR (100 MHz, $CDCl_3$): δ 145.2, 144.3, 139.9, 135.7, 129.5, 127.9, 127.5, 127.1, 124.2, 123.7, 122.8, 115.2, 114.6, 87.9, 42.0, 13.0.

3-(2,2-dibromovinyl)-10-dodecyl-10*H*-phenothiazine (6b):

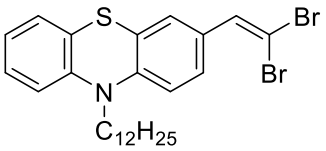

Time: 10 mins. Yield: 2.77 g, 96%. Highly viscous yellowish-green transparent liquid. ^{1}H NMR (400 MHz, $CDCl_3$): δ 7.36-7.29 (m, 2H) (PT-H), 7.31 (s, 1H) (-$CHBr_2$), 7.14 (t, *J* = 8.0 Hz, 1H) (PT-H), 7.11 (d, *J* = 8.0 Hz, 1H) (PT-H), 6.91 (t, *J* = 8.0 Hz, 1H) (PT-H), 6.84 (d, *J* = 8.0 Hz, 1H) (PT-H), 6.80 (d, *J* = 8.0 Hz, 1H) (PT-H), 3.82 (q, *J* = 8.0 Hz, 2H) (-CH_2-), 1.81 (qt, *J* = 7.2 Hz, 2H) (-CH_2-), 1.42 (qt, *J* = 8.0 Hz, 2H) (-CH_2-), 1.38-1.24 (m, 16H) (-CH_2-), 0.88 (t, *J* = 7.2 Hz, 3H) (-CH_3). ^{13}C NMR (100 MHz, $CDCl_3$): δ 145.5, 144.6, 135.7, 129.4, 127.8, 127.6, 127.4, 127.1, 124.7, 124.2, 122.8, 115.5, 114.9, 87.8, 47.6, 32.0, 29.8, 29.7, 29.5, 29.3, 27.0, 27.0, 26.9, 22.8, 14.3.

Synthesis of 3-(2,2-di(aryl-2-yl)vinyl)-10-alkyl-10*H*-phenothiazine [PT-Cn-$(Ar)_2$, where n=2 and 12 and Ar = phenyl, Naphthyl, anthracenyl, phenanthryl, and Pyrenyl] (1-5):

The following compounds were synthesized using the Suzuki-Miyaura cross-coupling mechanism.[4] In a one-necked round-bottom flask, compound **6** (1equiv.) was added in an oven-dried under N_2 atmosphere; then, a mixture of freshly distilled toluene/methanol (3:1) (24mL) was added into the flux under continuous N_2 purging. Then, potassium carbonate (5 equiv.) and Aryl-boronic acid (Ar-$B(OH)_2$) (2.5 equiv.) and $Pd(PPh_3)_4$ (0.08 equiv.) were added into the solution. The resulting mixture was purged with nitrogen gas for 20 min. Then the reaction mixture was allowed reflux at 80 °C under vigorous stirring overnight under the nitrogen gas atmosphere. The progress of the reaction was supervised through thin layer chromatography (TLC). As soon as the reaction was completed, the mixture was quenched with water and extracted with ethyl acetate (20 mL × 3). The combined organic layers were dried over anhydrous Na_2SO_4, filtered, and the filtrate was concentrated under a high vacuum. The crude product thus obtained was purified by silica-gel column chromatography using hexane-ethyl acetate mixtures (0-5% ethyl acetate in hexanes) as the eluant.

3-(2,2-diphenylvinyl)-10-ethyl-10*H*-phenothiazine [PT-C2-(Ph)$_2$] (1a):

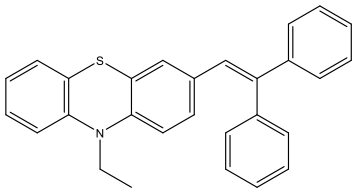

Time: 36h. Yield: 91%, 681.3 mg. Green solid. ^{1}H NMR (400 MHz, $CDCl_3$): δ 7.36 (s, 2H) (Ph-H), 7.85 (d, J = 1.6 Hz, 1H) (Ph-H), 7.30-7.29 (m, 5H) (Ph-H), 7.22-7.20 (m, 2H) (Ph-H), 7.10 (t, J = 8.0 Hz, 1H) (PT-H), 7.05 (t, J = 8.0 Hz, 1H) (PT-H), 6.86 (t, J = 8.0 Hz, 1H) (PT-H), 6.82 (s, 1H) (PT-CH(Ph_2)), 6.80 (d, J = 8.0 Hz, 1H) (PT-H), 6.76 (s, 1H) (PT-H), 6.76-6.73 (m, 1H) (PT-H), 6.58 (d, J = 8.0 Hz, 1H) (PT-H), 3.84 (q, J = 6.8 Hz, 2H) (-CH_2-), 1.36 (t, J = 6.8 Hz, 3H) (-CH_3). ^{13}C NMR (100 MHz, $CDCl_3$): δ 140.6, 130.4, 128.9, 128.7, 128.3, 127.56,127.52, 127.4, 127.3, 115.0, 114.4. HRMS (ESI-TOF) m/z: 406.1624 [M + H] $^+$ calcd. For $C_{28}H_{24}NS$, found 406.1600.

3-(2,2-diphenylvinyl)-10- dodecyl -10*H*-phenothiazine [PT-C2-(Ph)$_2$] (1b):

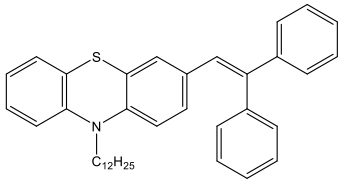

Time: 36h. Yield:91%, 681.3 mg. Sticky green solid. ^{1}H NMR (400 MHz, $CDCl_3$): δ 7.60 (s, J = 8 Hz, 1H) (Ph-H), 7.50-7.48 (m, 1H) (Ph-H), 7.48 (s, 1H) (Ph-H), 7.44 (t, J = 4 Hz, 1H) (Ph-H), 7.33-7.26 (m, 9H) (Ph-H), 7.16-7.10 (m, 3H) (PT-7.26.92 (t, J = 8 Hz, 1H) (PT-H), 6.85 (d, J = 8 Hz, 1H) (PT-H), 6.79 (d, J = 8 Hz, 1H) (PT-H), 3.83 (q, J = 7.2 Hz, 2H) (-CH_2-), 1.79 (qt, J = 7.2 Hz, 2H) (-CH_2-), 1.42 (qt, J = 7.2 Hz, 2H) (-CH_2-), 1.30-1.24 (m, 16H) (-CH_2-), 0.88 (t, J = 7.2 Hz, 3H) (-CH_3). ^{13}C NMR (100 MHz, $CDCl_3$): δ 130.4, 128.9, 128.6, 128.3, 127.5, 115.3, 114.7, 32.0, 29.8,29.7, 29.5, 29.4, 27.0, 22.8, 14.3. HRMS (ESI-TOF) m/z: 568.3008 [M + Na] $^+$ calcd. For $C_{38}H_{43}NSNa$, found 568.2979.

3-(2,2-di(naphthalen-2-yl)vinyl)-10-ethyl-10*H*-phenothiazine [PT-C2-(Nap)$_2$] (2a):

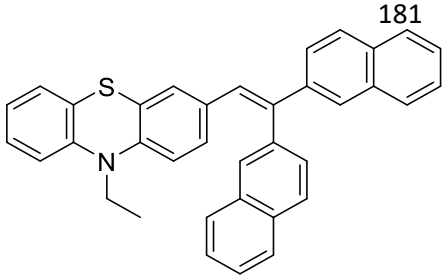

Time: 36h. Yield: 722 mg, 90 %. Bright yellow solid powder. ^{1}H NMR (400 MHz, $CDCl_3$): δ 7.90 (d, J = 8.0 Hz, 1H) (Nap-H), 7.85 (d, J = 8.4 Hz, 1H) (Nap-H), 7.83-7.70 (m, 4H) (Nap-H), 7.75 (s, 1H) (Nap-H), 7.68 (s, 1H) (Nap-H), 7.55-7.47 (m, 2H) (Nap-H), 7.50 (d, J = 8.8 Hz, 1H) (Nap-H), 7.47-7.41 (m, 2H) (Nap-H), 7.39 (d, J = 8.4 Hz, 1H) (Nap-H), 7.10 (t, J = 8.0 Hz, 1H) (PT-H), 7.04 (d, J = 6.0 Hz, 1H) (PT-H), 7.03 (s, 1H) (PT-CH($Nap)_2$), 6.93 (s, 1H) (PT-H), 6.86 (t, J = 7.2 Hz, 1H) (PT-H), 6.79 (d, J = 8.0 Hz, 1H) (PT-H), 6.73 (d, J = 8.4 Hz, 1H) (PT-H), 6.50 (d, J = 8.8 Hz, 1H) (PT-H), 3.81 (q, J = 7.2 Hz, 2H) (-CH_2-), 1.33 (t, J = 6.8 Hz, 3H) (-CH_3). ^{13}C NMR (100 MHz, $CDCl_3$): δ 144.5, 143.6, 141.1, 141.0, 138.2, 133.9, 133.5, 132.9, 132.87, 131.8, 129.5, 128.9, 128.8, 128.5, 128.4, 128.34, 128.32, 128.0, 127.9, 127.8, 127.6, 127.4, 127.3, 126.9, 126.3, 126.2, 126.1, 126.0, 125.8, 123.9, 123.5, 122.4, 115.0, 114.5, 41.8, 13.0. HRMS (ESI-TOF) m/z: 505.1864 [M]$^+$ calcd. For $C_{36}H_{27}NS$, found 505.1842.

3-(2,2-dinaphthalenvinyl)-10- dodecyl -10*H*-phenothiazine [PT-C12-(Nap)$_2$] (2b):

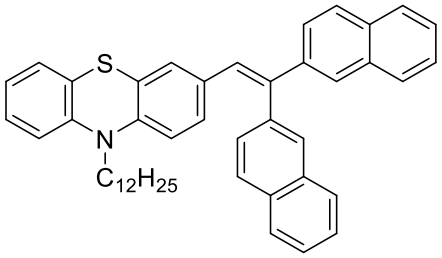

Time: 36h. Yield:91%, 681.3 mg. Highly sticky reddish-brown solid. ^{1}H NMR (400 MHz, $CDCl_3$): δ 7.90 (d, J = 8.0 Hz, 1H)(Nap-H), 7.85 (d, J = 8.4 Hz, 1H) (Nap-H), 7.82-7.80 (m, 1H) (Nap-H), 7.75 (s, 1H) (Nap-H), 7.75-7.70 (m, 3H) (Nap-H), 7.68 (s, 1H) (Nap-H), 7.54-7.42 (m, 5H) (Nap-H), 7.39 (d, J = 8.36 Hz, 1H) (Nap-H), 7.10 (t, J = 7.6 Hz, 1H) (PT-H), 7.04 (d, J = 8.12 Hz, 1H) (PT-H), 7.03 (s, 1H) (PT-CH(Nap_2)), 6.94 (s, 1H) (PT-H), 6.86 (t, J = 7.4 Hz, 1H) (PT-H), 6.78 (d, J = 8.0 Hz, 1H) (PT-H), 6.73 (d, J = 8.8 Hz, 1H) (PT-H), 6.49 (d, J = 8.4 Hz, 1H) (PT-H), 3.70 (t, J = 7.2 Hz, 2H) (-CH_2-), 1.71 (q, J = 6.8 Hz, 2H) (-CH_2-), 1.35 (q, J = 7.2 Hz, 2H) (-CH_2-), 1.3-1.23 (m, 16H) (-CH_2-), 0.88 (t, J = 7.2 Hz, 3H) (-CH_3). ^{13}C NMR (100 MHz, $CDCl_3$): δ 144.8, 144.0, 141.10, 141.0, 138.2, 133.9, 133.5, 132.91, 132.87, 131.8, 129.5, 128.9, 128.4, 128.3, 128.0, 127.9, 127.8, 127.6, 127.4, 127.2, 127.0, 126.3, 126.2, 126.1, 126.0, 125.8, 124.4, 124.0, 122.4, 115.3, 114.8, 47.5, 32.0, 29.83, 29.80, 29.75,29.72, 29.69,29.6, 29.5, 29.3, 27.0, 26.9, 22.8, 14.3. HRMS (ESI-TOF) m/z: 646.3502 $[M + H]^+$ calcd. For $C_{46}H_{48}NS$, found 646.3481.

3-(2,2-dianthracenvinyl)-10-ethyl-10*H*-phenothiazine: [PT-C2-($An)_2$] (3):

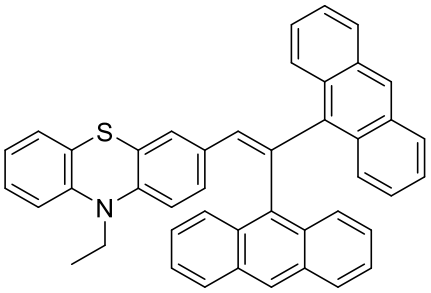

Time: 36 h. Yield: 439 mg, 78 %. Semi-crystalline orange solid. ^{1}H NMR (400 MHz, $CDCl_3$): δ 8.55 (d, J = 8.4 Hz, 2H) (An-H), 8.47 (s, 1H) (An-H), 8.42 (s, 1H) (An-H), 8.39 (d, J = 8.8 Hz, 2H) (An-H), 7.98 (d, J = 8.4 Hz, 4H) (An-H), 7.39-7.30 (m, 4H) (An-H), 7.31 (s, 1H) (PT-CH(An_2)), 7.24-7.13 (m, 3H) (An-H), 7.17 (d, J = 7.6 Hz, 1H) (An-H), 7.06 (t, J = 8.0 Hz, 1H) (PT-H), 6.97 (d, J = 7.6 Hz, 1H) (PT-H), 6.83 (t, J =7.2 Hz, 1H) (PT-H), 6.72 (d, J = 8.4 Hz, 1H) (PT-H), 6.64 (s, 1H) (PT-H), 6.41 (d, J = 8.4 Hz, 1H) (PT-H), 6.26 (d, J = 8.4 Hz, 1H) (PT-H), 3.70 (q, J = 6.4 Hz, 2H) (-CH_2-), 1.23 (t, J = 6.8 Hz, 3H) (-CH_3).^{13}C NMR (100 MHz, $CDCl_3$): δ 144.3, 143.9, 140.3, 141.9, 140.3, 136.3, 132.9, 132.0, 131.4, 131.3, 130.5, 129.1, 128.5, 128.3, 127.9, 127.3, 127.2, 127.1, 127.05, 126.20, 125.8, 125.1, 124.9, 123.7, 123.3, 122.4, 115.0, 114.3, 41.8, 12.8. HRMS (ESI-TOF) m/z: 605.2177 $[M]^+$ calcd. For $C_{44}H_{31}NS$, found 605.2147.

3-(2,2-diphenanthrenvinyl)-10-ethyl-10*H*-phenothiazine [PT-C2-($Pn)_2$] (4):

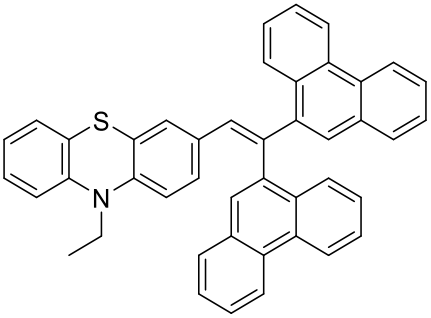

Time: 36h. Yield: 681 mg, 91%. Light yellow solid. ^{1}H NMR (400 MHz, $CDCl_3$): δ 8.80-8.71 (m, 3H) (Pn-H), 8.67 (s, 1H) (Pn-H), 8.65 (s, 1H) (Pn-H), 8.24 (d, J = 8.0 Hz, 1H) (Pn-H), 7.79 (s, 1H) (Pn-H), 7.78 (d, J = 6.4 Hz, 1H) (Pn-H), 7.70-7.64 (m, 4H) (Pn-H), 7.63-7.54 (m, 4H) (Pn-H), 7.50 (t, J = 7.6 Hz, 1H) (Pn-H), 7.43 (t, J = 6.8 Hz, 1H) (Pn-H), 7.10 (s, 1H) (PT-CH(Pn_2)), 7.07 (t, J = 7.2 Hz, 1H) (PT-H), 7.01 (d, J = 7.2 Hz, 1H) (PT-H), 6.91 (s, 1H) (PT-H), 6.84 (t, J = 7.6 Hz, 1H) (PT-H), 6.74 (d, J = 8.4 Hz, 1H) (PT-H), 6.70 (d, J = 8.8 Hz, 1H) (PT-H), 6.35 (d, J = 8.4 Hz, 1H) (PT-H), 3.71 (q, J = 6.8 Hz, 2H) (-CH_2-), 1.25 (t, J = 6.8 Hz, 3H) (-CH_3). ^{13}C NMR (100 MHz, $CDCl_3$): δ 144.5, 143.8, 140.6, 137.8, 136.7, 134.0, 132.0, 131.5, 131.4, 131.1, 130.5, 130.4, 130.0, 129.0, 128.9, 128.7, 127.8, 127.4, 127.3, 127.2, 126.9, 126.8, 126.77, 126.7, 126.5, 123.5, 123.3, 123.1, 122.7, 122.5, 122.4, 115.0, 114.6, 41.8, 12.9. HRMS (ESI-TOF) m/z: 605.2177 $[M]^+$ calcd. For $C_{44}H_{31}NS$, found 605.2150.

3-(2,2-diphenanthrenvinyl)-10-ethyl-10*H*-pyrene [PT-C2-($Pr)_2$] (5):

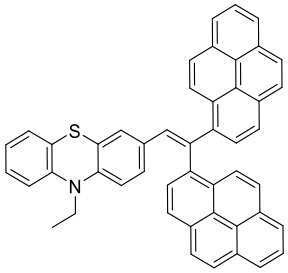

Time: 36h. Yield: 371.2 mg, 68%. Orange solid. ^{1}H NMR (500 MHz, $CDCl_3$): δ 8.94 (d, J = 9.5 Hz, 1H) (Pr-H), 8.31 (d, J = 9.5 Hz, 1H) (Pr-H), 8.20-8.16 (m, 4H) (Pr-H), 8.13-8.08 (m, 4H) (Pr-H), 8.06-7.96 (m, 5H) (Pr-H), 7.93 (d, J = 8.0 Hz, 1H) (Pr-H), 7.88 (d, J = 9.5 Hz, 1H) (Pr-H), 7.71 (d, J = 8.0 Hz, 1H) (Pr-H), 7.20 (s, 1H) (PT-CH(Pr_2)), 7.06 (t, 1H) (PT-H), 7.01-6.96 (m, 1H) (PT-H), 6.90 (d, J = 2.0 Hz, 1H) (PT-H), 6.85-6.81 (m, 1H) (PT-H), 6.73 (d, J = 8.0 Hz, 1H) (PT-H), 6.59-6.55 (m, 1H) (PT-H), 6.33 (d, J = 8.5 Hz, 1H) (PT-H), 3.71 (q, J = 7.0 Hz, 2H) (-CH_2-), 1.23 (t, J = 7.0 Hz, 3H) (-CH_3). HRMS (ESI-TOF) m/z: 654.2250 $[M]^+$ calcd. For $C_{48}H_{31}NS$, found 654.2176.

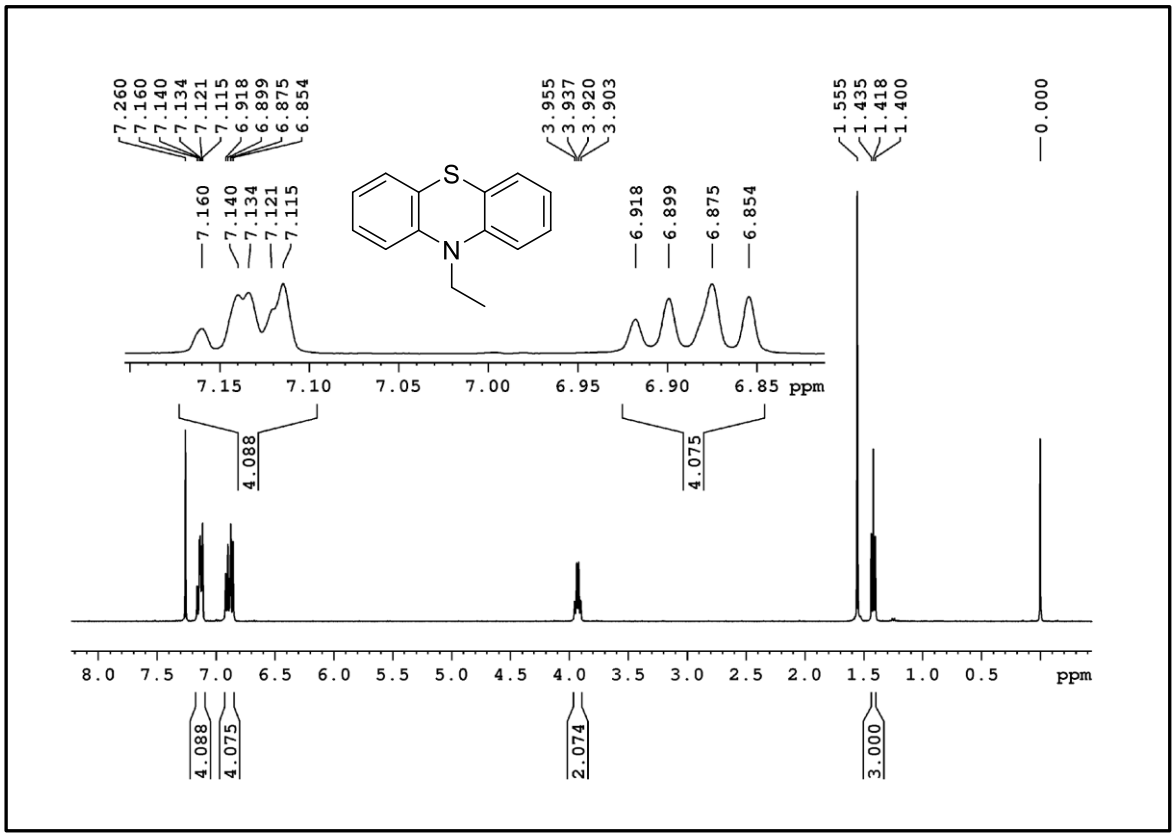

Figure S1. 400 MHz ^{1}H NMR spectrum of **8a** in $CDCl_3$.

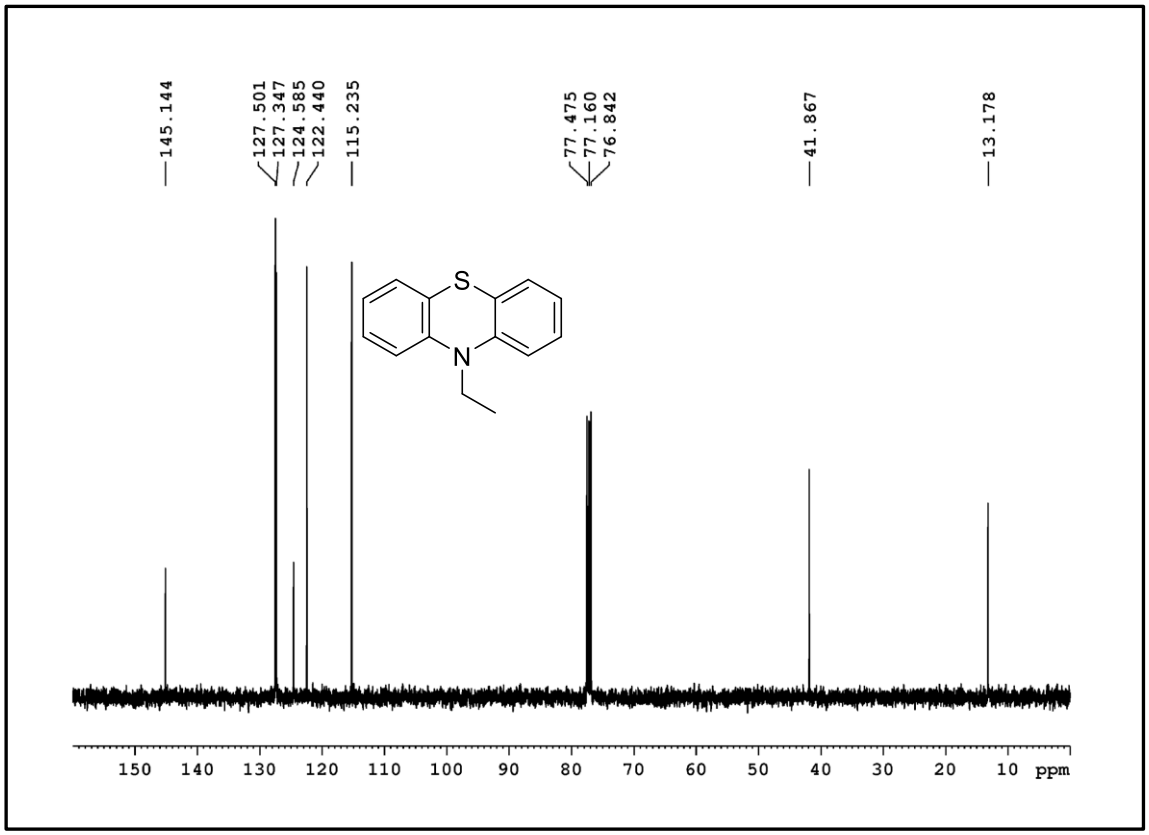

244

245 **Figure S2.** 100 MHz ^{13}C NMR spectrum of **8a** in $CDCl_3$.

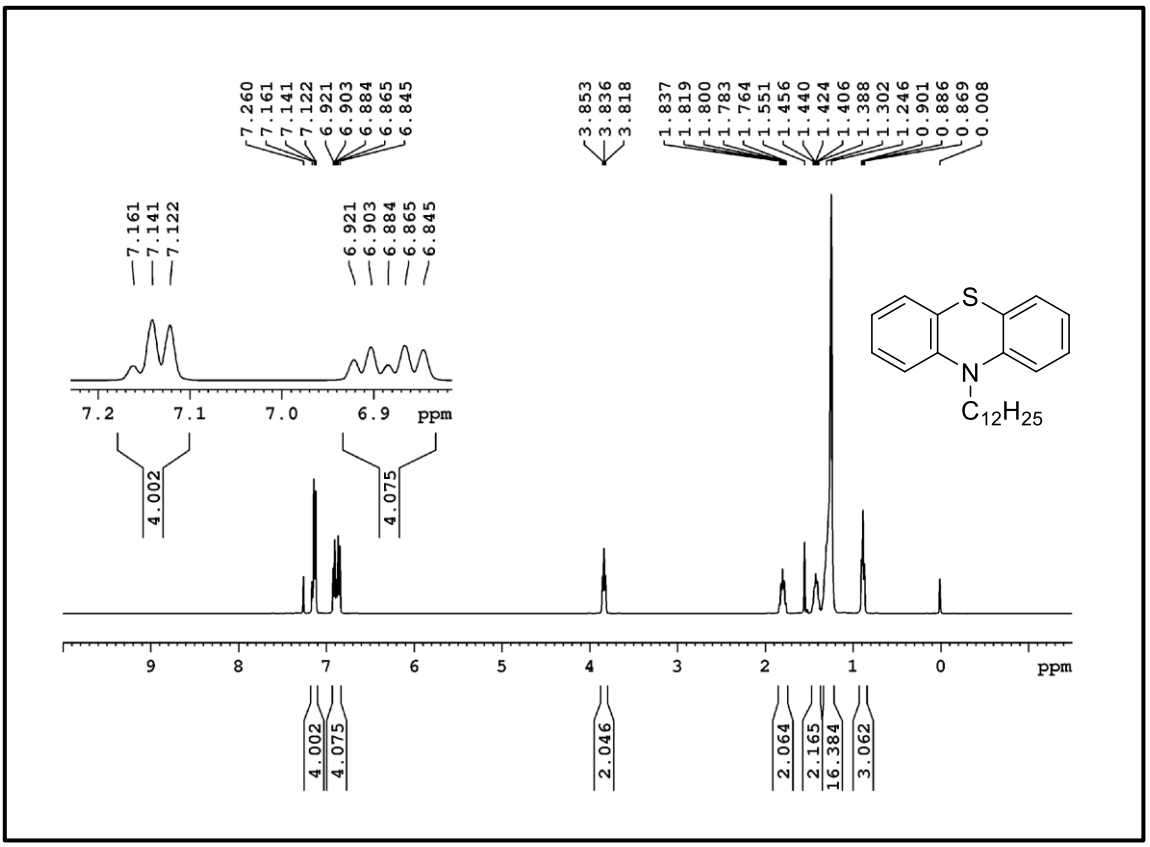

246

247 **Figure S3.** 400 MHz ^{1}H NMR spectrum of **8b** in $CDCl_3$.

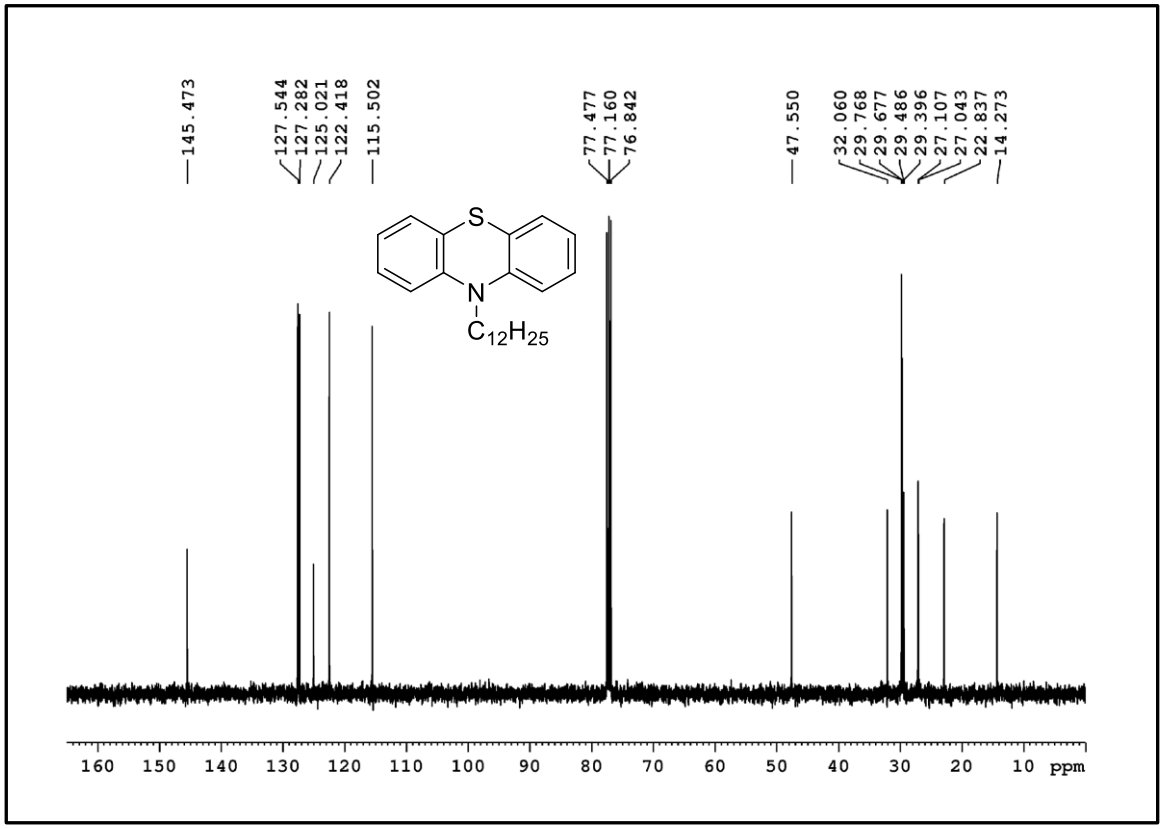

248

249 **Figure S4.** 400 MHz ^{13}C NMR spectrum of **8b** in $CDCl_3$.

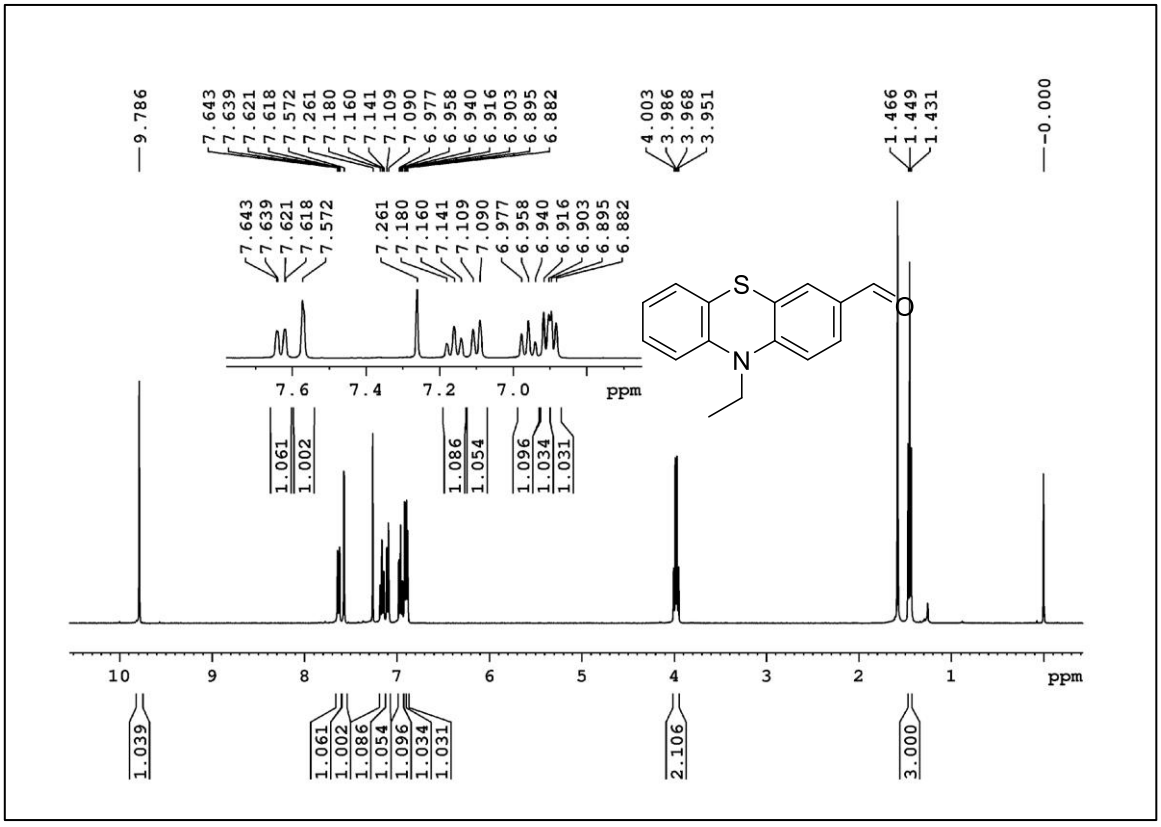

250

251 **Figure S5.** 400 MHz ^{1}H NMR spectrum of **7a** in $CDCl_3$.

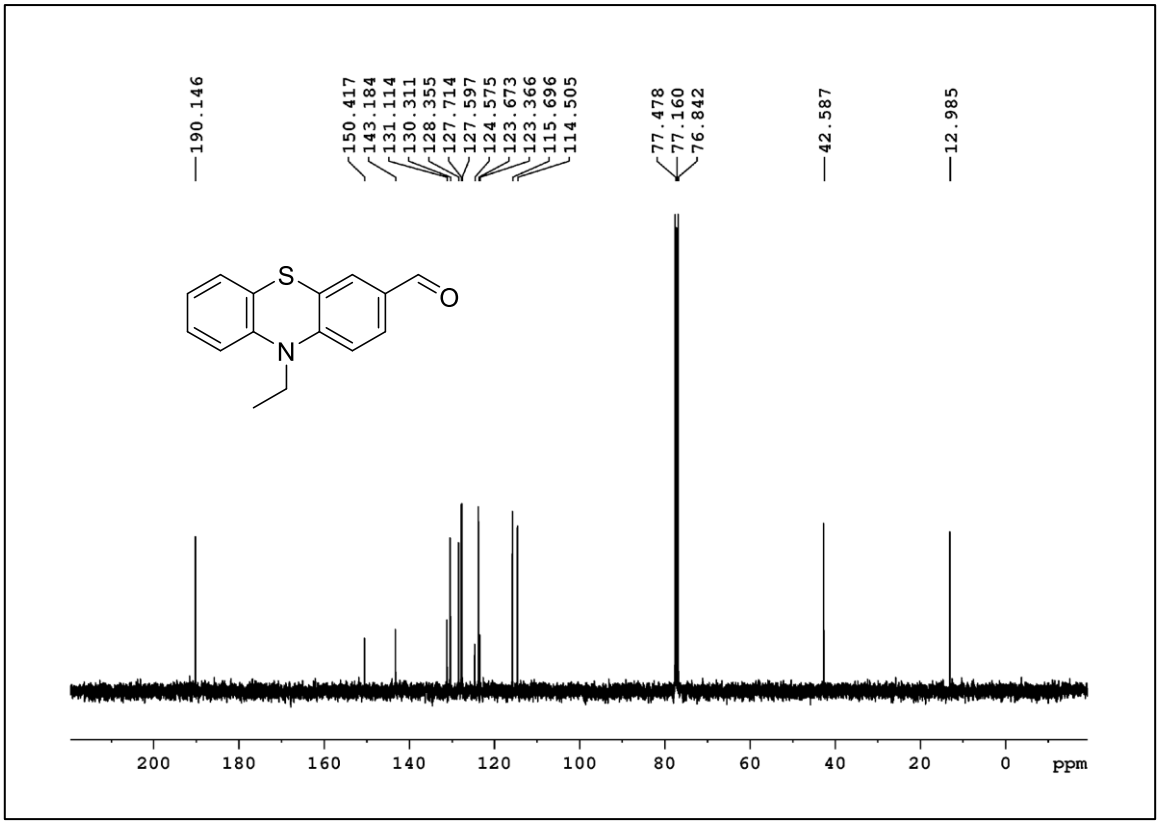

252

253 **Figure S6.** 400 MHz ^{13}C NMR spectrum of **7a** in $CDCl_3$.

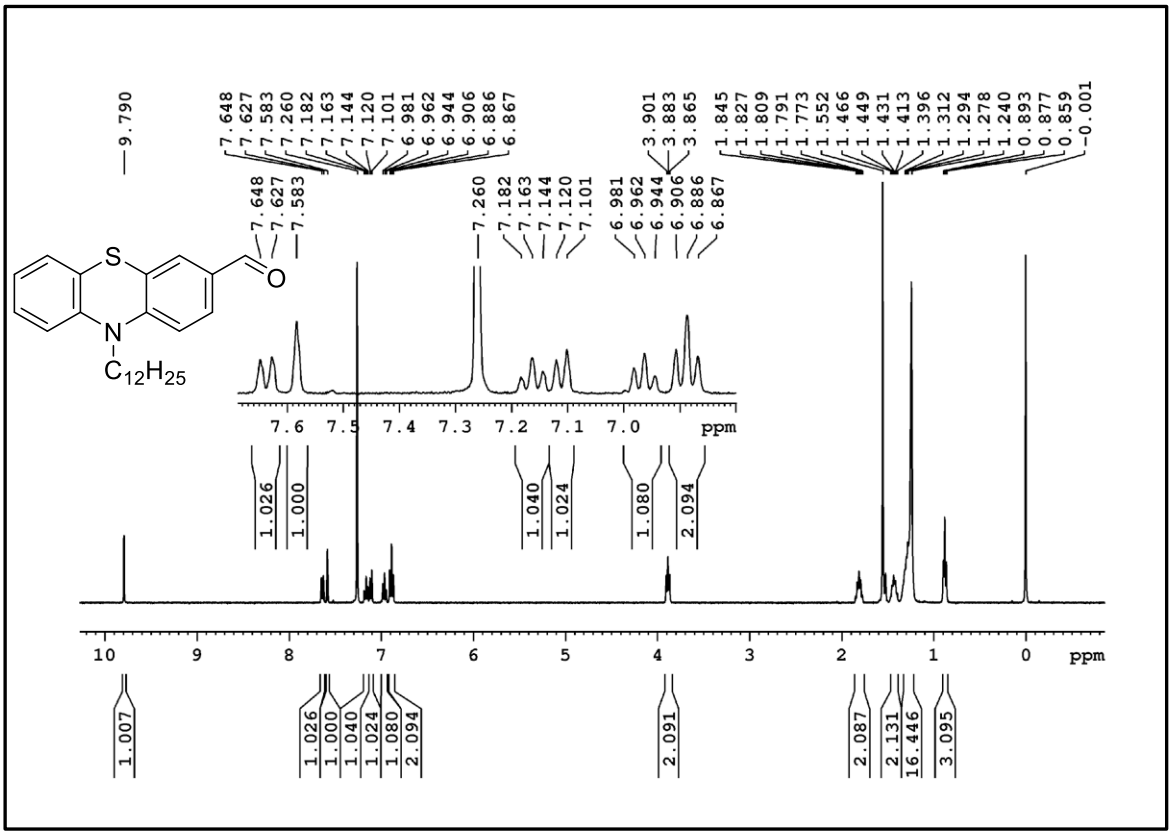

254

255 **Figure S7.** 400 MHz ^{1}H NMR spectrum of **7b** in $CDCl_3$.

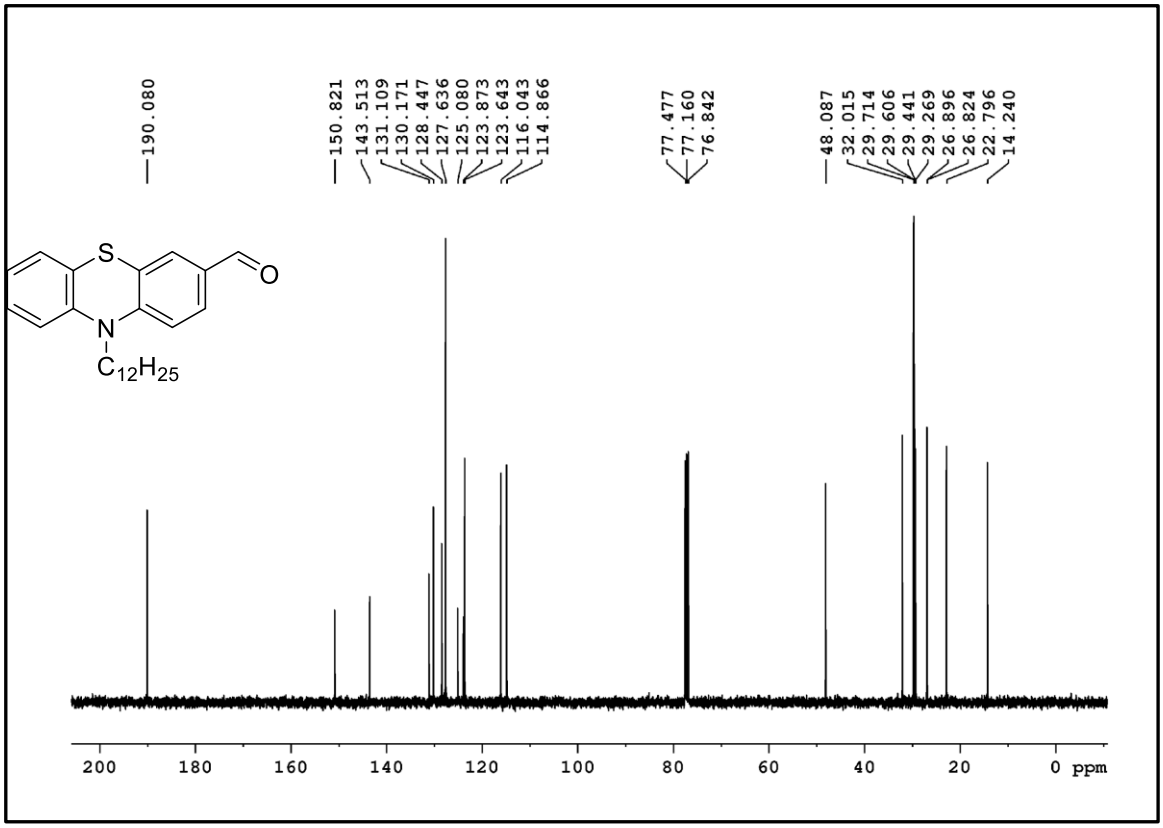

256

257 **Figure S8.** 400 MHz ^{13}C NMR spectrum of **7b** in $CDCl_3$.

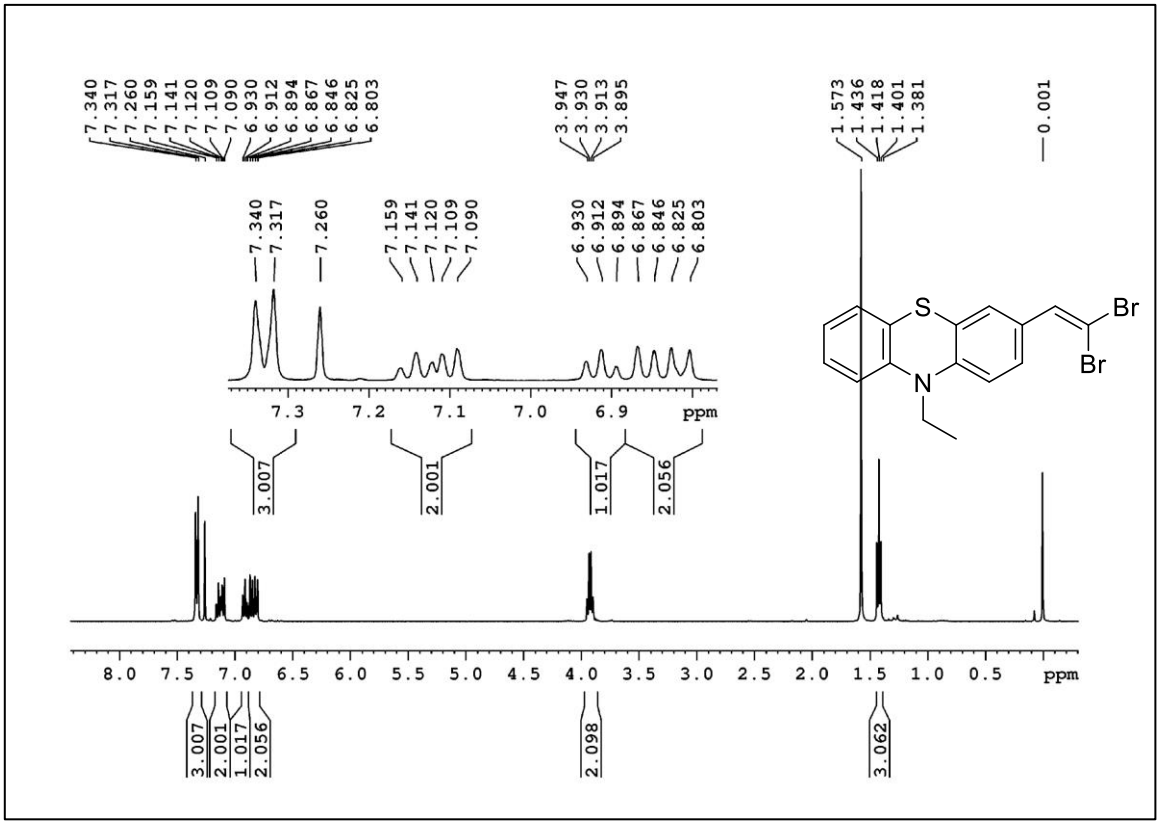

258

259 **Figure S9.** 400 MHz ^{1}H NMR spectrum of **6a** in $CDCl_3$.

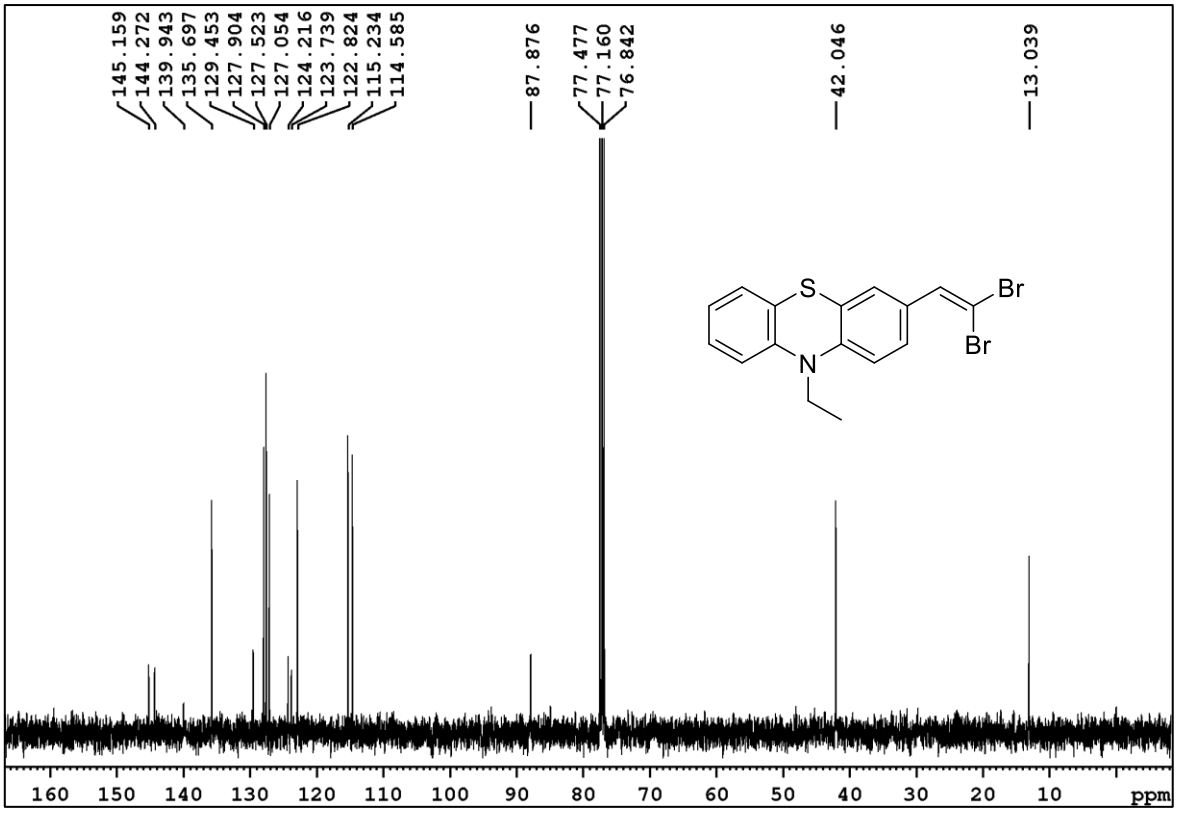

Figure S10. 400 MHz ^{1}H NMR spectrum of **6a** in $CDCl_3$.

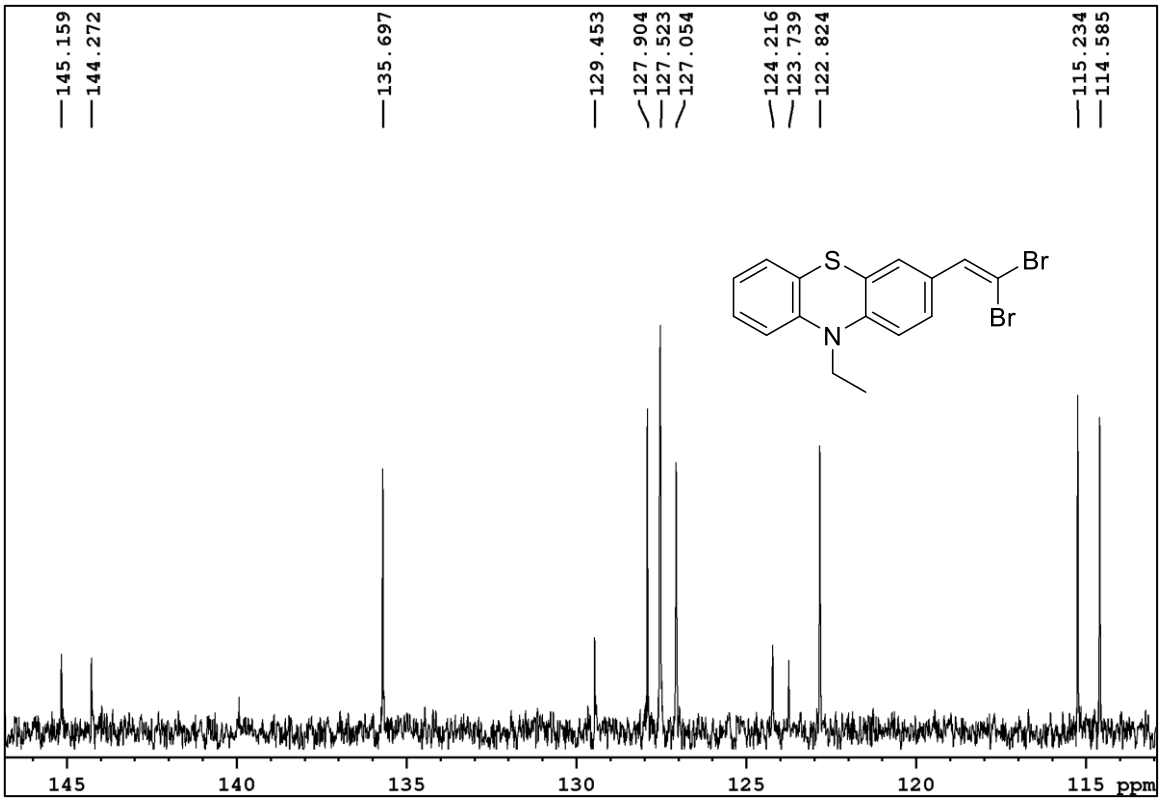

Figure S11. 400 MHz ^{1}H NMR spectrum of **6a** in $CDCl_3$.

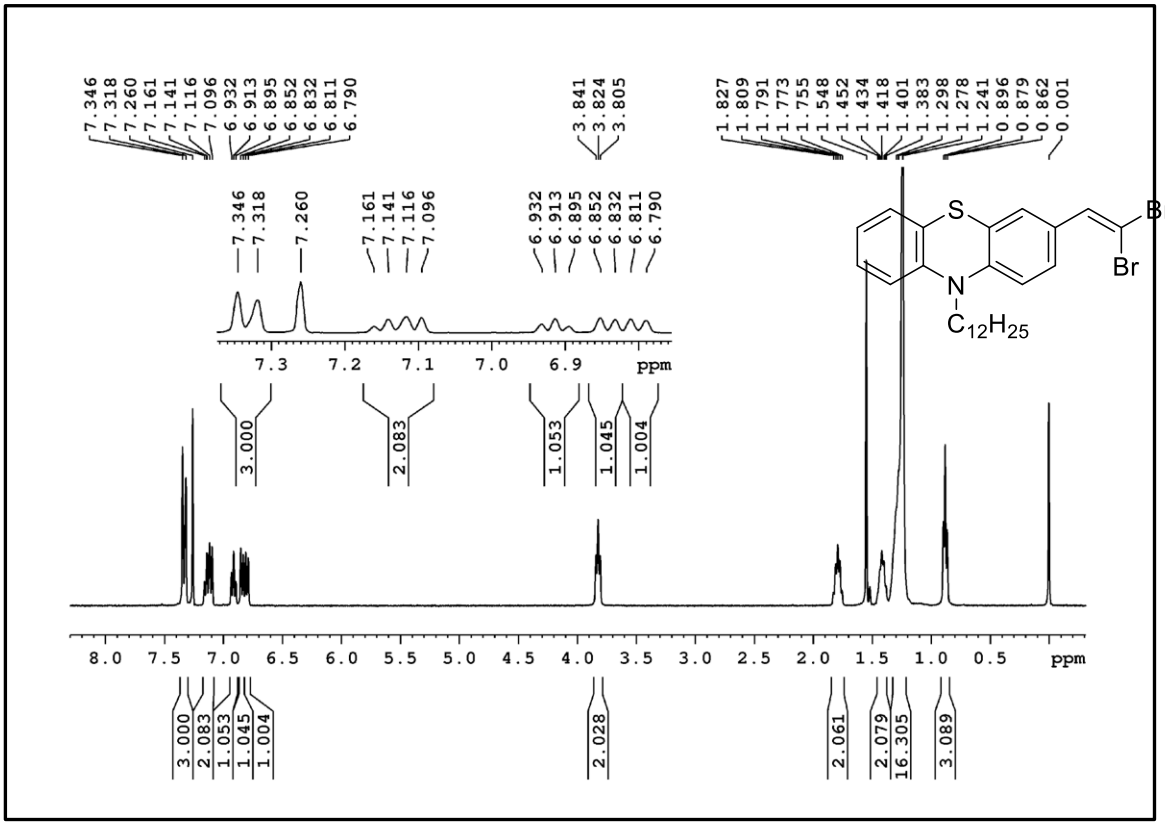

265

266 **Figure S12.** 400 MHz ^{1}H NMR spectrum of **6b** in $CDCl_3$.

267

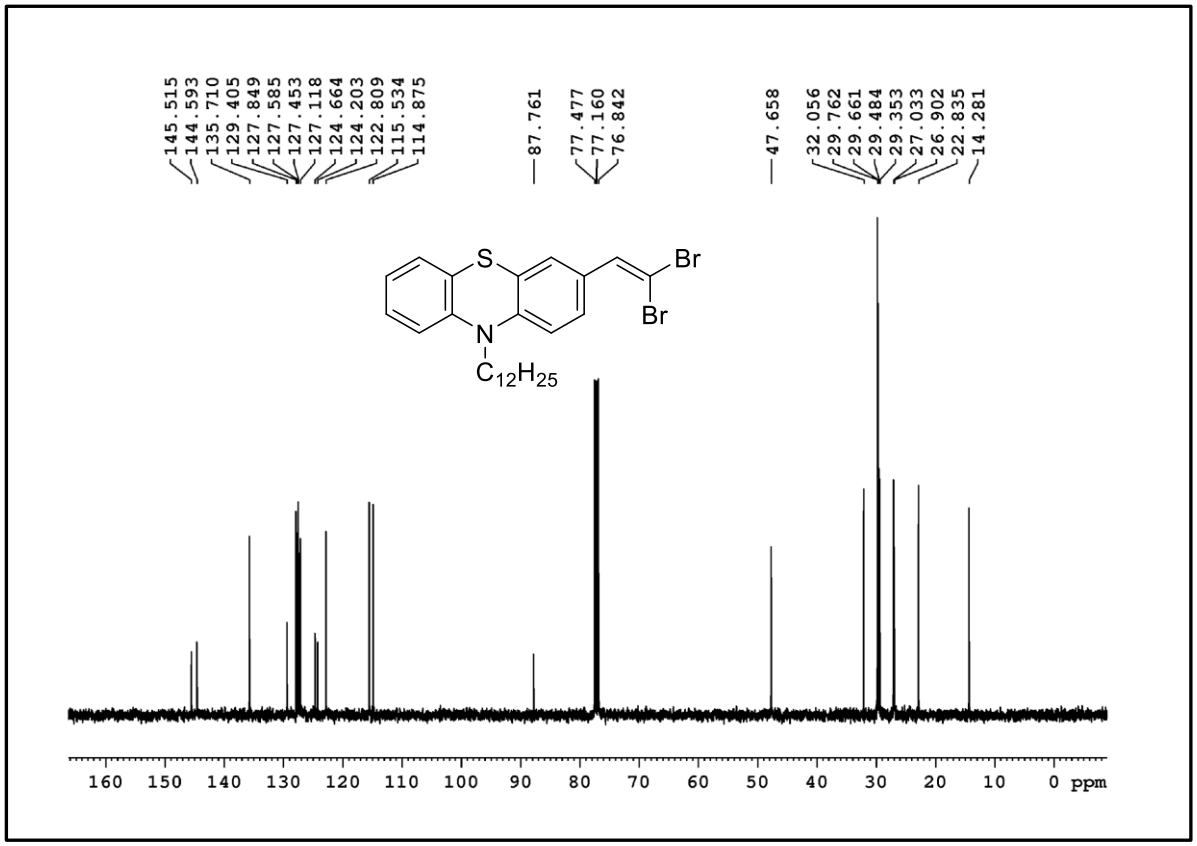

268

269 **Figure S13.** 400 MHz ^{13}C NMR spectrum of **6b** in $CDCl_3$.

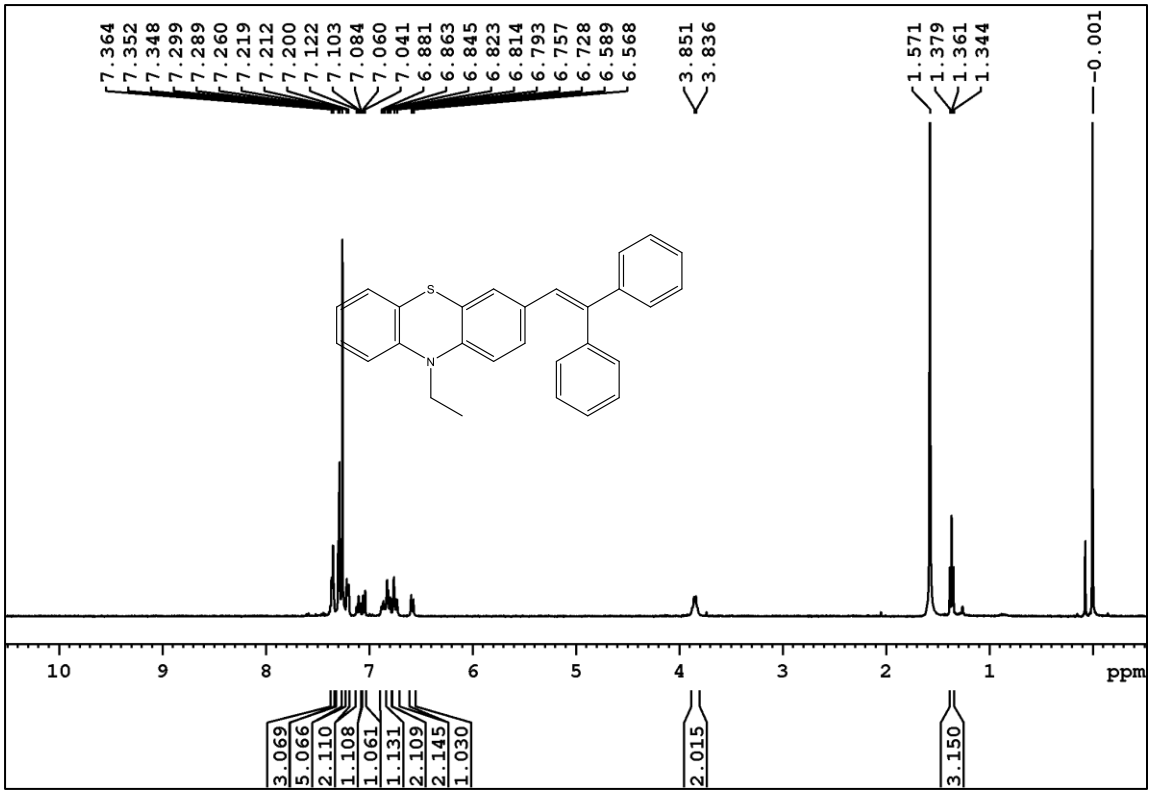

Figure S14. 400 MHz ^{1}H NMR spectrum of **1a** in $CDCl_3$.

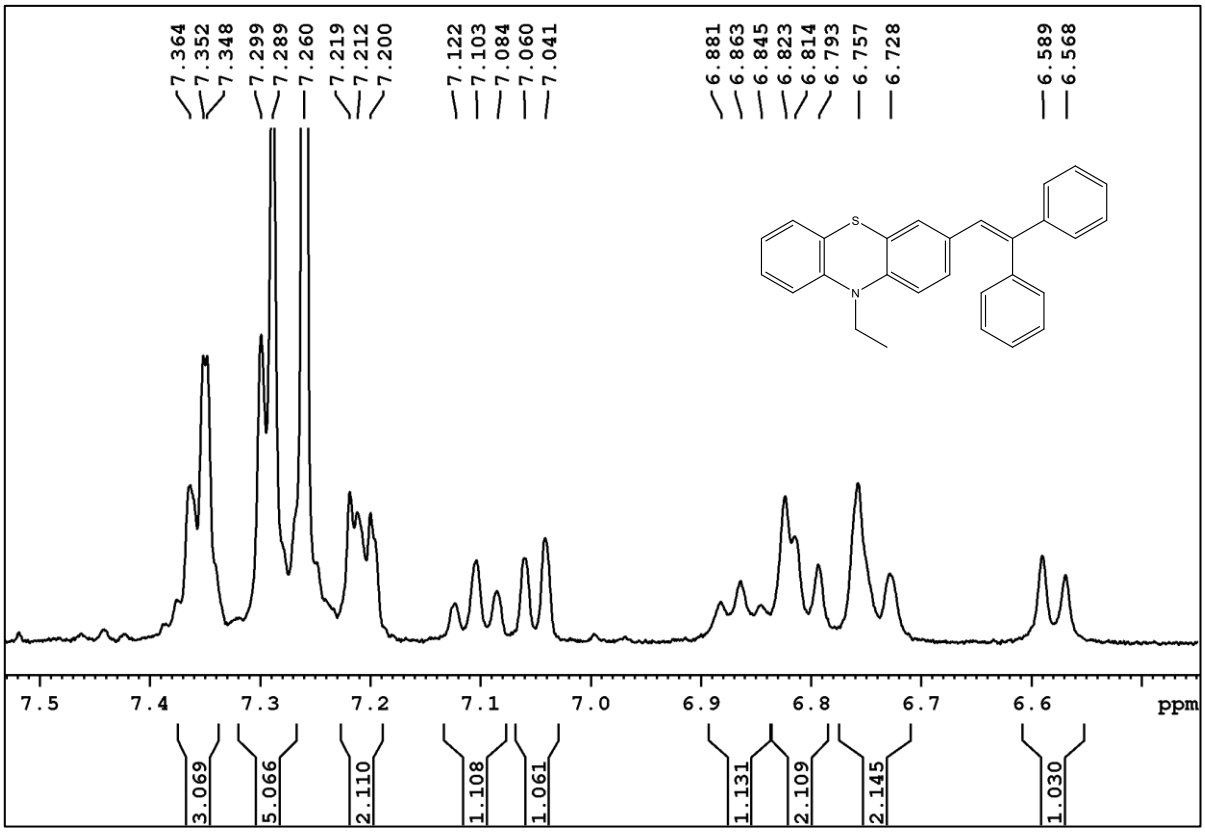

Figure S15. 400 MHz ^{1}H NMR (expanded) spectrum of **1a** in $CDCl_3$.

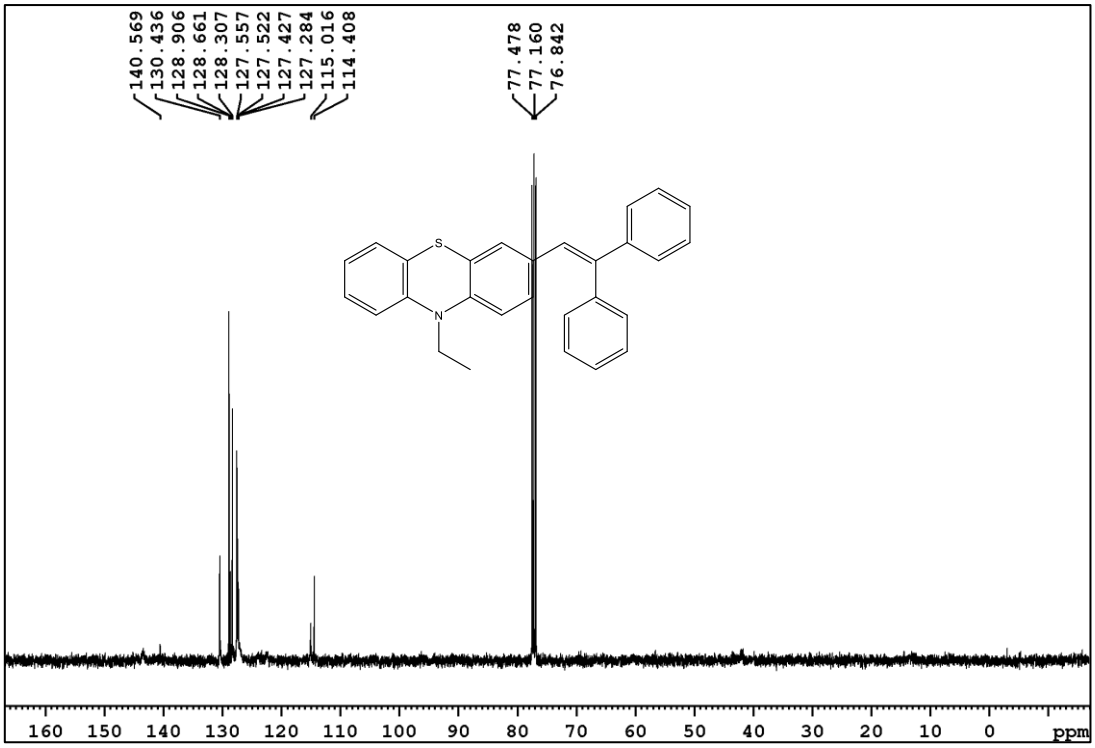

Figure S16. 400 MHz ^{13}C NMR spectrum of **1a** in $CDCl_3$.

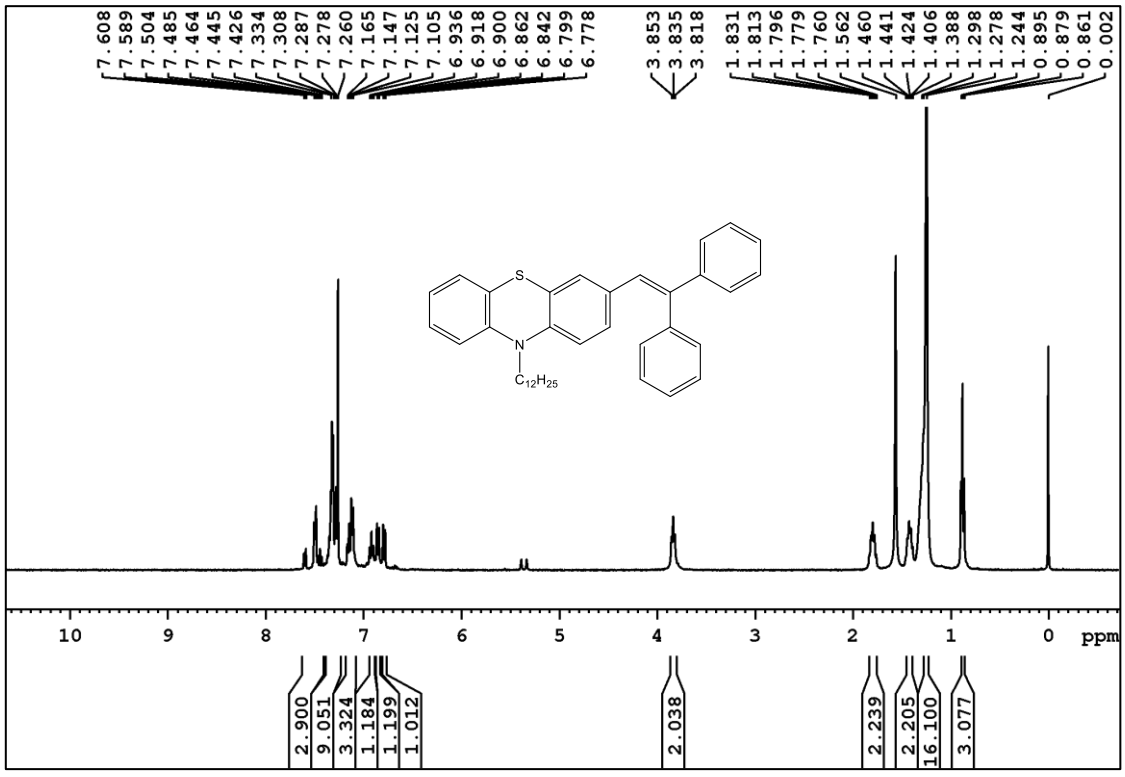

Figure S17. 400 MHz ^{1}H NMR spectrum of **2a** in $CDCl_3$.

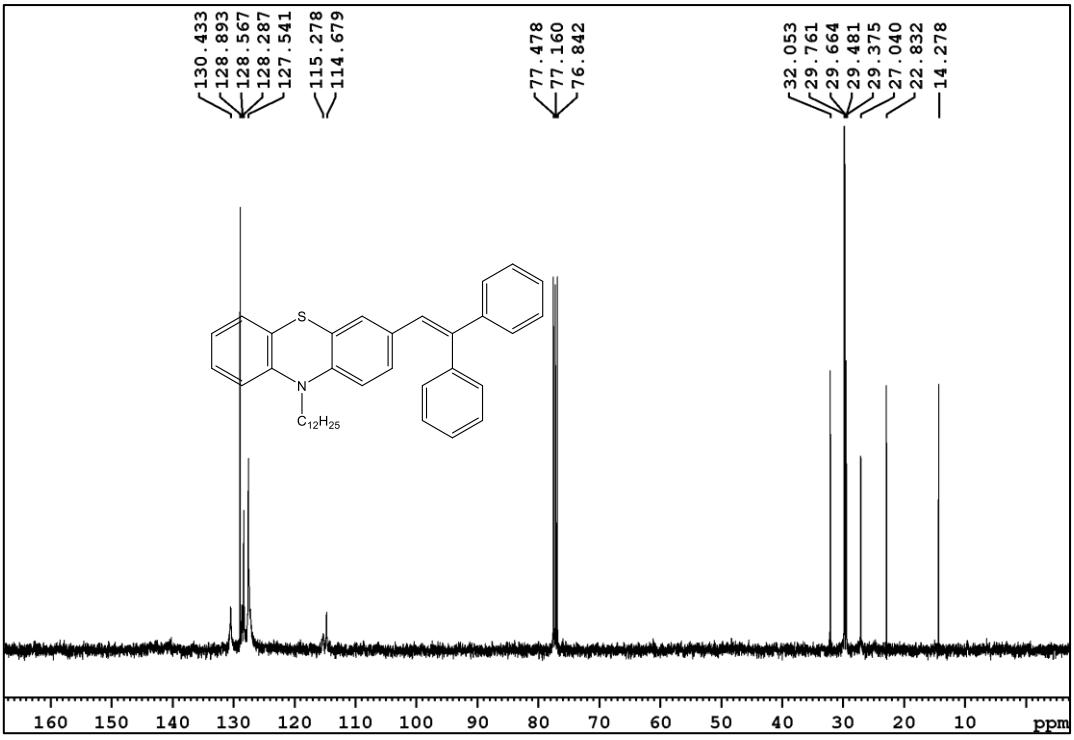

281

282 **Figure S18.** 400 MHz ^{13}C NMR spectrum of **1b** in $CDCl_3$.

283

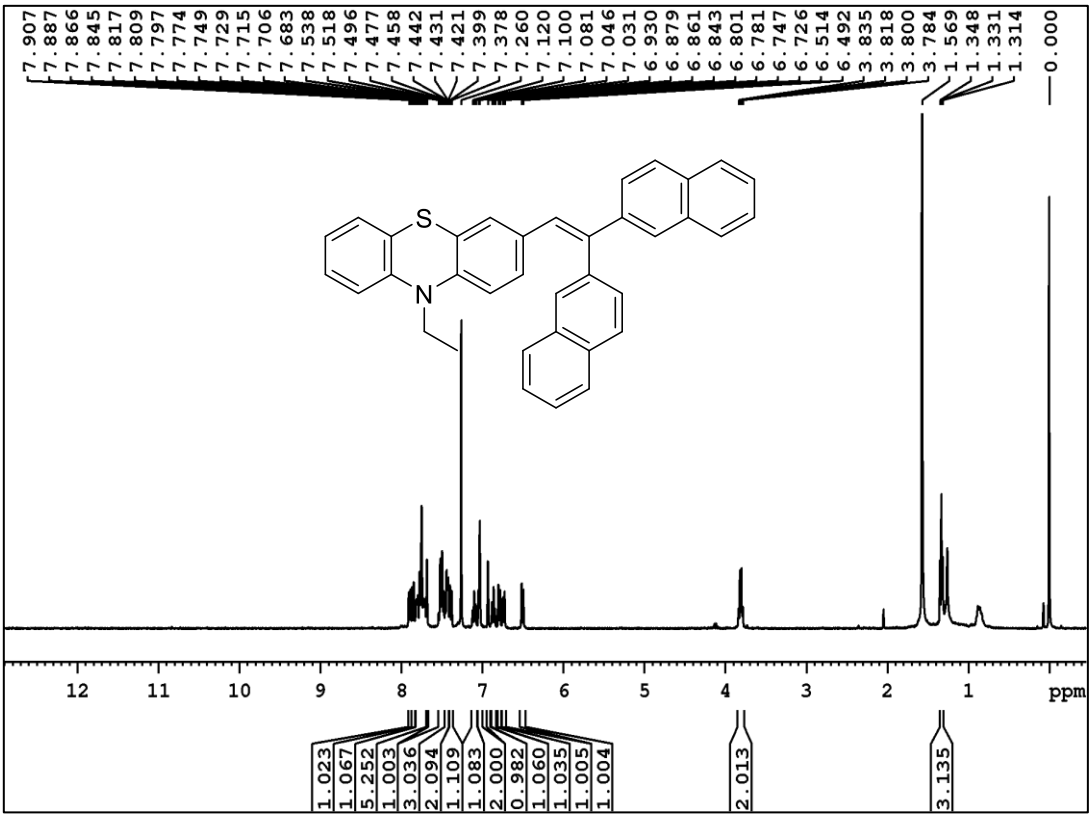

284

285 **Figure S19.** 400 MHz ^{1}H NMR spectrum of **2a** in $CDCl_3$.

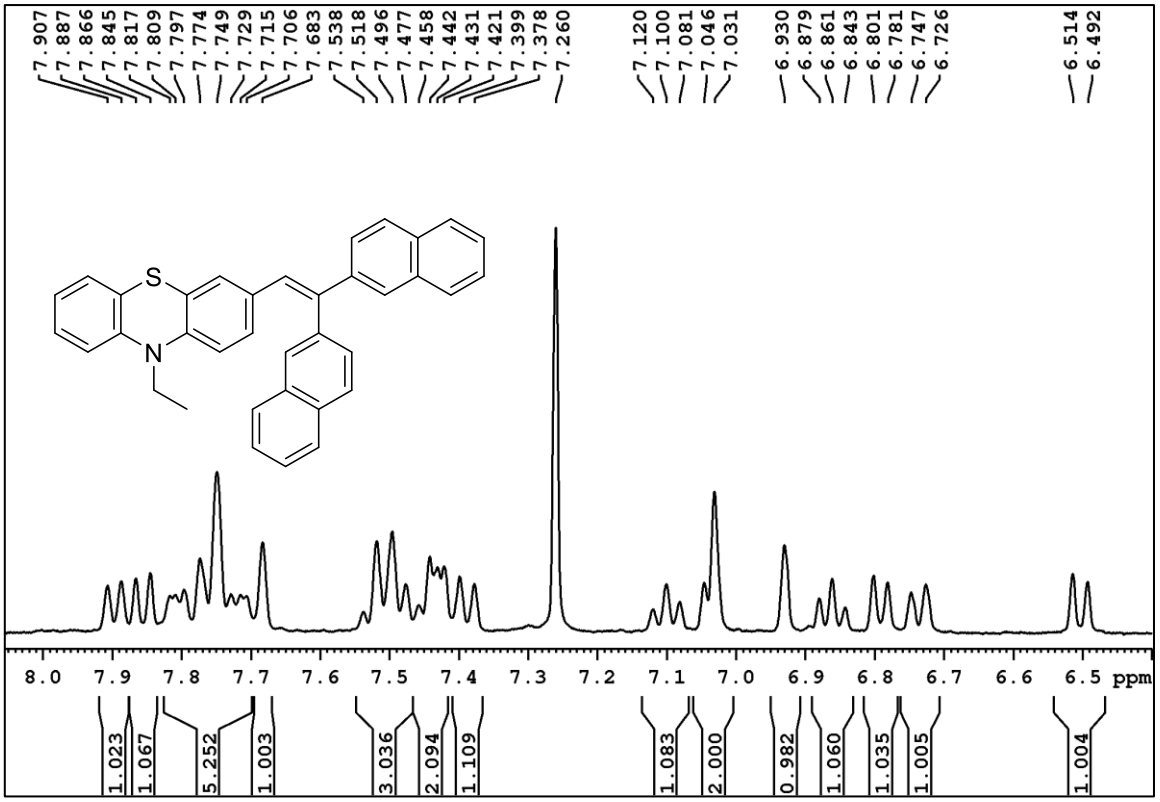

Figure S20. 400 MHz ^{1}H NMR (expanded) spectrum of **2a** in $CDCl_3$.

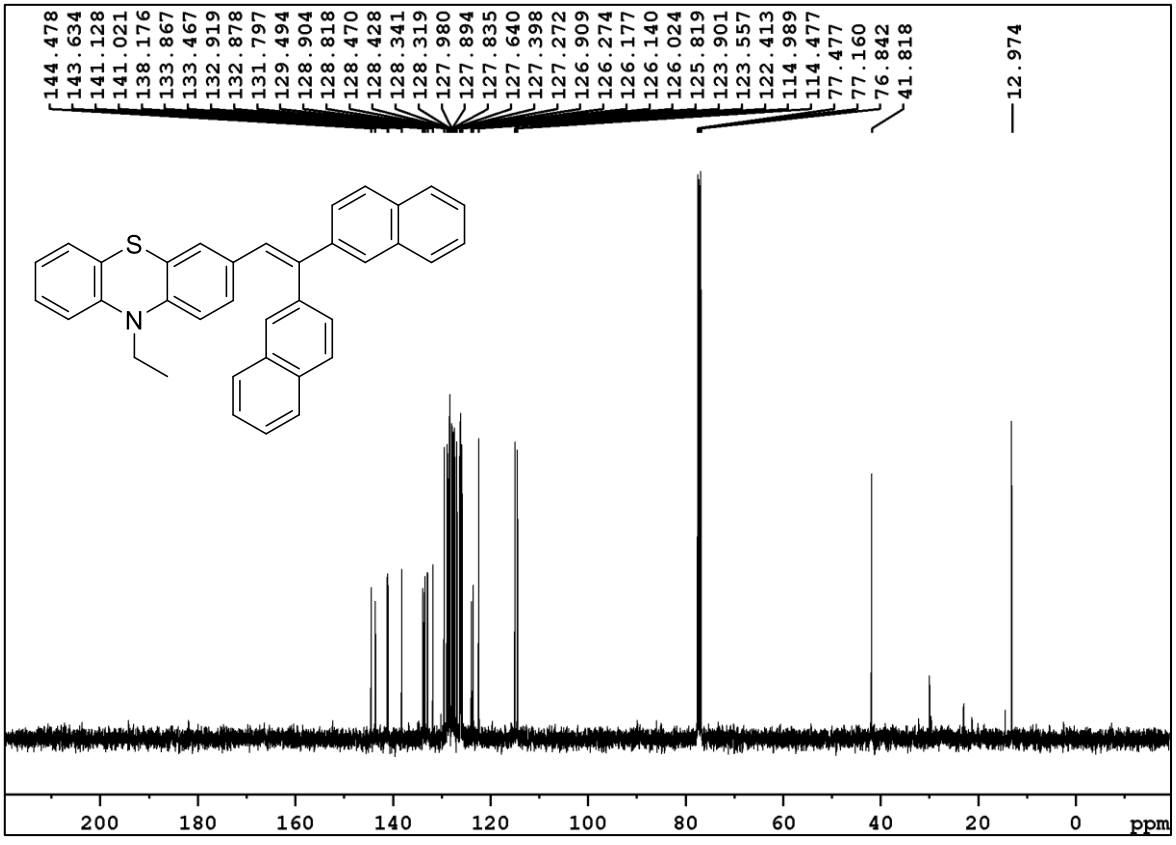

Figure S21. 100 MHz ^{13}C NMR spectrum of **2a** in $CDCl_3$.

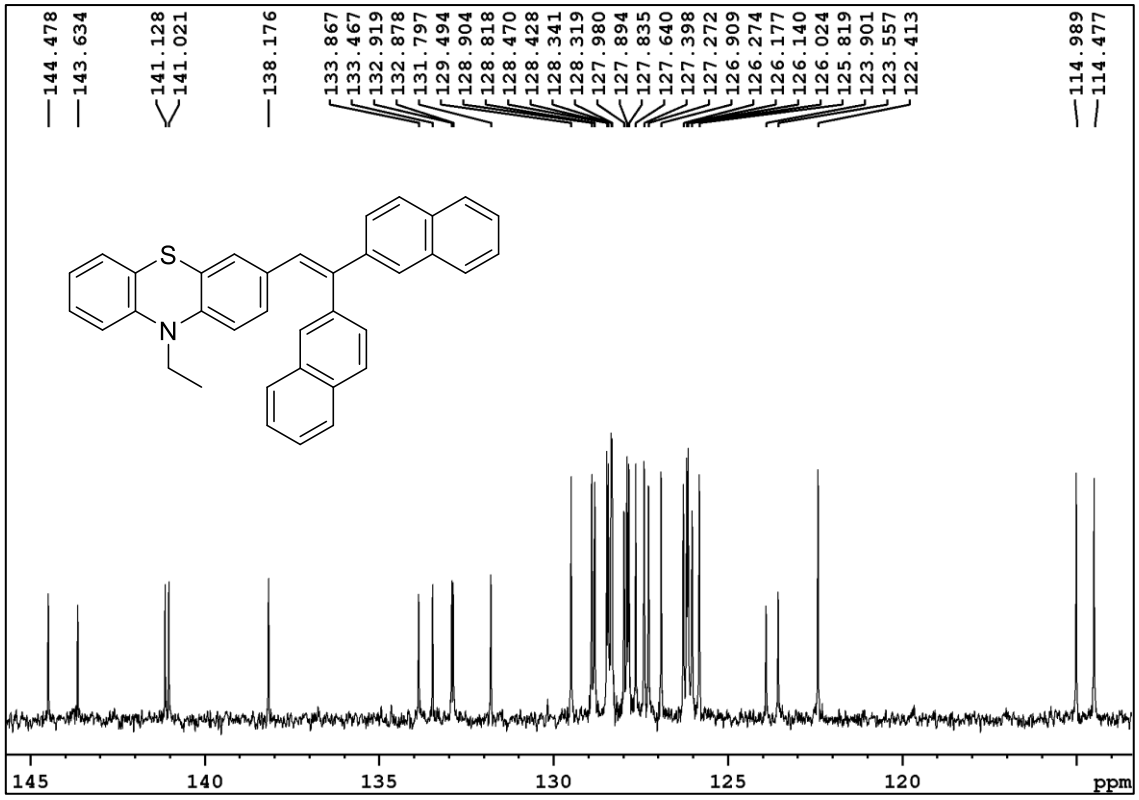

Figure S22. 100 MHz ^{13}C NMR (expanded) spectrum of **2a** in $CDCl_3$.

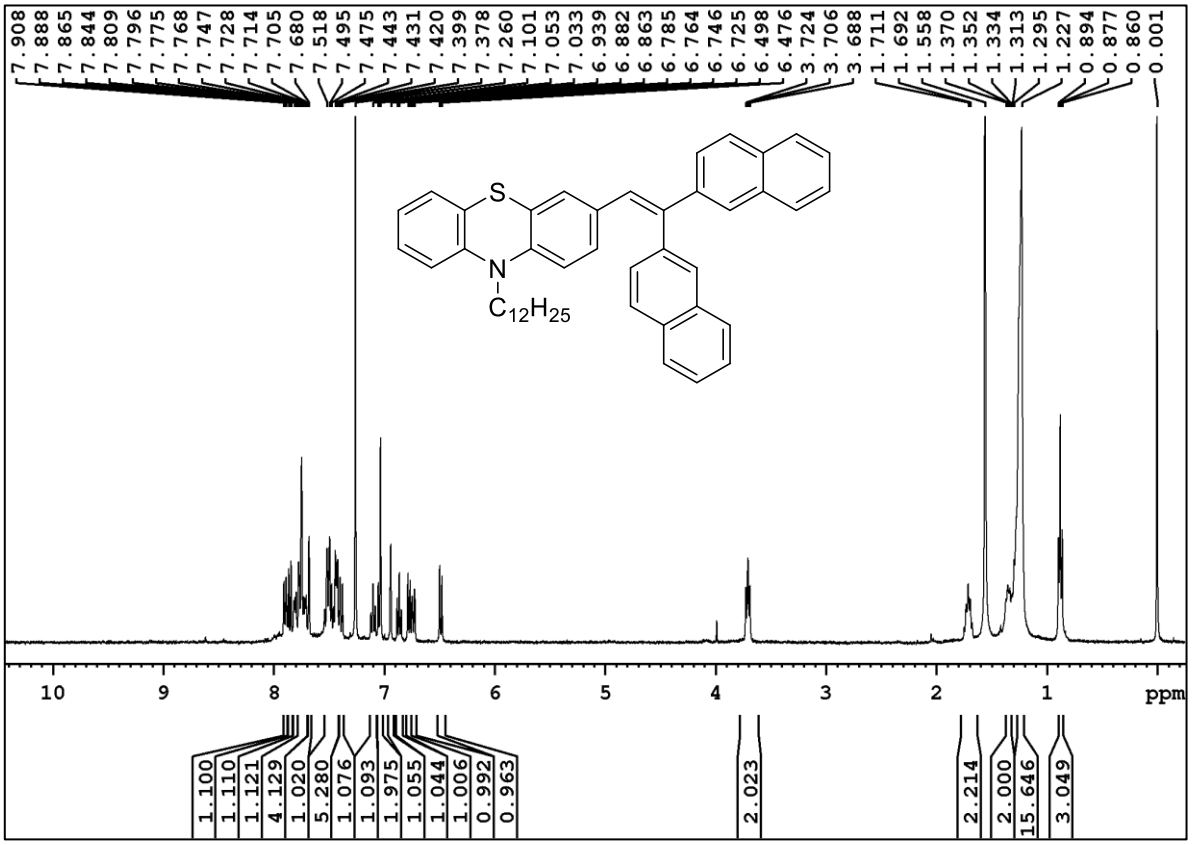

Figure S23. 400 MHz ^{1}H NMR spectrum of **2b** in $CDCl_3$.

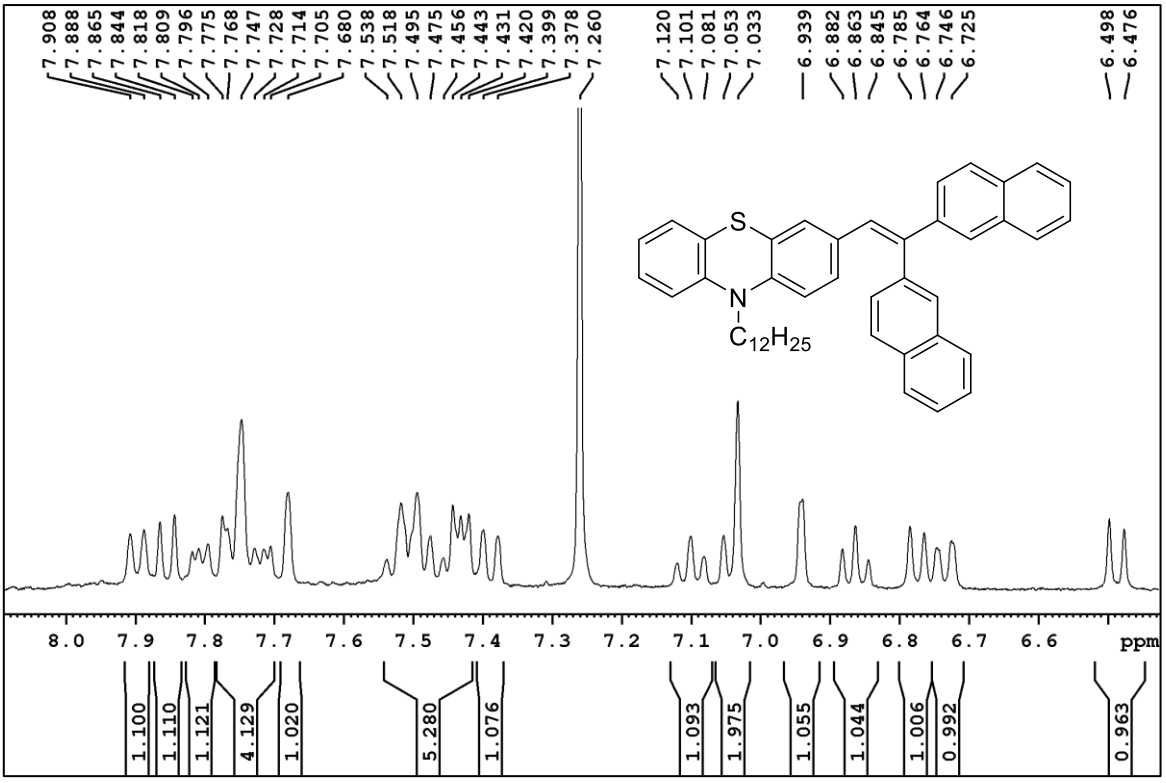

295

296 **Figure S24.** 400 MHz ^{1}H NMR (expanded) spectrum of **2b** in $CDCl_3$.

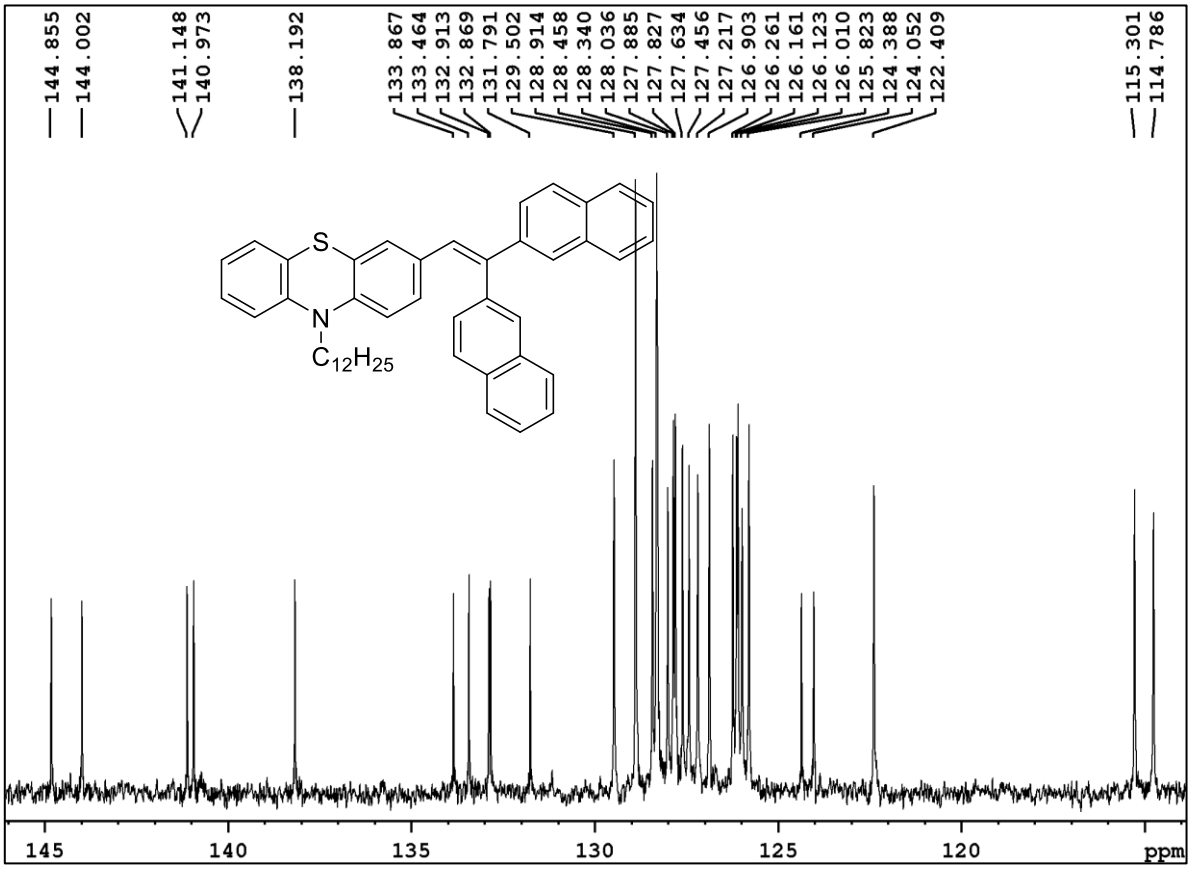

297

298 **Figure S25.** 400 MHz ^{1}H NMR (expanded) spectrum of **2b** in $CDCl_3$.

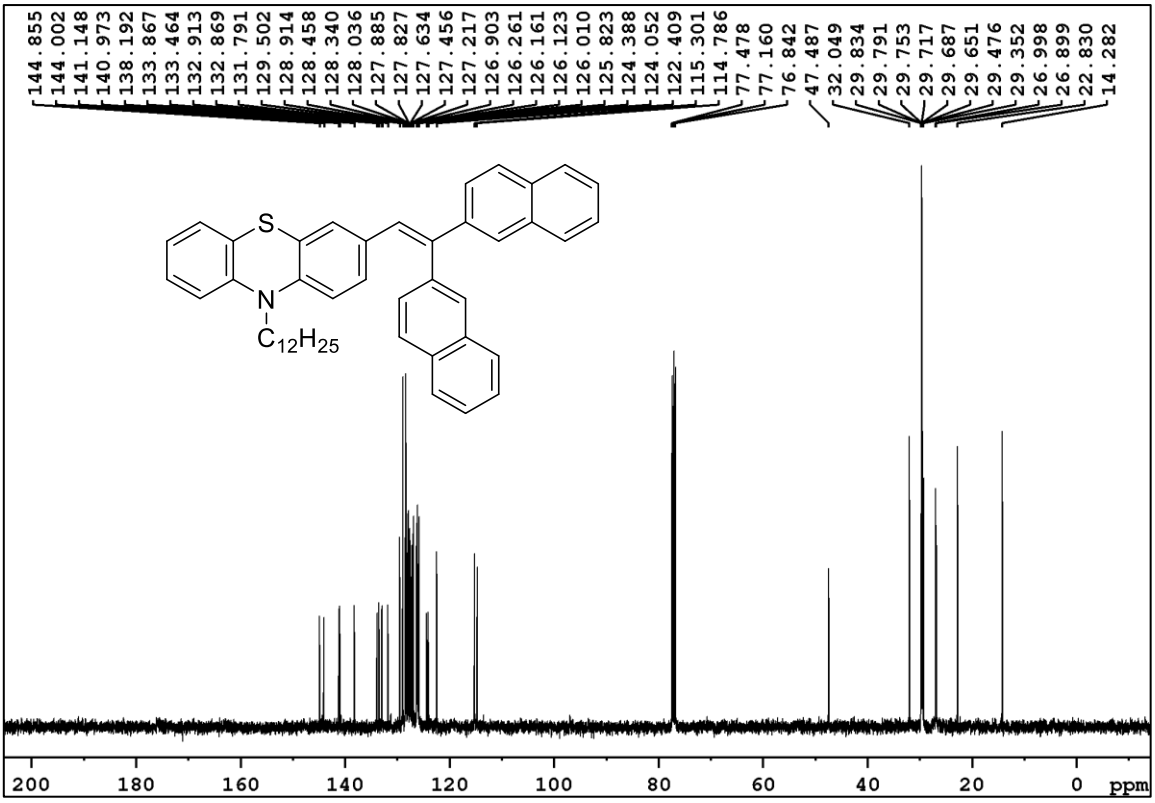

299

300 **Figure S26.** 400 MHz ^{1}H NMR spectrum of **2b** in $CDCl_3$.

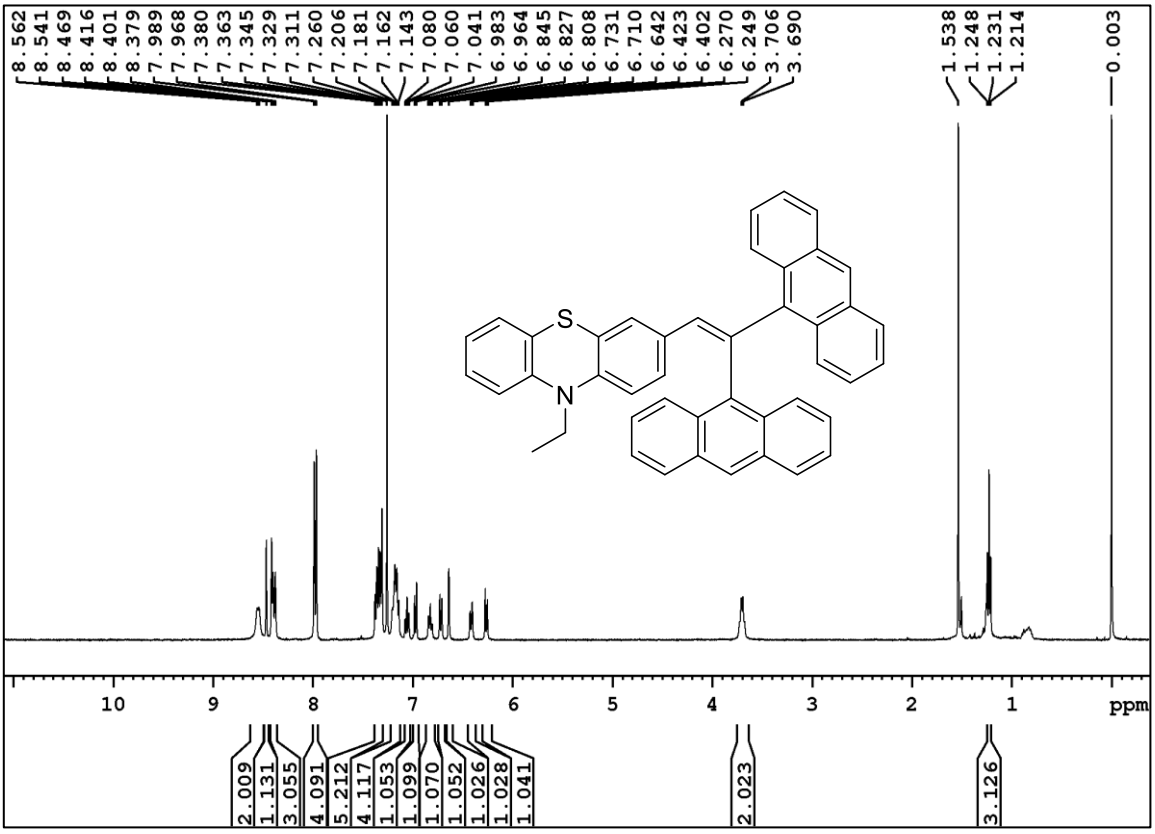

301

302 **Figure S27.** 400 MHz ^{1}H NMR spectrum of **3** in $CDCl_3$.

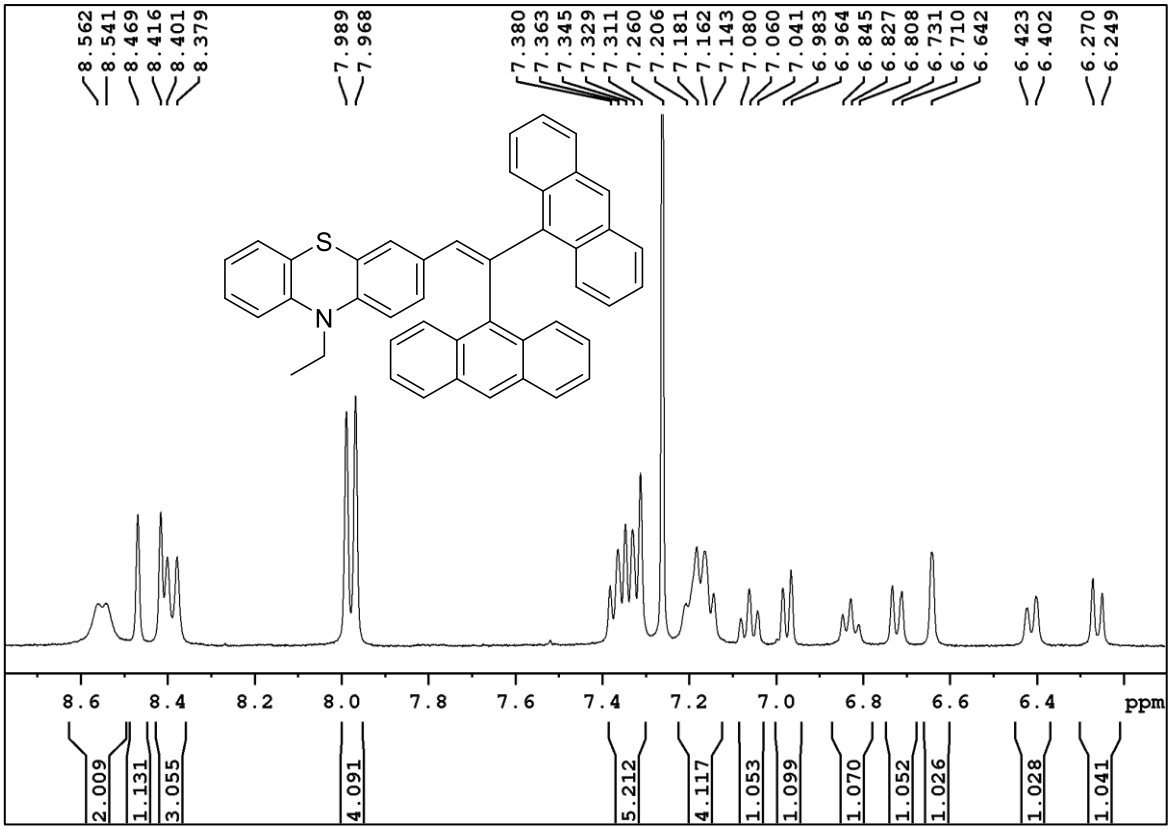

303

304 **Figure S28.** 400 MHz ^{1}H NMR (expanded) spectrum of **3** in $CDCl_3$.

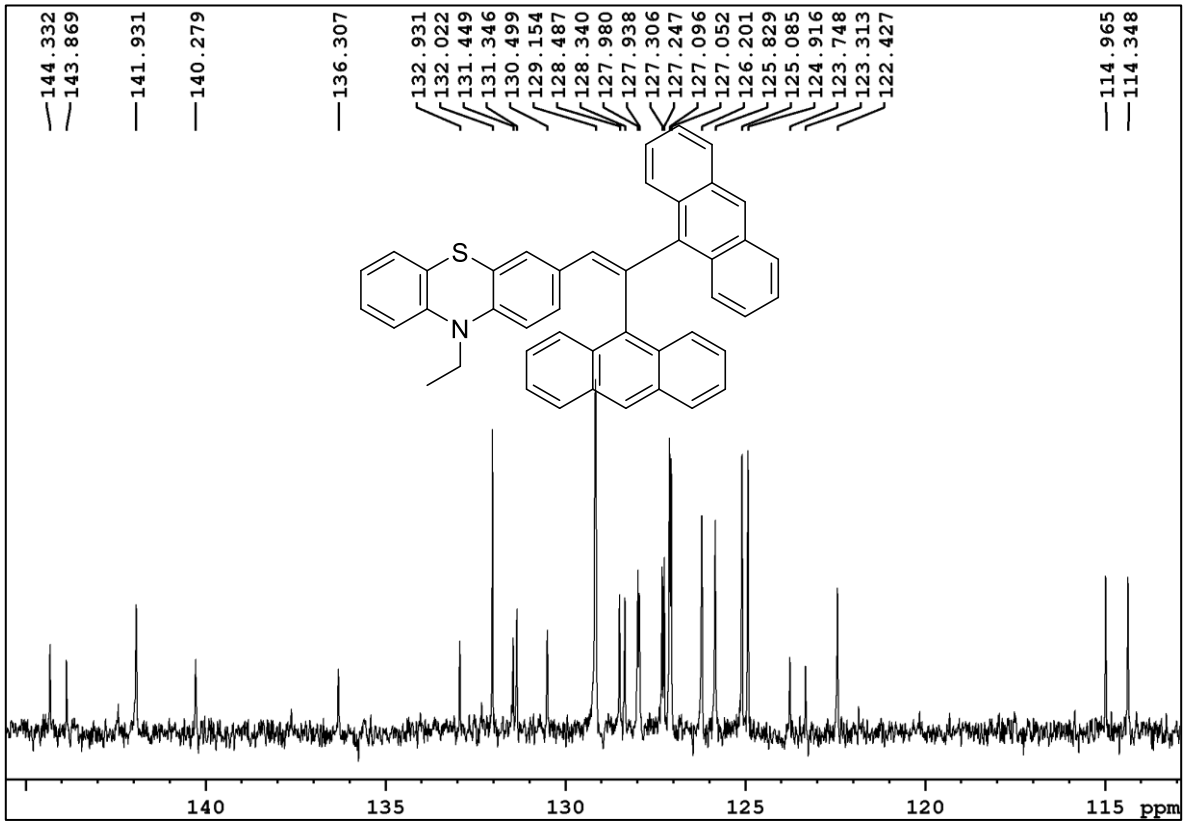

305

306 **Figure S29.** 100 MHz ^{13}C NMR (expanded) spectrum of **3** in $CDCl_3$

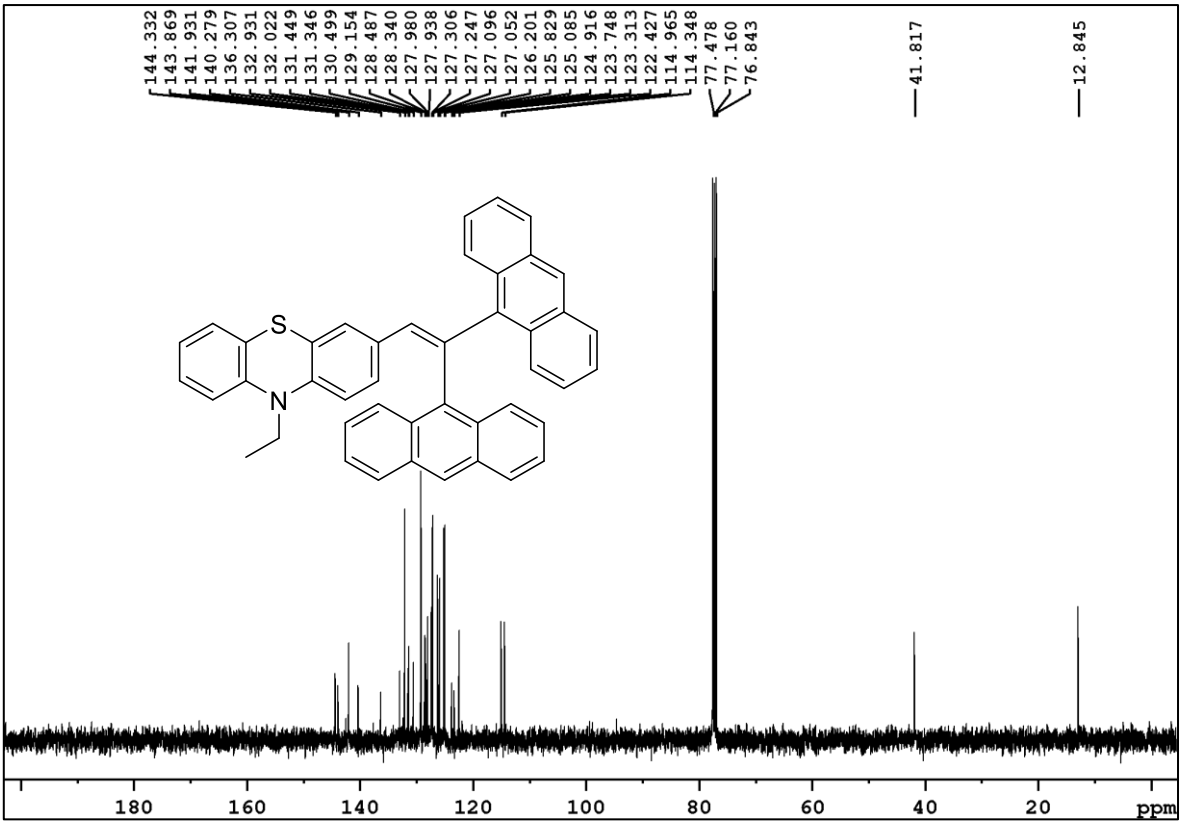

307

308 **Figure S30.** 100 MHz ^{13}C NMR spectrum of **3** in $CDCl_3$.

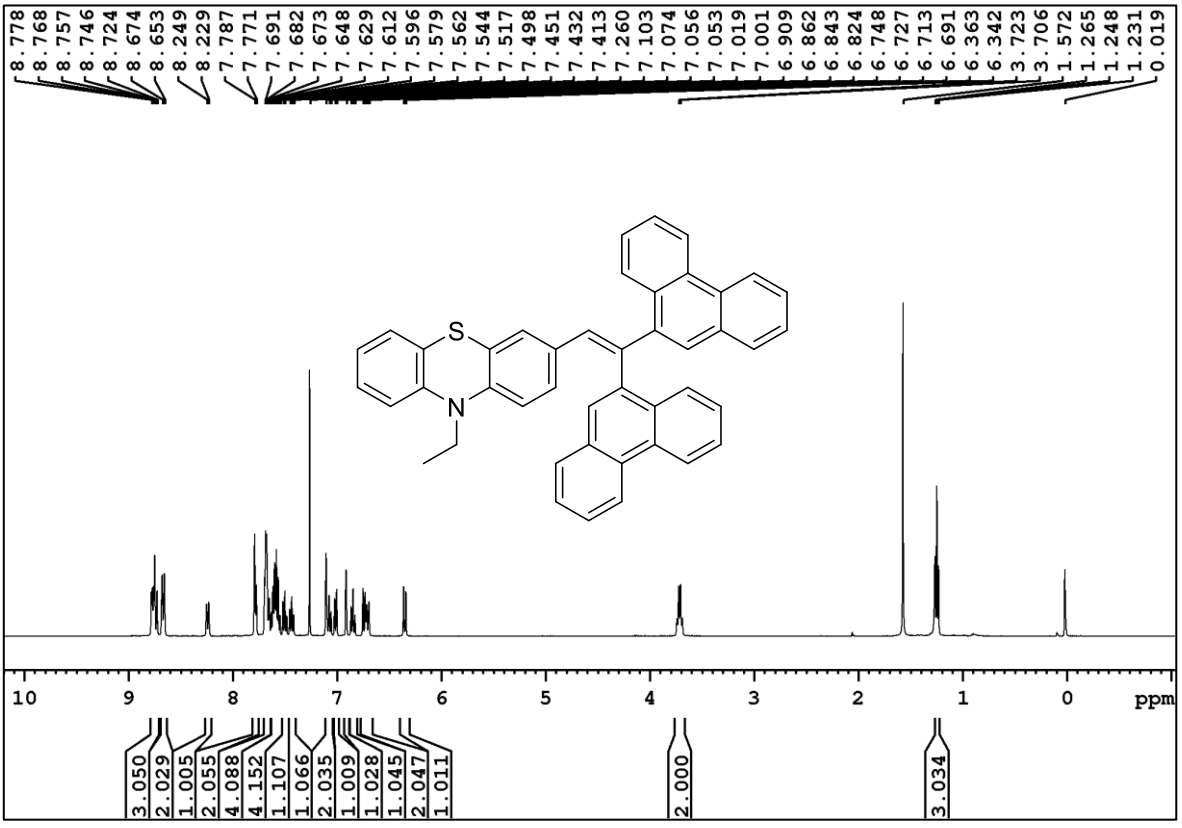

309

310 **Figure S31.** 400 MHz ^{1}H NMR spectrum of **4** in $CDCl_3$.

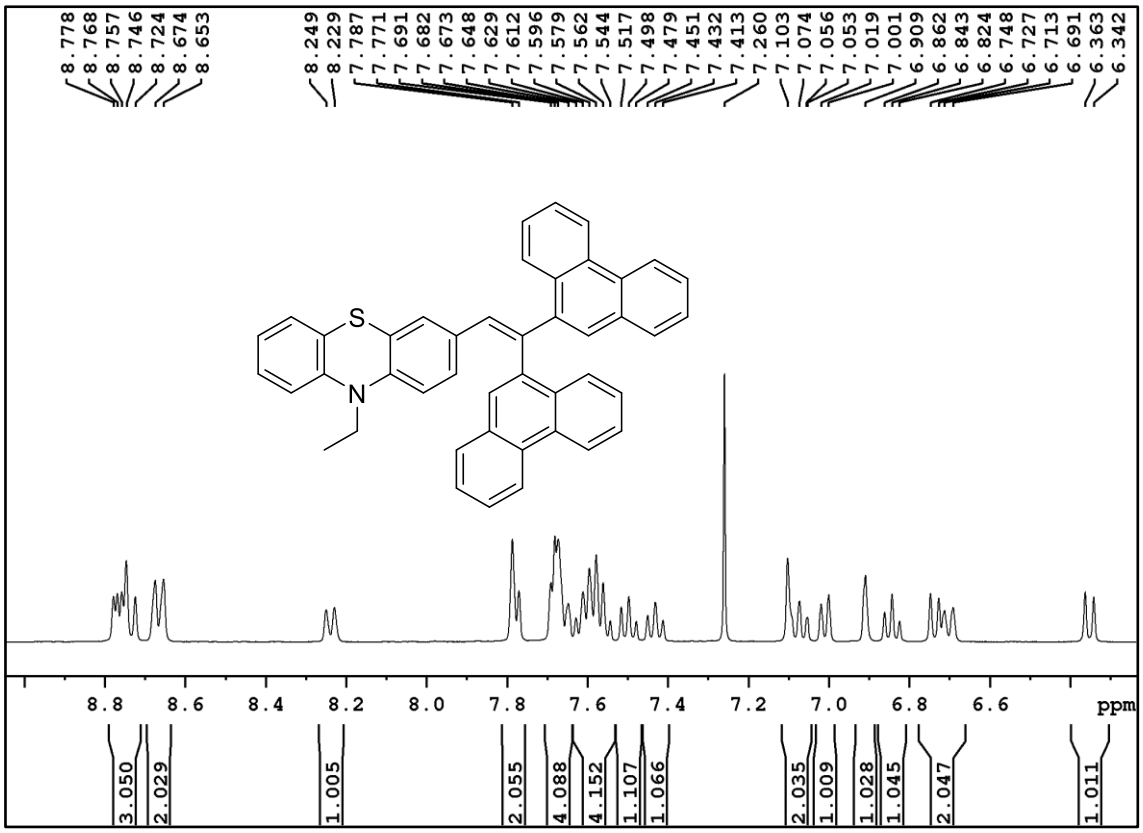

311

312 **Figure S32.** 400 MHz ^{1}H NMR (expanded) spectrum of **4** in $CDCl_3$.

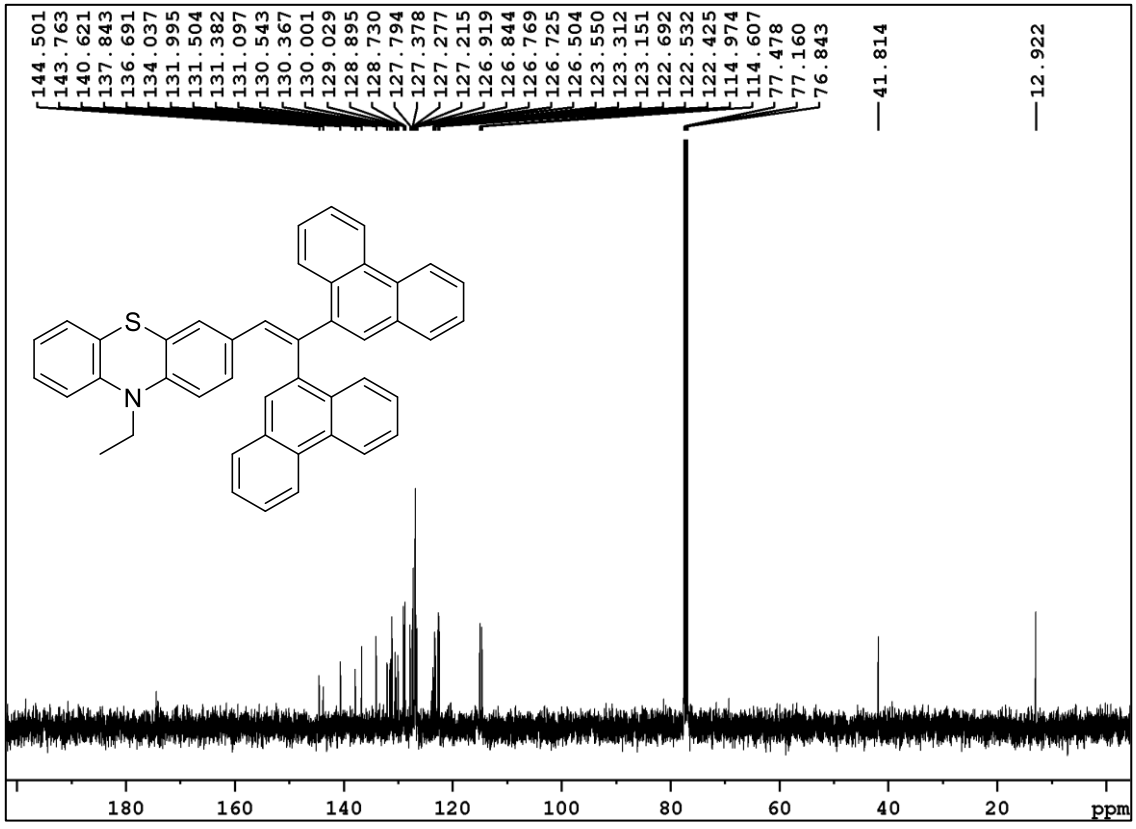

313

314 **Figure S33.** 100 MHz ^{13}C NMR spectrum of **4** in $CDCl_3$.

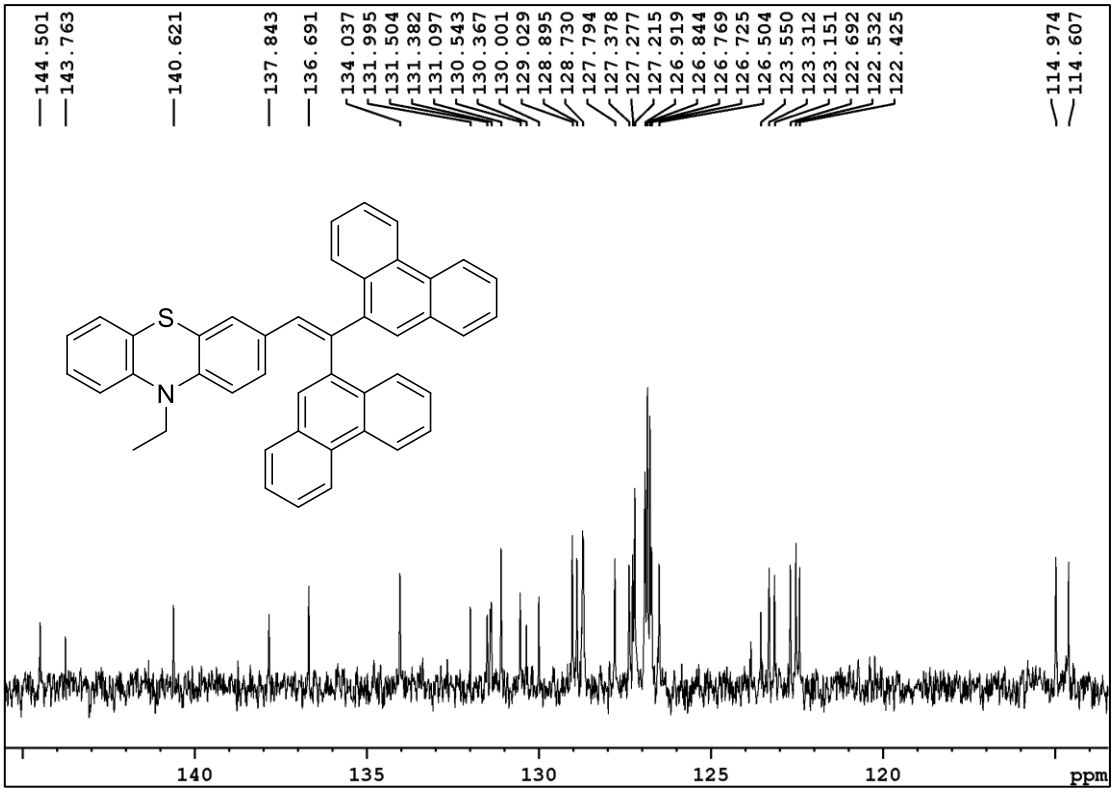

315

316 **Figure S34.** 100 MHz ^{13}C NMR (expanded) spectrum of **4** in $CDCl_3$.

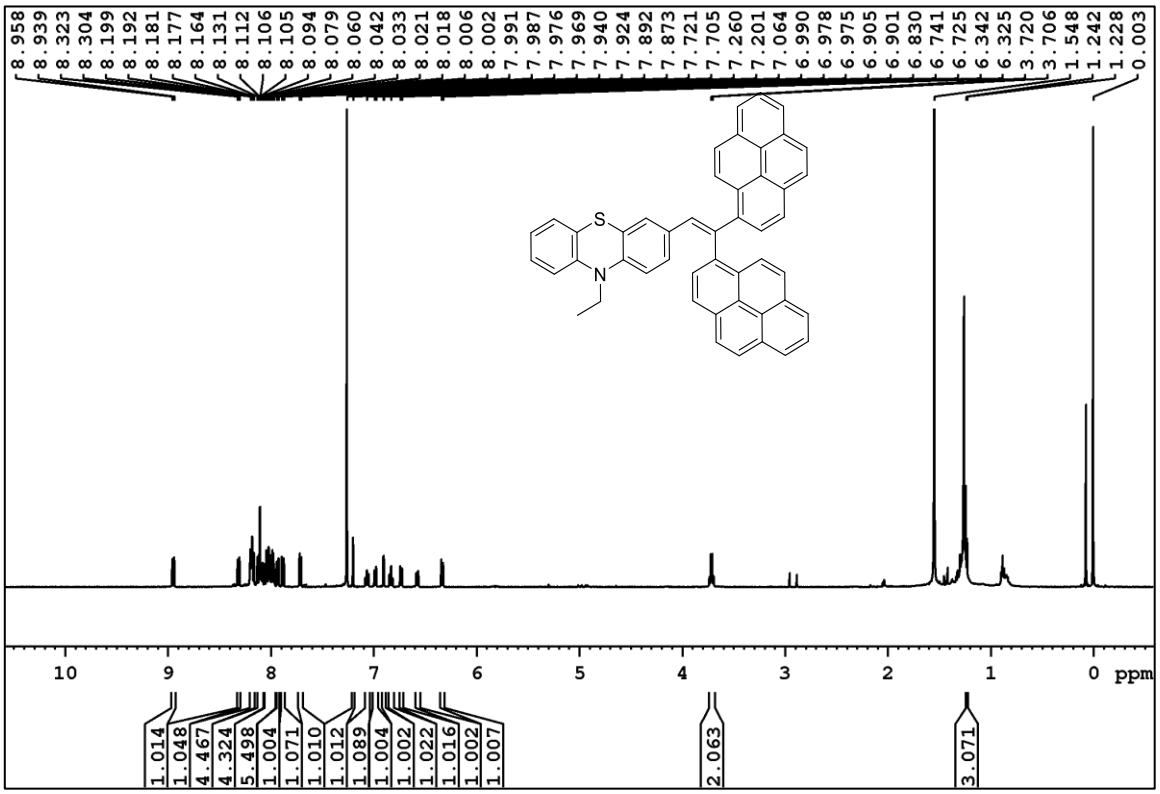

317

318 **Figure S35.** 100 MHz ^{1}H NMR spectrum of **5** in $CDCl_3$.

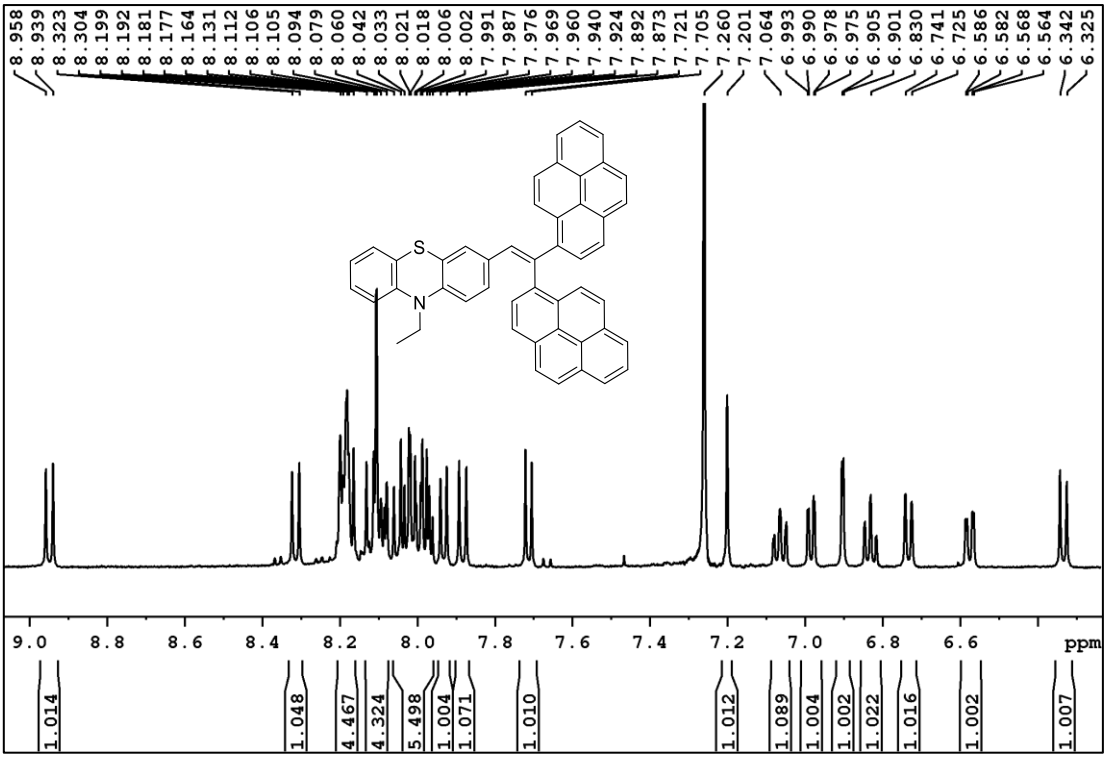

Figure S36. 100 MHz 1H NMR (expanded) spectrum of **5** in $CDCl_3$.

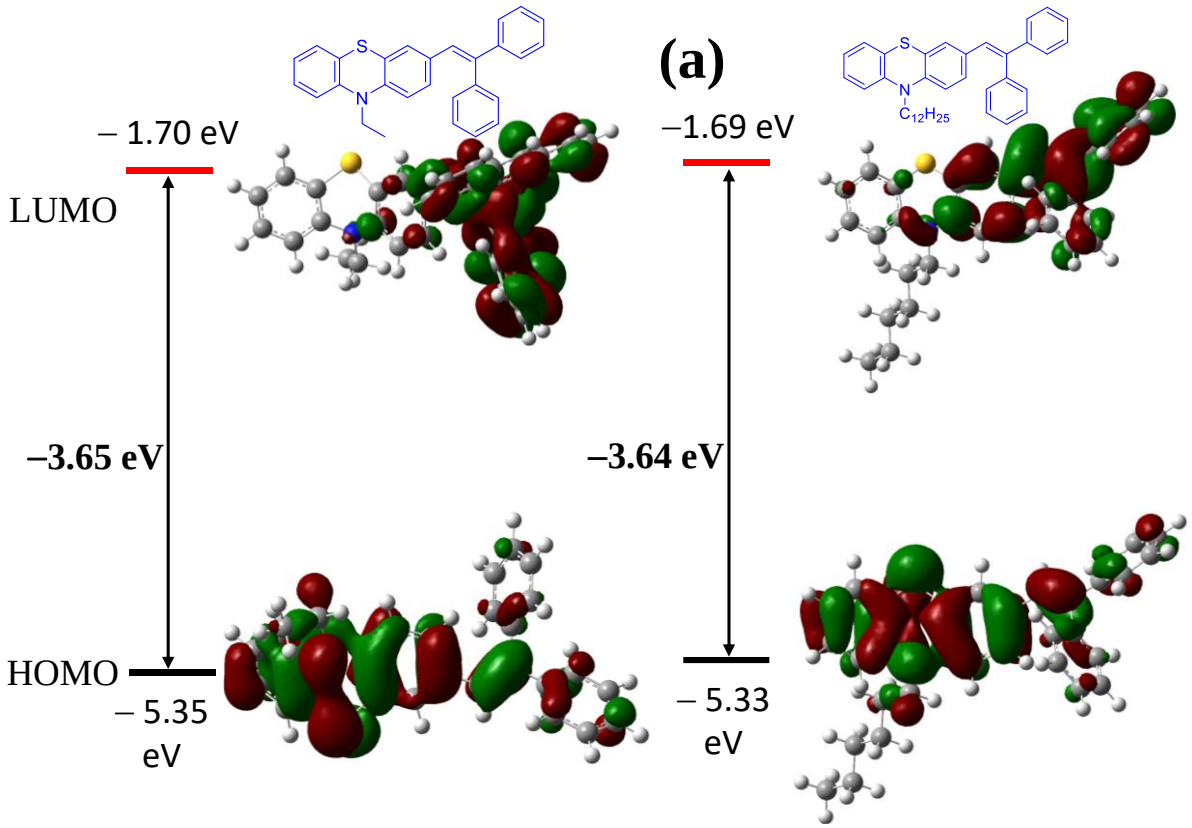

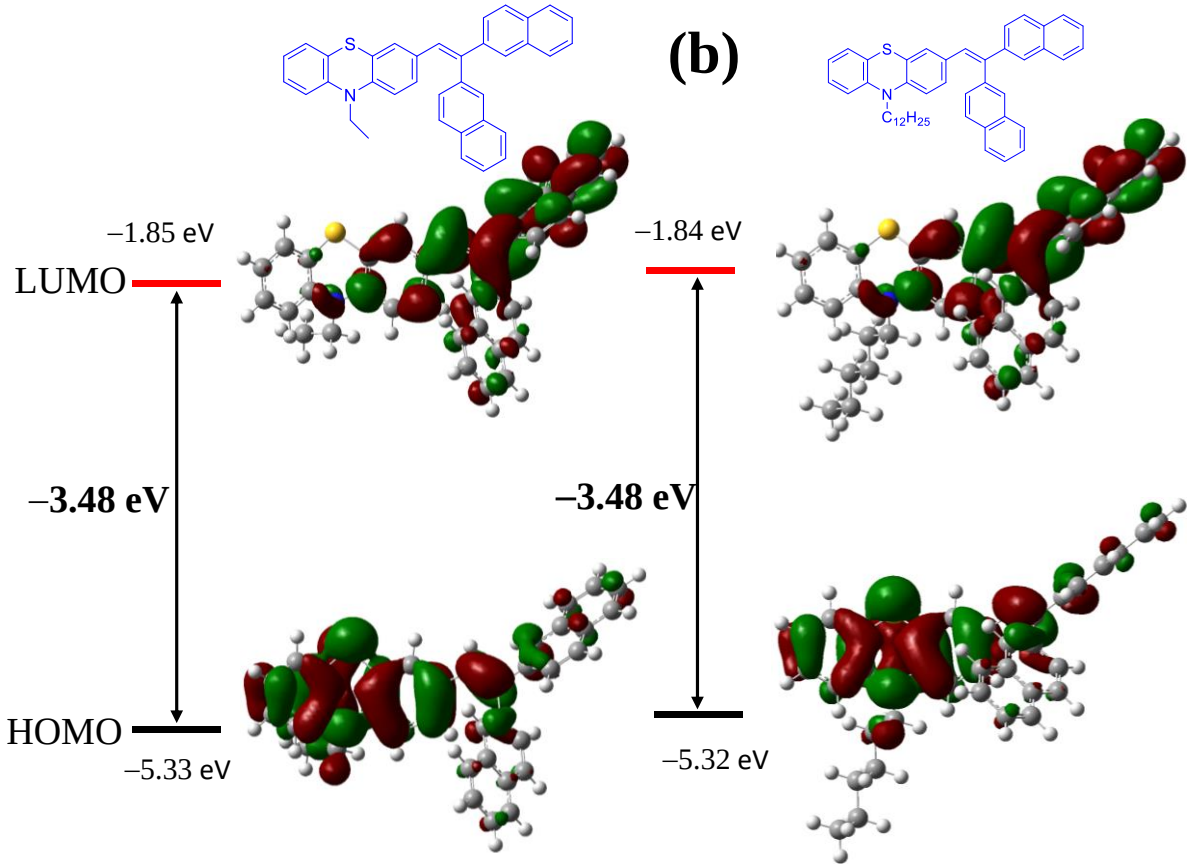

323

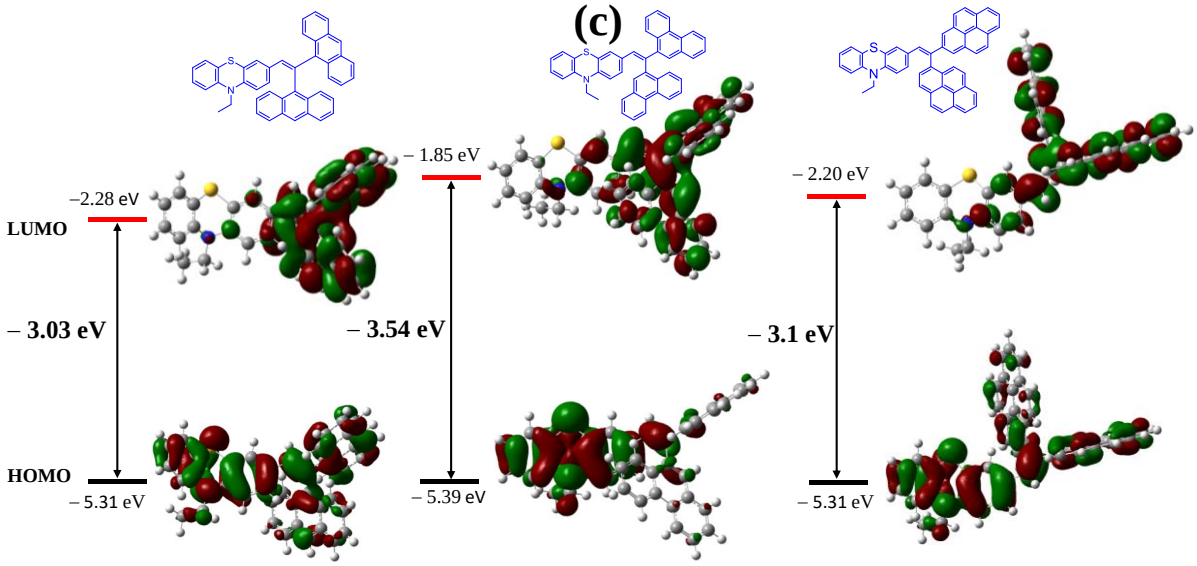

324

325 **Figure S37.** (a) (PT-C2-(Ph)$_2$ and PT-C12-(Ph)$_2$), (b) (PT-C2-(Nap)$_2$ and PT-C12-(Nap)$_2$), (c) (PT-C2-(An)$_2$, PT-C2-(Pn)$_2$) and PT-C2-(Pr)$_2$ obtained by the ground state
326 optimization via b3lyp/6-311+g (d, p) level of theory.

Table S1. Properties obtained from ground state and excited state optimization of PT derivatives

Compound	[a]HOMO (eV)	[b]LUMO (eV)	ΔE (eV)	[c]ϕ (°)	[d]Dev	[e]θ(°)	μ_g (D)	μ_e (D)
PT-C2-$(Ph)_2$	−5.35	−1.70	−3.65	175, −8	5,8	117	3.46	3.80
PT-C12-$(Ph)_2$	−5.33	−1.69	−3.64	175, −8	5,8	117	3.55	3.92
PT-C2-$(Nap)_2$	−5.33	−1.85	−3.48	174, −8	6,8	116	3.54	3.97
PT-C12-$(Nap)_2$	−5.32	−1.84	−3.48	174, −8	6,8	116	3.63	4.08
PT-C2-$(An)_2$	−5.31	−2.28	−3.03	−172, 8	8,8	120	3.55	4.24
PT-C2-$(Pn)_2$	−5.38	−1.85	−3.53	169, −4	11,4	117	3.60	4.0
PT-C2-$(Pr)_2$	−5.31	−2.21	−3.10	172, 9	8,9	120	3.13	3.93

Where a, b represents theoretically obtained HOMO and LUMO of the compounds in their ground state; c represents the dihedral angle connecting the phenyl ring of PT unit and the phenyl ring of the Ar unit; d represents the deviation from linearity, and e represents the angle between the two Ar units. Also, μ_g and μ_e represent the ground and excited state dipole moment of the molecule.

Determination of Fluorescence quantum yields

The fluorescence quantum yield (QY) measurements of the as-synthesized PT derivatives were accomplished utilizing freshly distilled nitrogen purged dichloromethane (CH_2Cl_2) solutions. The concentrations of PT derivatives in dichloromethane solutions were prepared in such a manner that their maximum absorbance at λ = 372 nm was ca. 0.05 to 0.1. The emission spectrum of the solutions was recorded in the right-angle mode (387-800 nm). Coumarin152 in cyclohexane (Φ_f = 0.97) was taken as the reference for the QY calculation. Both the PT- derivatives and the Coumarin152 were excited at 372 nm, keeping both the excitation and emission slit widths at 1nm. Three independent determinations were recorded, and the average of the corresponding QY values was reported. The QY for the as-synthesized compounds were calculated using the following formula:

$$\Phi_f = \Phi_s \times (A_s/A_f) \times (I_f/I_s) \times (\eta_f/\eta_s)^2 \quad \text{..... (1)}$$

where the subscripts "s" and "f" refer to standard and PT derivatives, A_s and A_f refer to the absorbances of the standard and test compounds under considerations at the excitation wavelength 372 nm, I_f and I_s refer to the integrated emission intensities (i.e., areas under the emission curves) of the test sample and the standard, and η_f and η_s to the refractive indexes of the corresponding solutions (pure solvents are assumed).

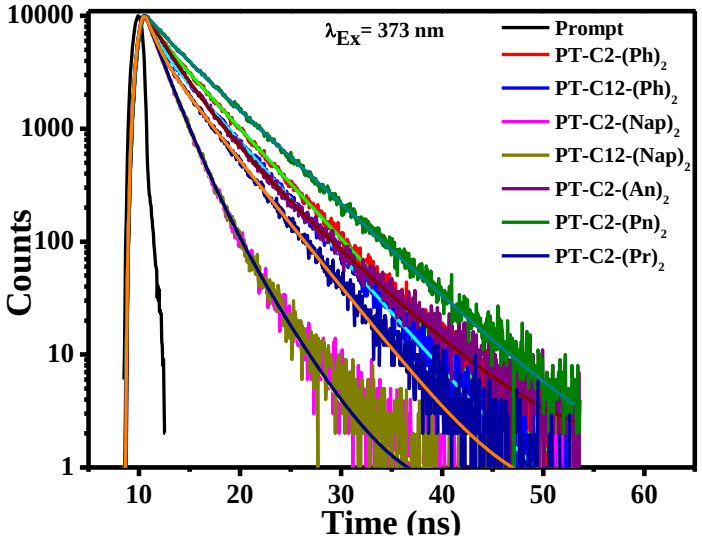

Figure S38. Time resolved fluorescence decay of (a) PT-C2-$(Ph)_2$, (b) PT-C12-$(Ph)_2$, (c) PT-C2-$(Nap)_2$, (d) PT-C12-$(Nap)_2$, (e) PT-C2-$(An)_2$, (f) PT-C2-$(Pn)_2$ and (g) PT-C2-$(Pr)_2$ (luminogen conc. ca.10 μM) in DCM (λ_{Ex}= 373 nm).

352 **Table S2.** Time-resolved fluorescence decay parameters of PT derivatives in DCM (λ_{Ex} = 370 nm, luminogen concentration ca. 10 μM).

Compounds, Em (nm)	α_1	α_2	τ_1 (ns)	τ_2 (ns)	τ_f (ns)	χ^2	φ_f	φ_{nr}	K_r	K_{nr}
PT-C2-$(Ph)_2$ (527)	0.099	0.901	0.993	4.460	4.377	1.167	0.410	0.590	0.094	0.135
PT-C2-$(Ph)_2$ (582)	0.087	0.914	1.990	4.640	4.537	1.155	0.410	0.590	0.090	0.130
PT-C12-$(Ph)_2$ (527)	0.169	0.830	0.865	4.290	4.155	1.075	0.430	0.570	0.103	0.137
PT-C12-$(Ph)_2$ (582)	0.066	0.934	1.070	4.420	4.363	1.200	0.430	0.570	0.099	0.131
PT-C2-$(Nap)_2$ (546)	0.719	0.281	1.530	2.960	2.145	1.120	0.150	0.850	0.070	0.396
PT-C2-$(Nap)_2$ (582)	0.724	0.276	1.610	2.960	2.166	0.999	0.150	0.850	0.069	0.392
PT-C12-$(Nap)_2$ (544)	0.803	0.197	1.680	3.220	2.172	1.020	0.140	0.860	0.064	0.396
PT-C12-$(Nap)_2$ (587)	0.717	0.283	1.660	2.840	2.135	1.190	0.140	0.860	0.066	0.403
PT-C2-$(An)_2$ (548)	0.589	0.411	2.560	5.420	4.264	1.180	0.070	0.930	0.016	0.218
PT-C2-$(An)_2$ (600)	0.530	0.470	2.560	4.790	3.952	0.991	0.070	0.930	0.018	0.235
PT-C2-$(Pn)_2$ (533)	0.098	0.902	2.080	5.280	5.149	1.230	0.440	0.560	0.085	0.109
PT-C2-$(Pn)_2$ (580)	0.199	0.801	3.240	5.710	5.405	1.128	0.440	0.560	0.081	0.104
PT-C2-$(Pr)_2$ (548)	0.249	0.751	1.010	3.880	3.652	1.023	0.170	0.830	0.047	0.227
PT-C2-$(Pr)_2$ (594)	0.144	0.856	1.650	3.960	3.808	1.075	0.170	0.830	0.045	0.218

353

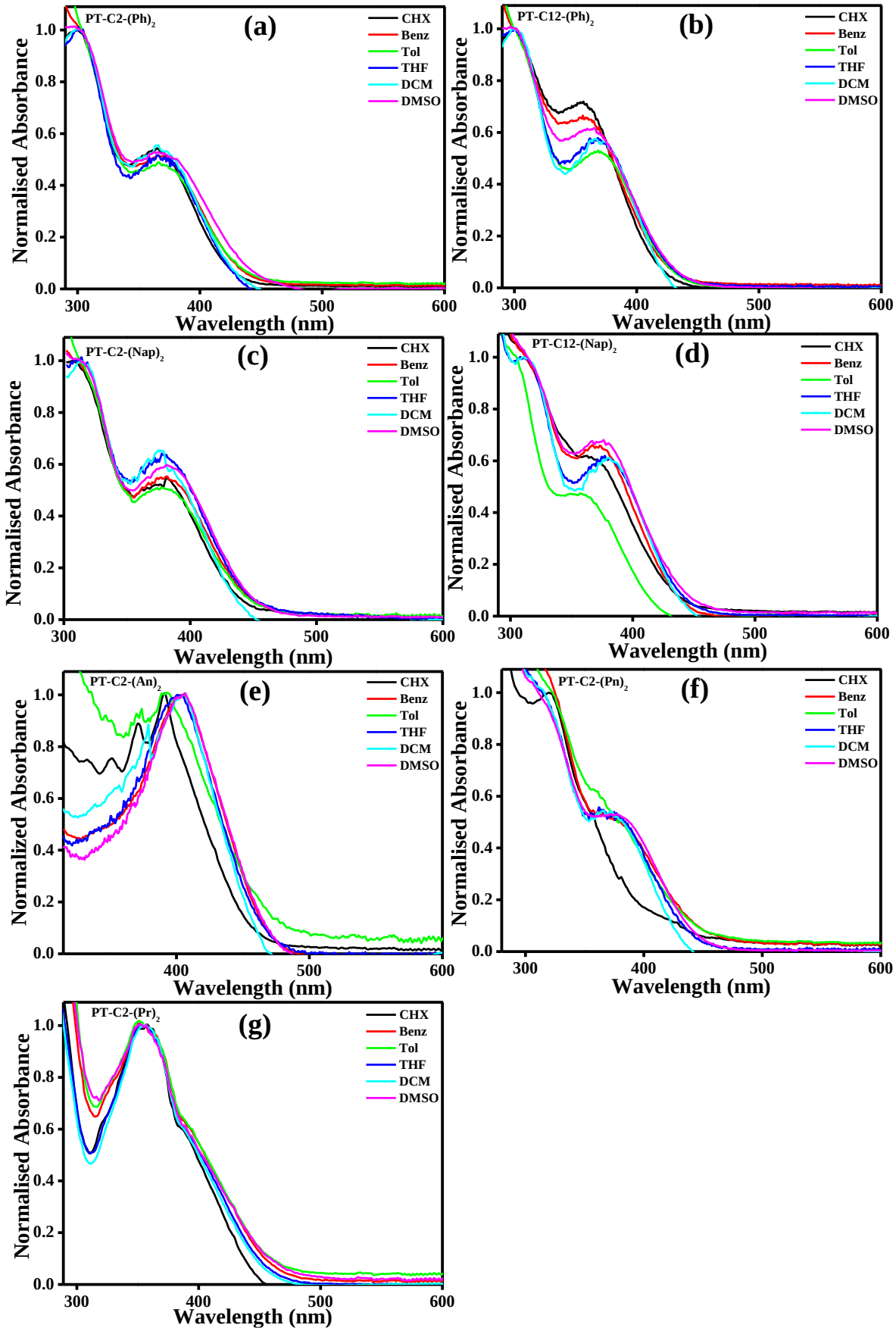

Figure S39. Absorption spectra of (a) PT-C2-(Ph)$_2$, (b) PT-C12-(Ph)$_2$, (c) PT-C2-(Nap)$_2$, (d) PT-C12-(Nap)$_2$, (e) PT-C2-(An)$_2$ and (f) PT-C2-(Pn)$_2$ and (g) PT-C2-(Pr)$_2$ in solvents (Cyclohexane (CHX), Benzene (Benz), Toluene (Tol), DCM, THF, and DMSO) of varying polarity.

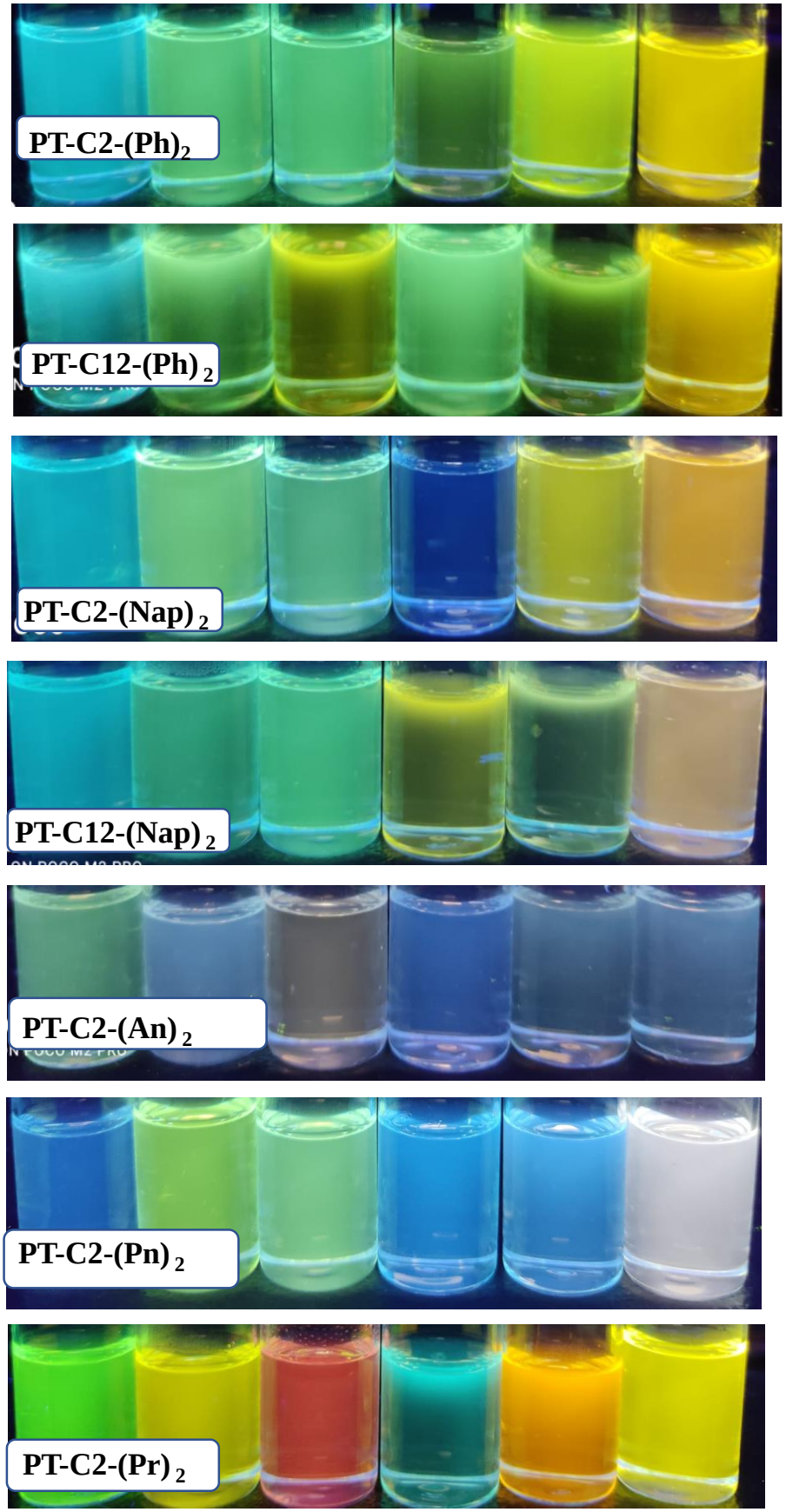

Figure S40. Photographs of PT-C2-$(Ph)_2$, PT-C12-$(Ph)_2$, PT-C2-$(Nap)_2$, PT-C12-$(Nap)_2$, PT-C2-$(An)_2$, PT-C2-$(Pn)_2$ and PT-C2-$(Pr)_2$ (top to bottom) (luminogen conc. ca.10 μM) in different solvents with increasing polarity taken under 365 nm UV illumination (Cyclohexane (CHX), Benzene (Benz), Toluene (Tol), DCM, THF and DMSO).

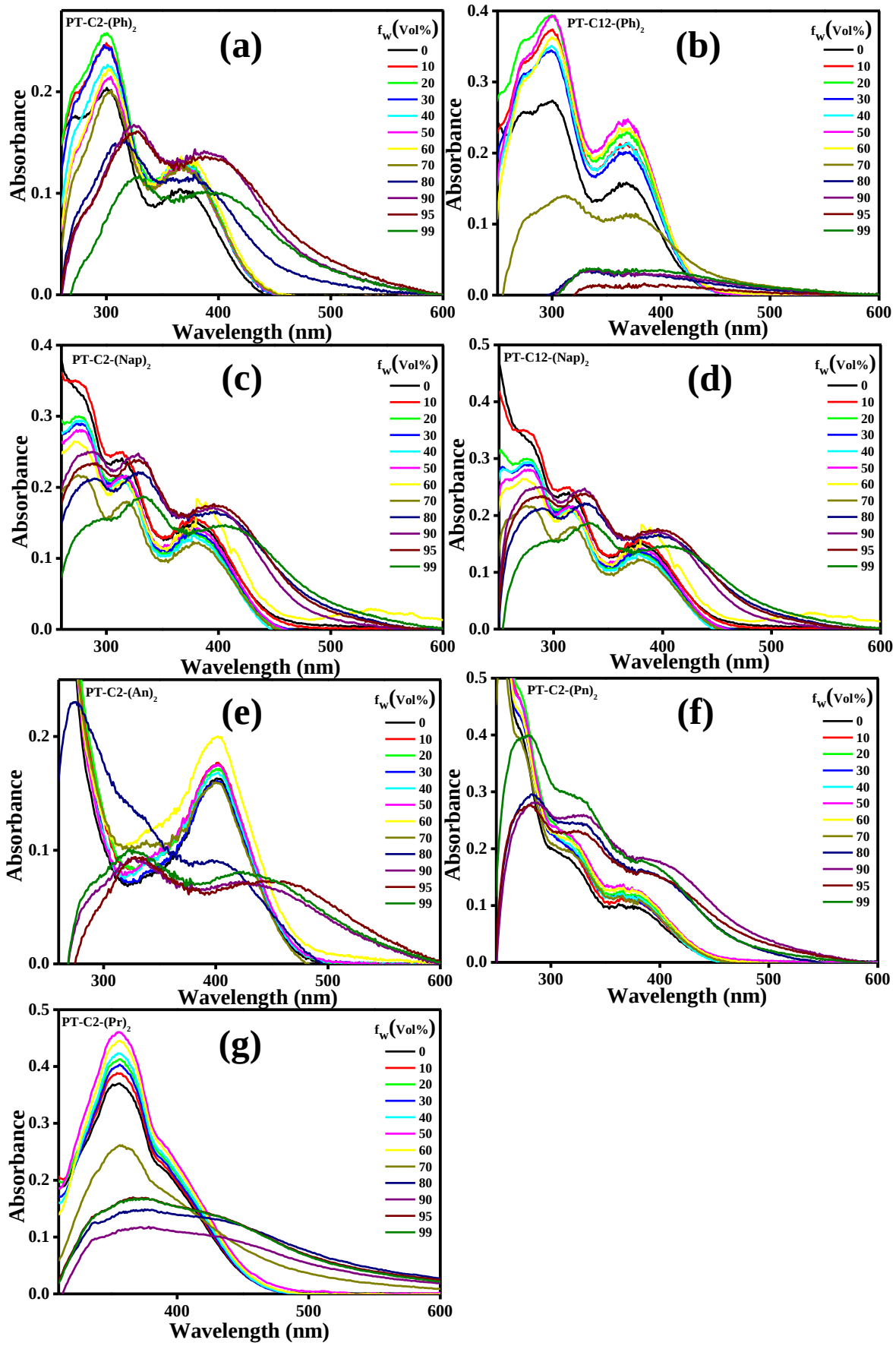

361

362 **Figure S41.** Absorption spectra of (a) PT-C2-(Ph)$_2$, (b) PT-C12-(Ph)$_2$, (c) PT-C2-(Nap)$_2$, (d) PT-C12-(Nap)$_2$, (e) PT-C2-(An)$_2$, (f) PT-C2-(Pn)$_2$ and (g) PT-C2-
363 (Pr)$_2$ in THF–water mixtures with different water fractions (fw (%)) (luminogen conc. 10 μM).

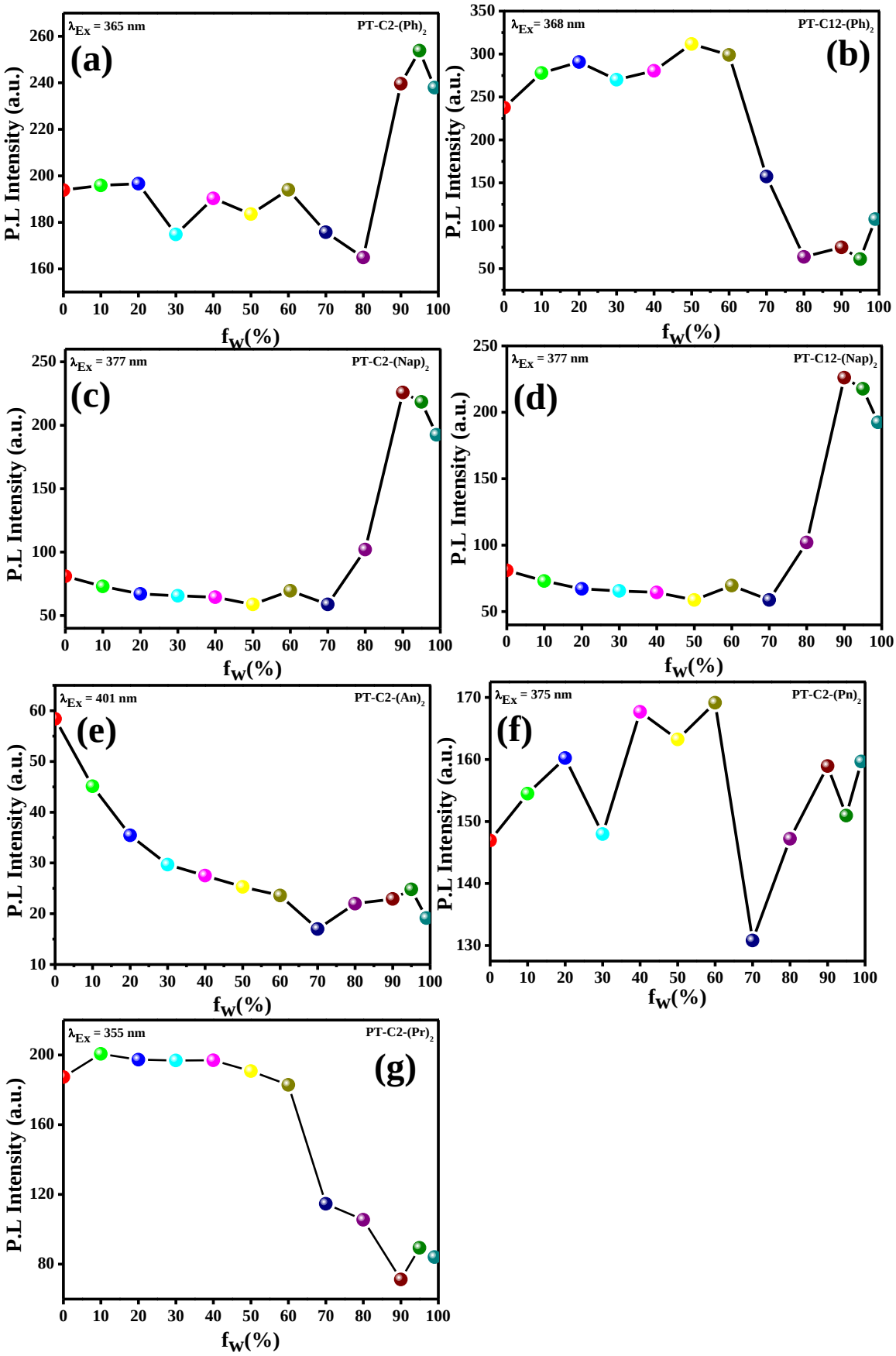

Figure S42. P.L intensity (Imax) vs. water fraction (fw) % [intensity calculated at Imax (Imax with the highest intensity considered for the calculation)] of (a) PT-C2-$(Ph)_2$, (b) PT-C12-$(Ph)_2$, (c) PT-C2-$(Nap)_2$, (d) PT-C12-$(Nap)_2$, (e) PT-C2-$(An)_2$, (f) PT-C2-$(Pn)_2$ and (g) PT-C2-$(Pr)_2$ in THF–water mixtures with different water fractions (fw (%)) (luminogen conc. 10 μM).

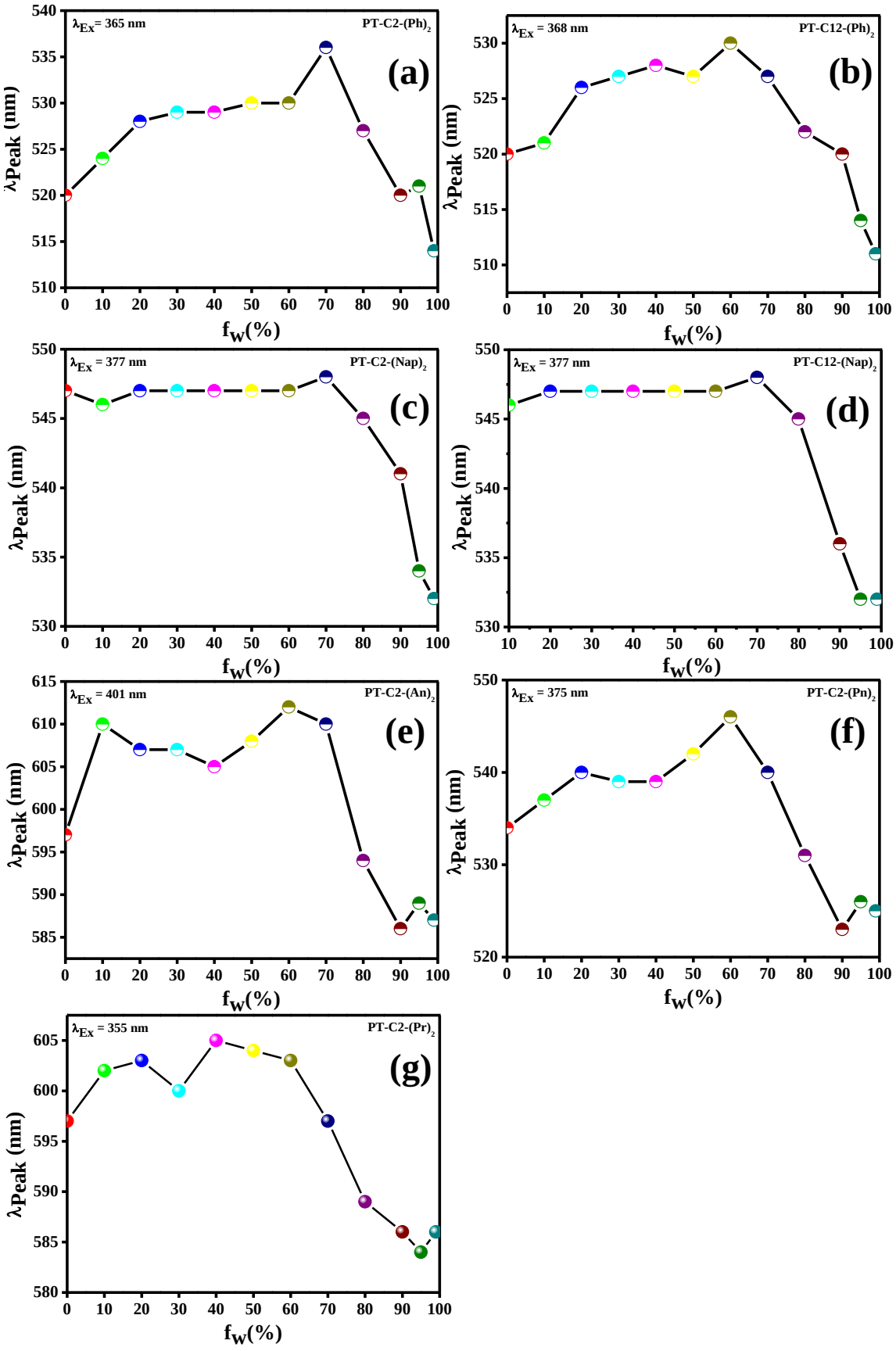

Figure S43. Emission wavelength (λPeak) vs. water fraction (fw) % [intensity calculated at λmax (λmax with the highest intensity considered for the calculation)] of (a) PT-C2-$(Ph)_2$, (b) PT-C12-$(Ph)_2$, (c) PT-C2-$(Nap)_2$, (d) PT-C12-$(Nap)_2$, (e) PT-C2-$(An)_2$ and (f) PT-C2-$(Pn)_2$ and (g) PT-C2-$(Pr)_2$ in THF–water mixtures with different water fractions (f_w (%)) (luminogen conc. 10 μM).

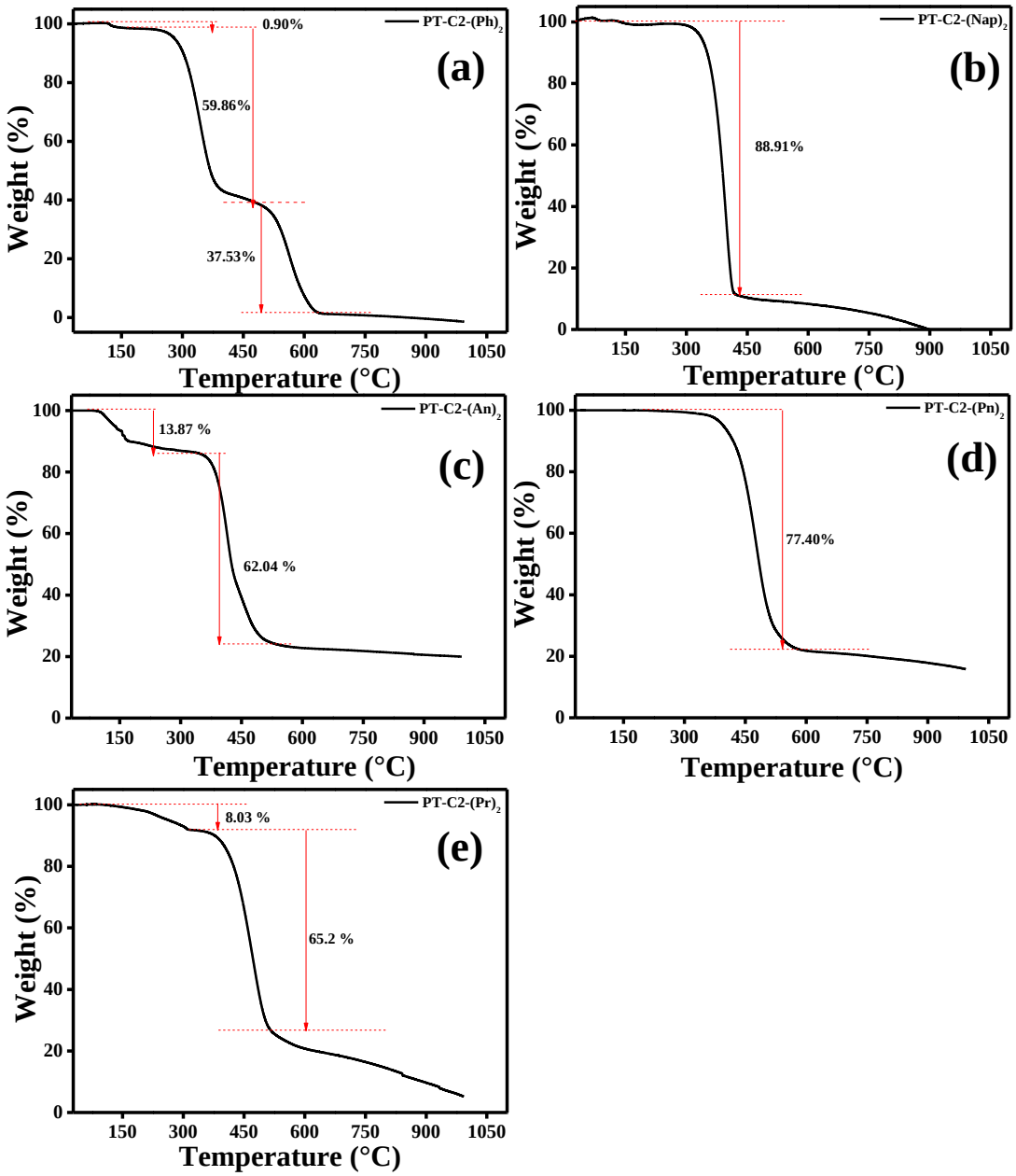

Figure S44. Thermal gravimetric analysis of the five PT-derivatives, and the T_d of (a) PT-C2-$(Ph)_2$, (b) PT-C2-$(Nap)_2$, (c)PT-C2-$(An)_2$, (d) PT-C2-$(Pn)_2$ and (e) PT-C2-$(Pr)_2$.

Extraction of HOMO values from the CV data

From the cyclic voltammograms given below, the HOMO values have been calculated by considering the onset oxidation potential of the ethynyldiaryl- & dodecyldiaryl-phenothiazine derivatives and the compounds with the ferrocene (FC) using the following equation (2). The tabulated values are documented in **Table S3.** The formula for the HOMO value calculation from the CV data using the Fc/Fc^+ as the internal standard is:

$$E_{HOMO}\ (eV) = -\left(E_{OX}^{onset} - E_{Fc/Fc^+}^{onset}\right) - 4.80\ eV \qquad \ldots\ldots\ldots\ldots\ldots\ldots\ldots\ (2)$$

The energy values were calculated by using ferrocene as the internal standard with the HOMO value –4.8 eV against vacuum level as zero. Here, E_{OX}^{onset} and $E_{Fc/Fc+}^{onset}$ are the onset oxidation potentials of the ethynyldiaryl- & dodecyldiaryl-phenothiazine derivatives and of the ferrocene against Ag/AgCl electrode. The obtained ferrocene onset value was found to be in good agreement with the literature value.

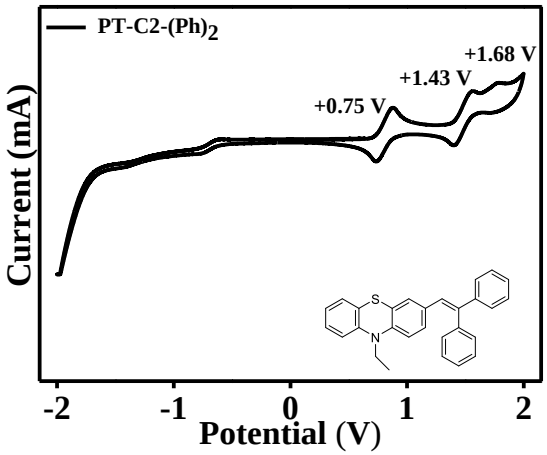

385

386 **Figure S45.** Cyclic voltammograms of PT-C2-$(Ph)_2$ in DCM.

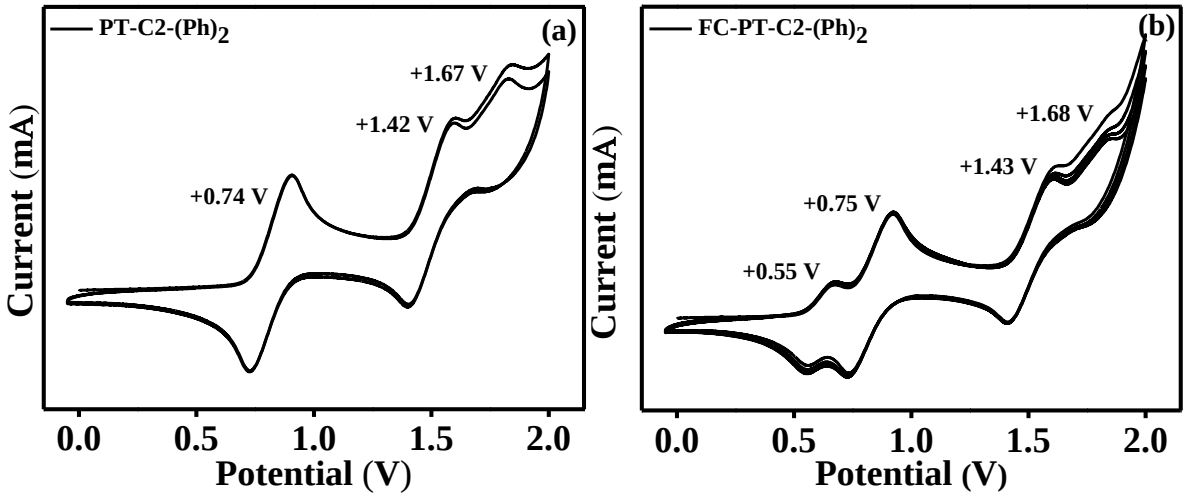

387

388 **Figure S46.** Cyclic voltammograms (100 mV/sec) of PT-C2-$(Ph)_2$ without Fc/Fc^+ (a) and with Fc/Fc^+ (b) in DCM.

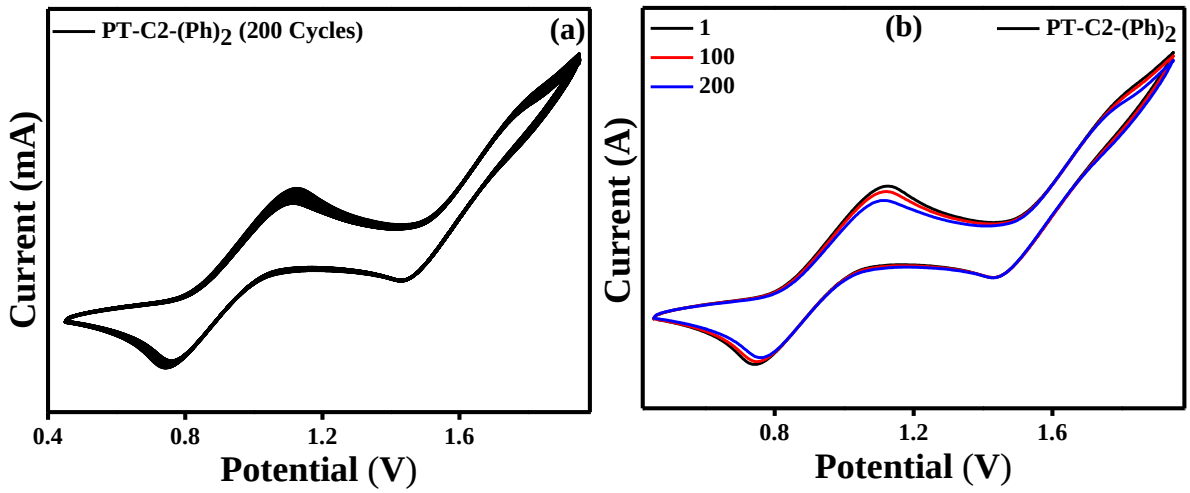

389

390 **Figure S47.** Cyclic voltammograms (200 mV/sec) of PT-C2-$(Ph)_2$ (200 cycles) (a) and (1st, 100th and 200th cycles) (b) in DCM.

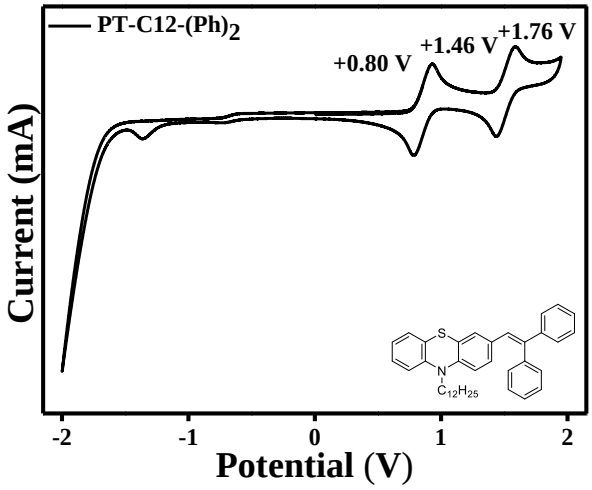

Figure S48. Cyclic voltammograms of PT-C12-$(Ph)_2$ in DCM.

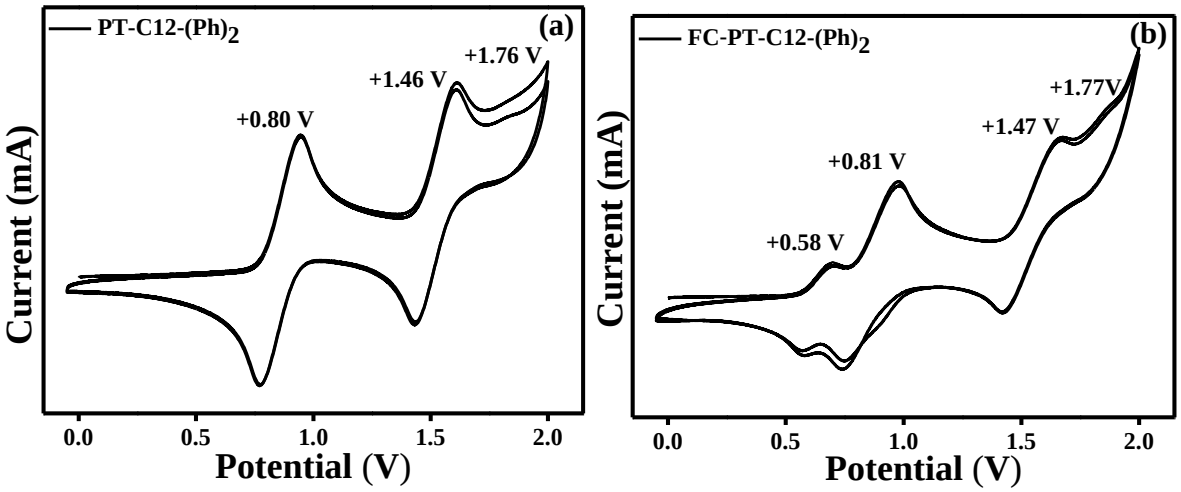

Figure S49. Cyclic voltammograms (100 mV/sec) of PT-C12-$(Ph)_2$ without Fc/Fc^+ (a) and with Fc/Fc^+ (b) in DCM.

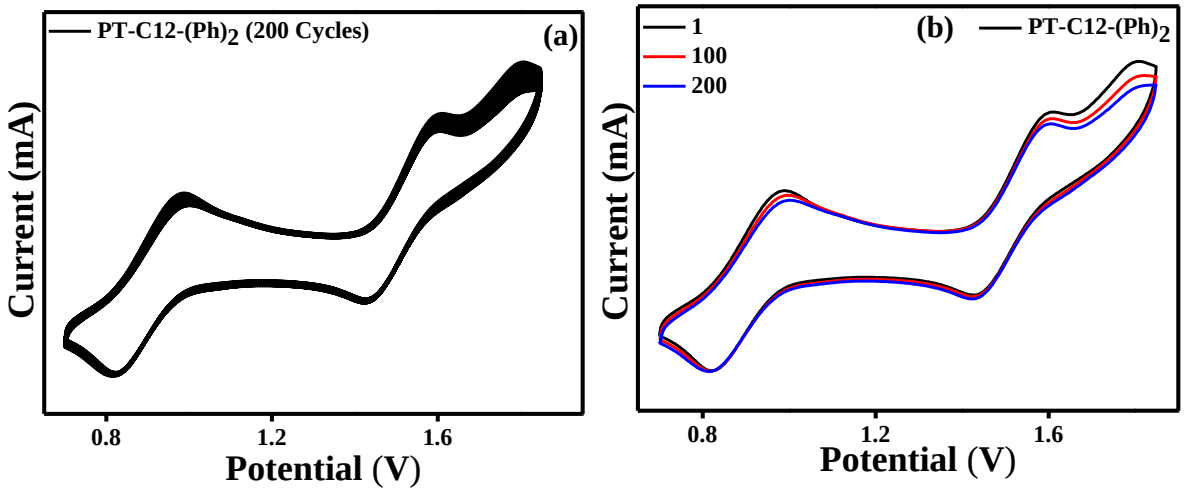

Figure S50. Cyclic voltammograms (200 mV/sec) of PT-C12-$(Ph)_2$ (200 cycles) (a) and (1st, 100th and 200th cycles) (b) in DCM.

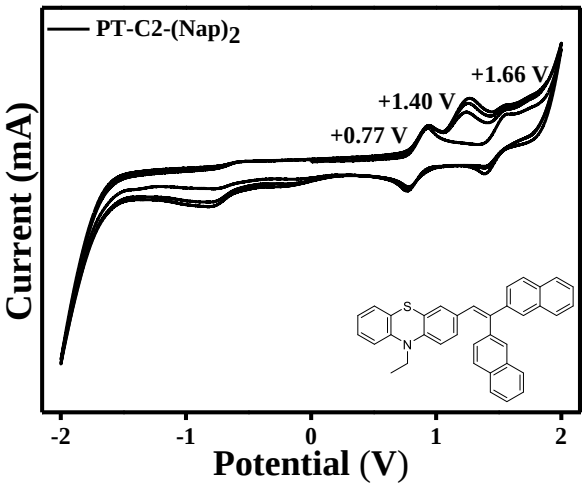

398

399 **Figure S51.** Cyclic voltammograms of PT-C2-$(Nap)_2$ in DCM.

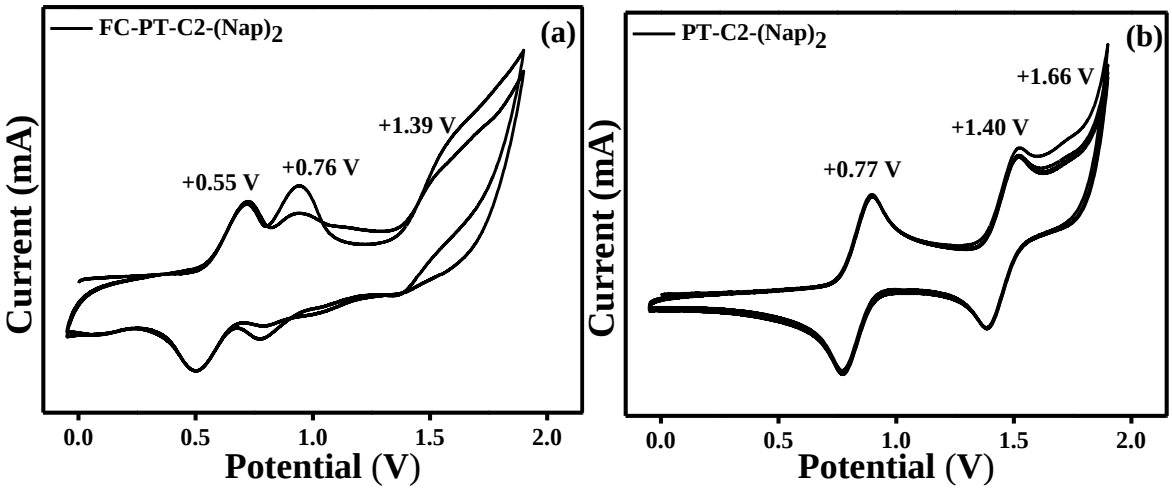

400

401 **Figure S52.** Cyclic voltammograms (100 mV/sec) of PT-C2-$(Nap)_2$ without Fc/Fc^+ (a) and with Fc/Fc^+ (b) in DCM.

402

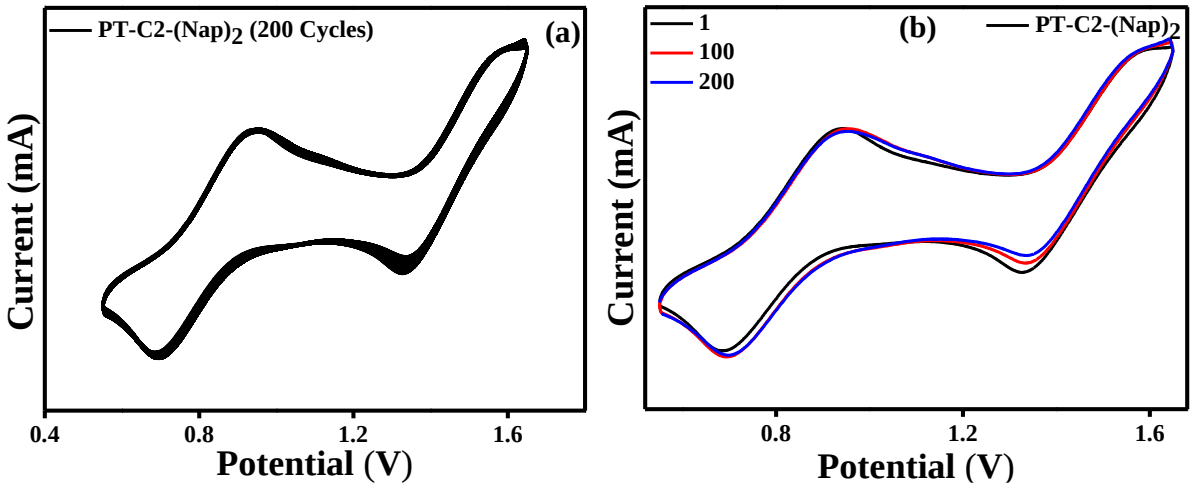

403

404 **Figure S53.** Cyclic voltammograms (200 mV/sec) of PT-C2-$(Nap)_2$ (200 cycles) (a) and (1st, 100th and 200th cycles) (b) in DCM.

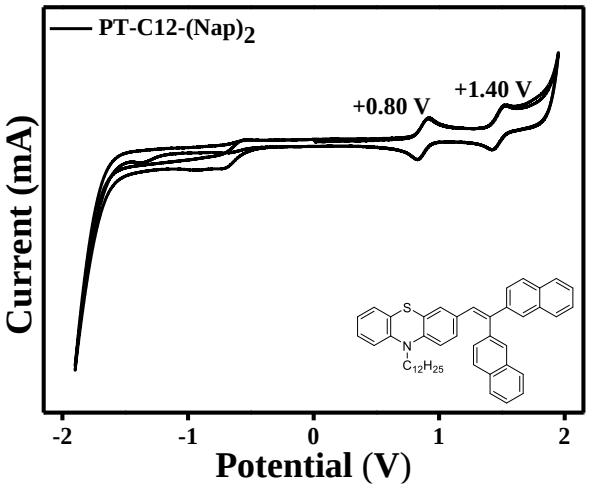

405

406 **Figure S54.** Cyclic voltammograms of PT-C12-$(Nap)_2$ in DCM.

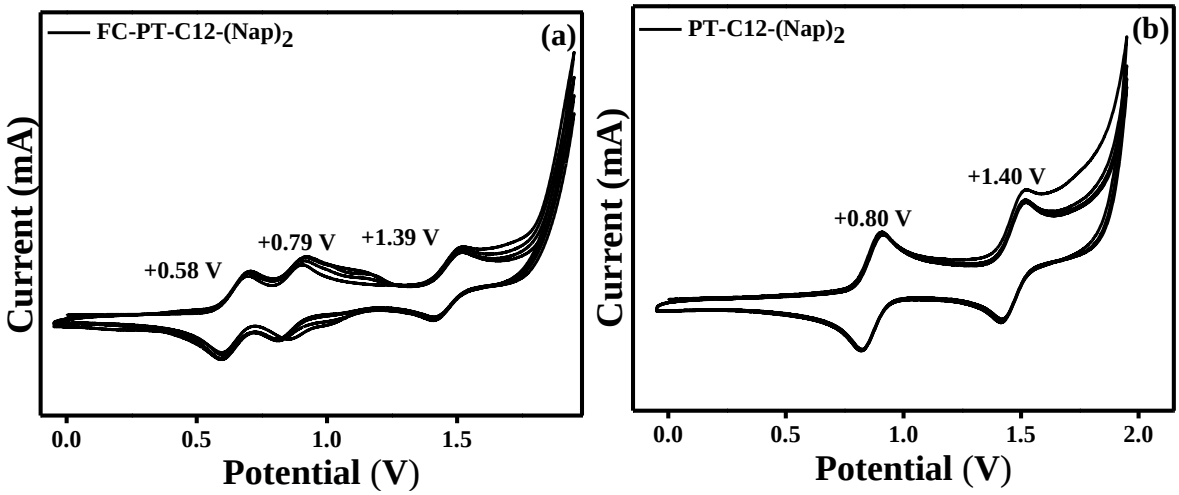

407

408 **Figure S55.** Cyclic voltammograms (100 mV/sec) of PT-C12-$(Nap)_2$ without Fc/Fc^+ (a) and with Fc/Fc^+ (b) in DCM.

409

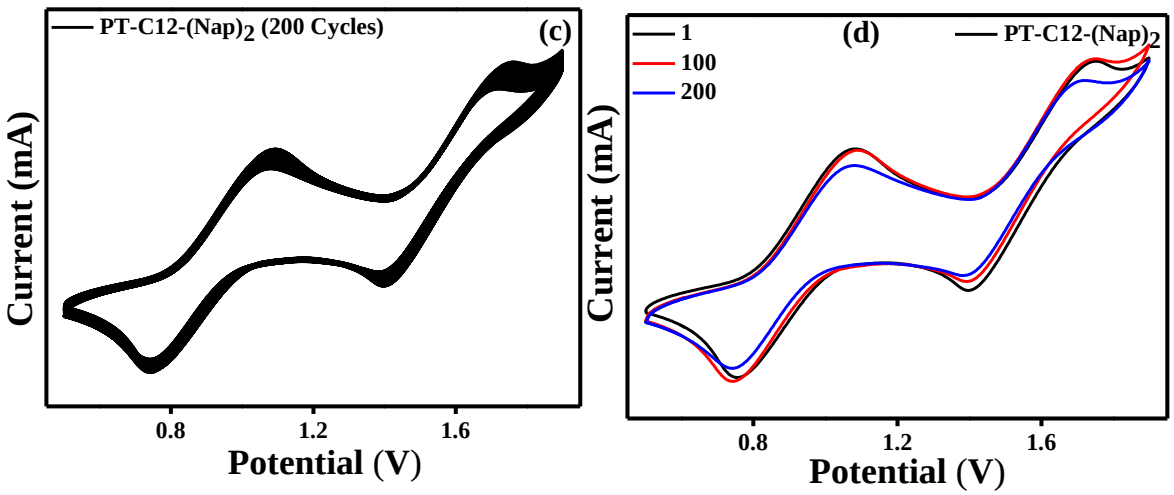

410

411 **Figure S56.** Cyclic voltammograms (200 mV/sec) of PT-C12-$(Nap)_2$ (200 cycles) (a) and (1st, 100th and 200th cycles) (b) in DCM.

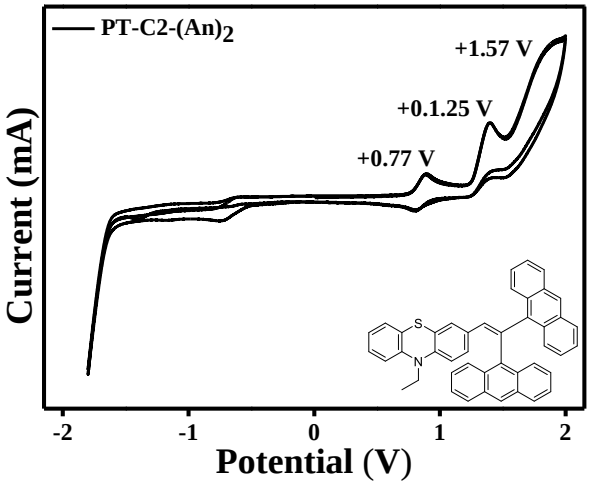

412

413 **Figure S57.** Cyclic voltammograms of PT-C2-$(An)_2$ in DCM.

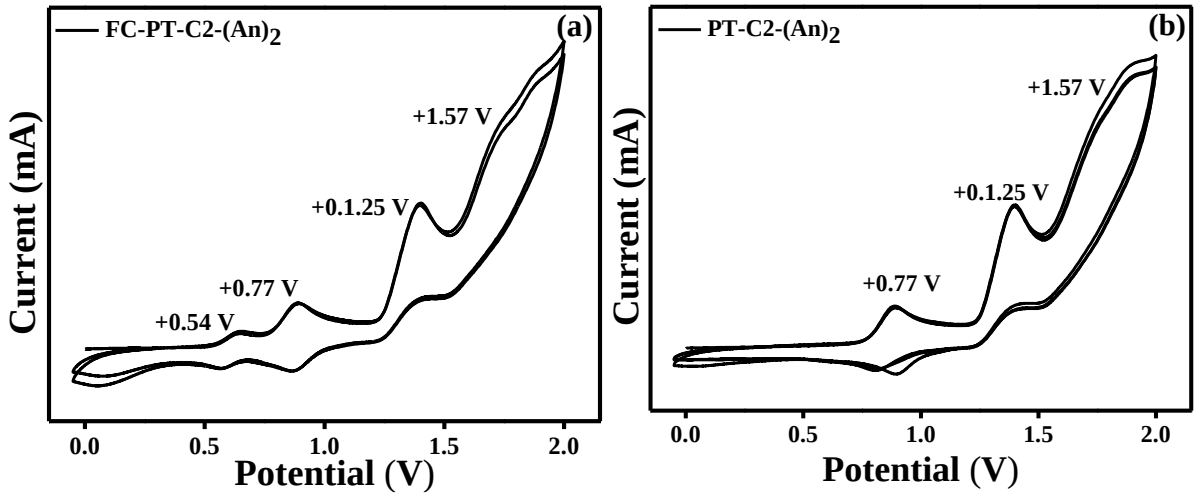

414

415 **Figure S58.** Cyclic voltammograms (100 mV/sec) of PT-C2-$(An)_2$ without Fc/Fc^+ (a) and with Fc/Fc^+ (b) in DCM.

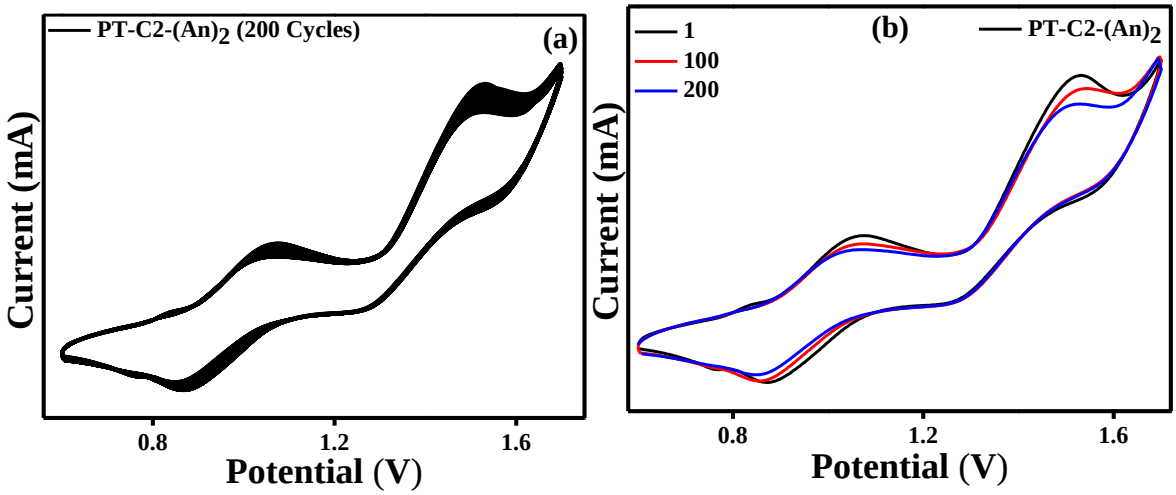

416

417 **Figure S59.** Cyclic voltammograms (200 mV/sec) of PT-C2-$(An)_2$ (200 cycles) (a) and (1st, 100th and 200th cycles) (b) in DCM.

418

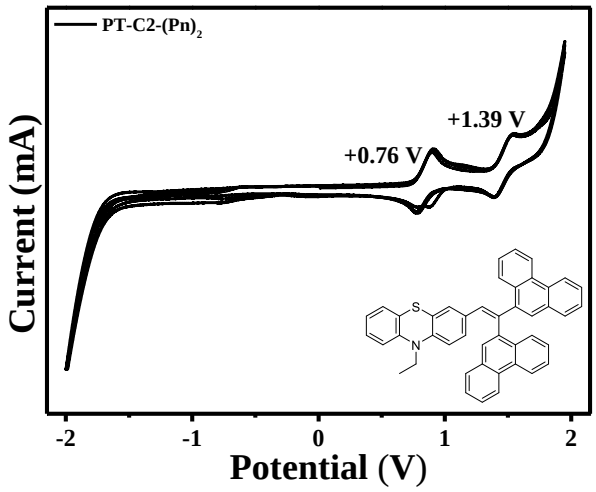

419

420 **Figure S60.** Cyclic voltammograms of PT-C2-$(Pn)_2$ in DCM.

421

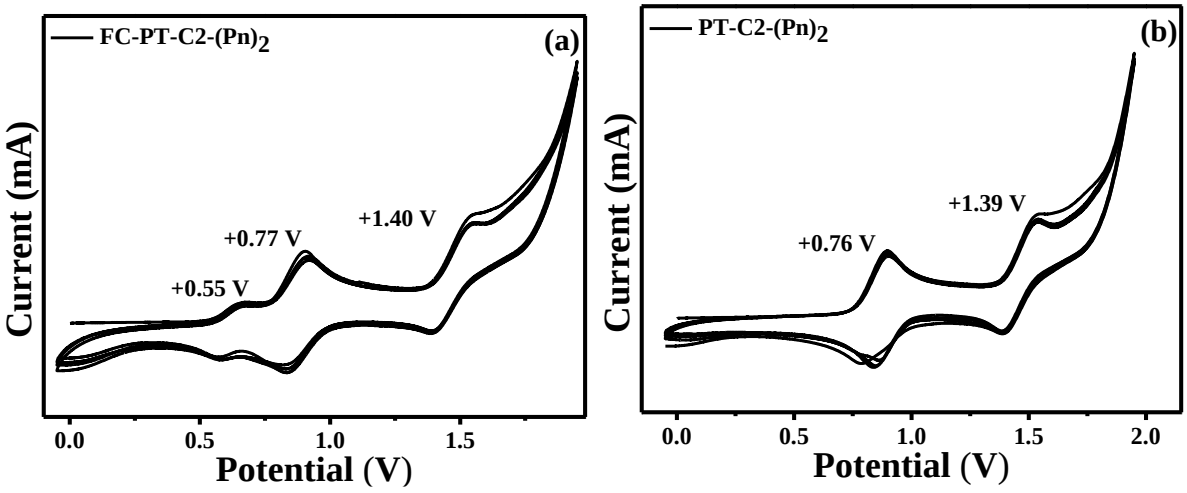

422

423 **Figure S61.** Cyclic voltammograms (100 mV/sec) of PT-C2-$(Pn)_2$ without Fc/Fc^+ (a) and with Fc/Fc^+ (b) in DCM.

424

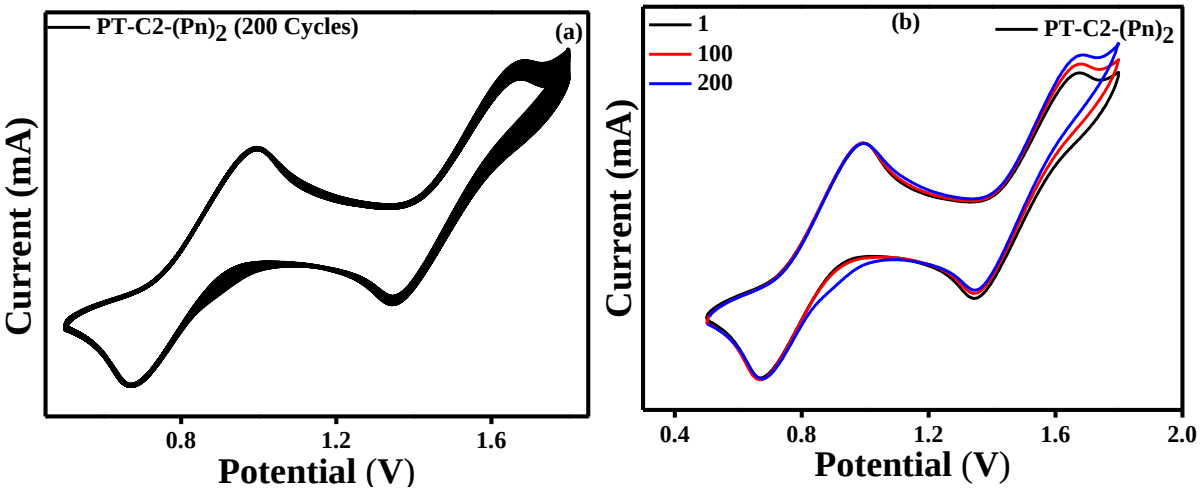

425

426 **Figure S62.** Cyclic voltammograms (200 mV/sec) of PT-C2-$(Pn)_2$ (200 cycles) (a) and (1st, 100th and 200th cycles) (b) in DCM.

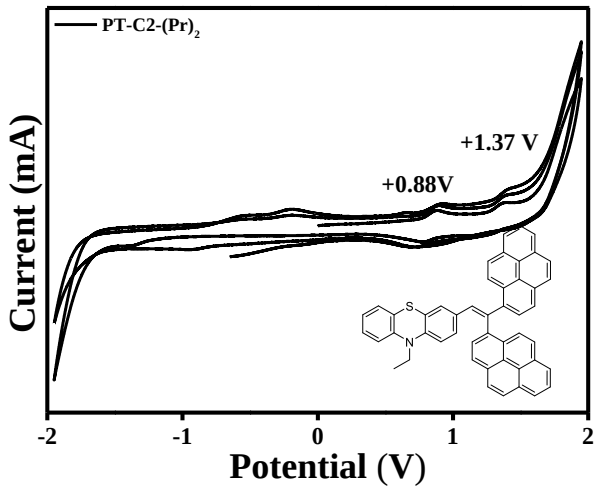

427

428 **Figure S63.** Cyclic voltammograms of PT-C2-$(Pr)_2$ in DCM.

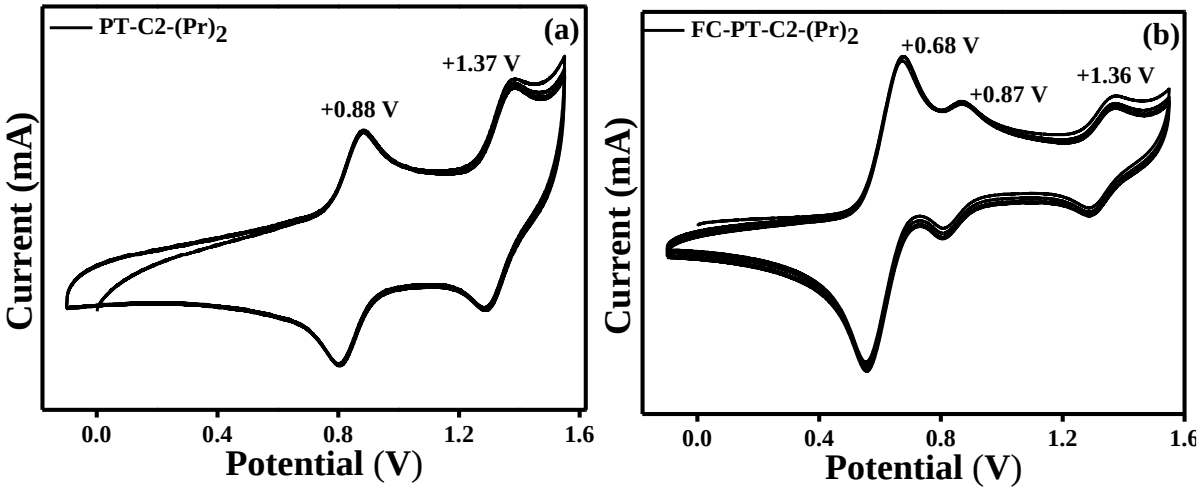

429

430 **Figure S64.** Cyclic voltammograms (100 mV/sec) of PT-C2-$(Pr)_2$ without Fc/Fc^+ (a) and with Fc/Fc^+ (b) in DCM.

431

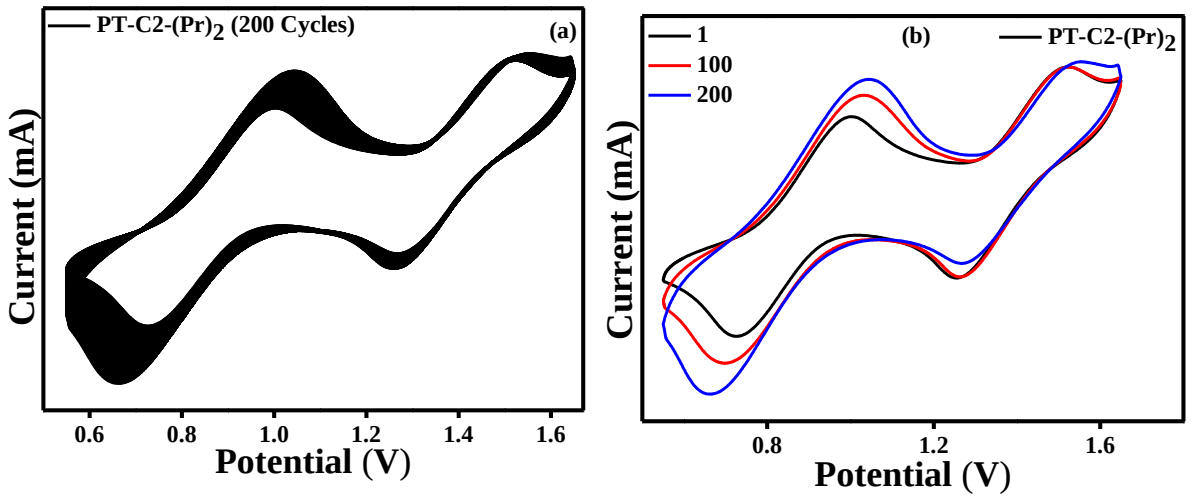

432

433 **Figure S65.** Cyclic voltammograms (200 mV/sec) of PT-C2-$(Pr)_2$ (200 cycles) (a) and (1st, 100th and 200th cycles) (b) in DCM.

434 **Table S3.** Calculated HOMO energy values for the compounds.

S.No.	Compound	Eox (onset, V)	Fc/Fc+, Eox (onset, V)	EHOMO (eV)
1.	PT-C2-$(Ph)_2$	+0.75, +1.43, +1.68	+0.55	−5.00
2.	PT-C12-$(Ph)_2$	+0.81, +1.47, +1.77	+0.58	−5.03
3.	PT-C2-$(Nap)_2$	+0.76, +1.39	+0.55	−5.01
4.	PT-C12-$(Nap)_2$	+0.79, +1.39	+0.58	−5.01
5.	PT-C2-$(An)_2$	+0.77, + 1.25, +1.57	+0.54	−5.03
6.	PT-C2-$(Pn)_2$	+0.77, +1.40	+0.55	−5.02
7.	PT-C2-$(Pr)_2$	+0.87, +1.36	+0.68	−5.00

LUMO value calculation from the UV-visible spectra and cyclic voltammogram

The LUMO values[5] were derived by summing up the HOMO values (E_{HOMO}, obtained from the first oxidation of the cyclic voltammogram, i.e., peak maximum in DPV) with the energy gap (E_g, obtained from the onset of the UV-visible absorption spectrum), which was obtained from the onset of the UV-visible absorption spectrum. The equation[5] is as follows, and the values are tabulated in **Table S4**.

$$E_{LUMO} = E_{HOMO} + E_g \quad \text{…….. (3)}$$

Table S4. Calculation of LUMO energy levels of ethynyldiaryl- & dodecyldiaryl-phenothiazine derivatives.

S.No.	Compound	λ_{onset} [nm], E_g [eV]	E_{HOMO} [eV]	E_{LUMO} [eV]
1.	PT-C2-$(Ph)_2$	381, 2.84	−5.00	−2.16
2.	PT-C12-$(Ph)_2$	370, 2.86	−5.03	−2.17
3.	PT-C2-$(Nap)_2$	381, 2.78	−5.01	−2.23
4.	PT-C12-$(Nap)_2$	381, 2.80	−5.01	−2.21
5.	PT-C2-$(An)_2$	405, 2.67	−5.03	−2.36
6.	PT-C2-$(Pn)_2$	365, 2.85	−5.02	−2.17
7.	PT-C2-$(Pr)_2$	460, 2.69	−5.00	−2.31

Note: $E_{LUMO} = E_{HOMO} + E_g$.

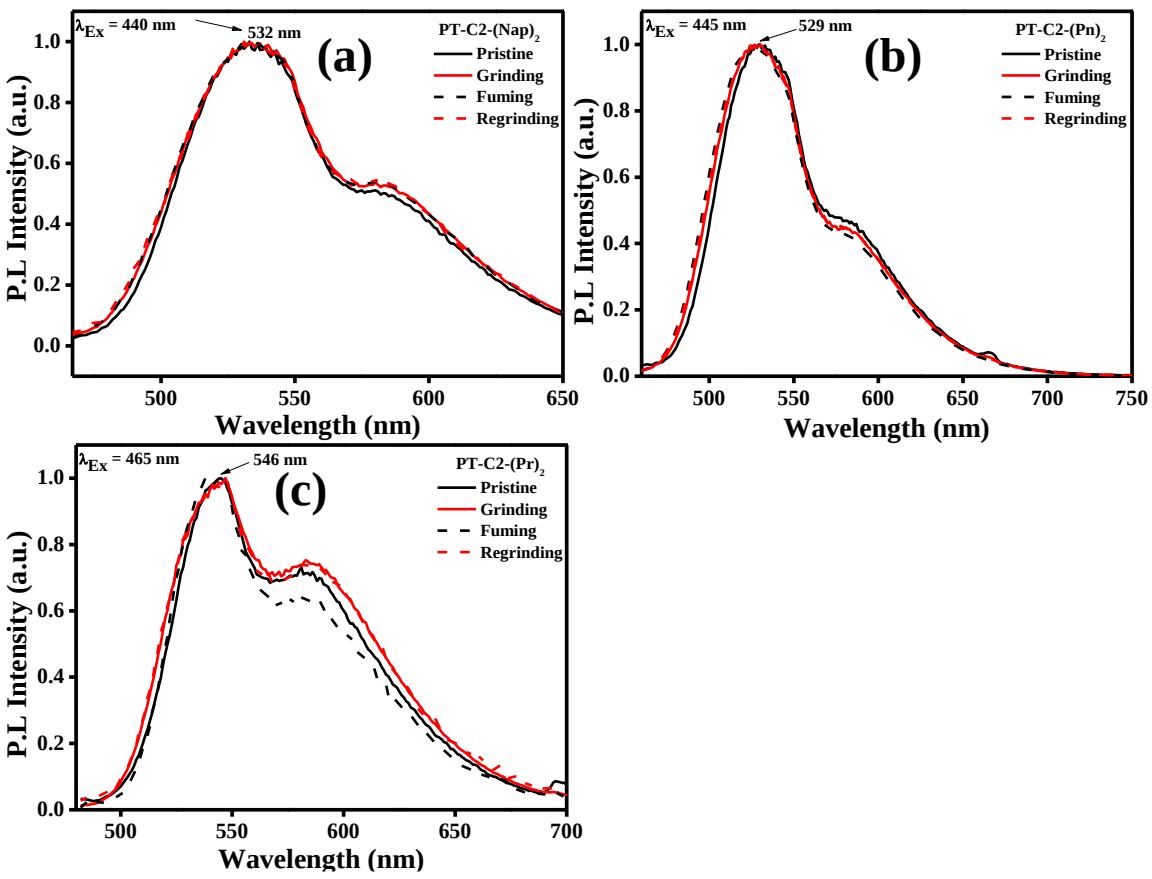

444

445 **Figure S66.** Fluorescence spectra of PT-derivatives upon grinding–fuming cycles.

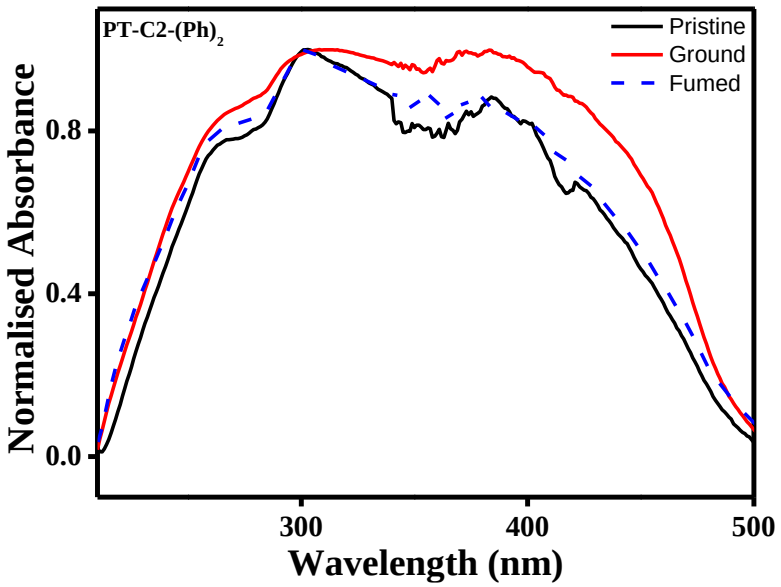

446

447 **Figure S67**. Absorption spectra of PT-C2-$(Ph)_2$ upon grinding–fuming cycles.

448 **Table S5.** Time-resolved fluorescence decay parameters of solid PT-C2-$(Ph)_2$ in its pristine (PT-C2-$(Ph)_2$-P) and ground (PT-C2-$(Ph)_2$-G) states (λ_{Ex} = 405 nm).

Compounds, λ_{Ex} = 405 (nm)	α_1	α_2	α_3	τ_1 (ns)	τ_2 (ns)	τ_3 (ns)	τ_f	χ_2
PT-C2-$(Ph)_2$-P	0.36	0.05	0.59	1.94	0.18	4.77	4.19	1.61
PT-C2-$(Ph)_2$-G	0.05	0.63	0.32	0.13	4.86	8.03	6.29	1.74

449

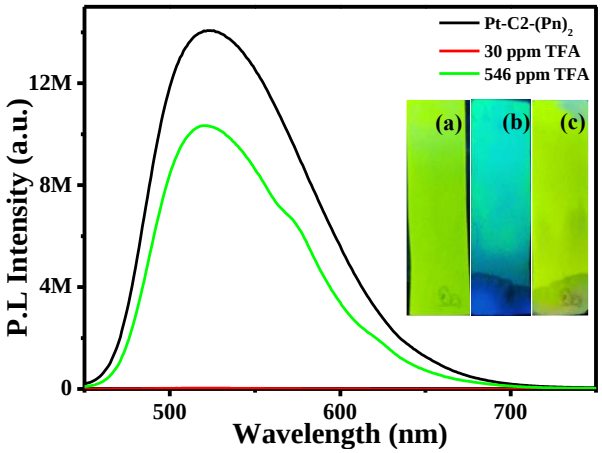

450

451 **Figure S68.** Fluorescence emission spectra of PT-C2-$(Pn)_2$ thin film, recorded under the saturated vapors of TFA and TEA. Inset showing the color change of PT-
452 C2-$(Pn)_2$ thin film (a) before and (b) after addition of TFA followed by the addition of (c)TEA.

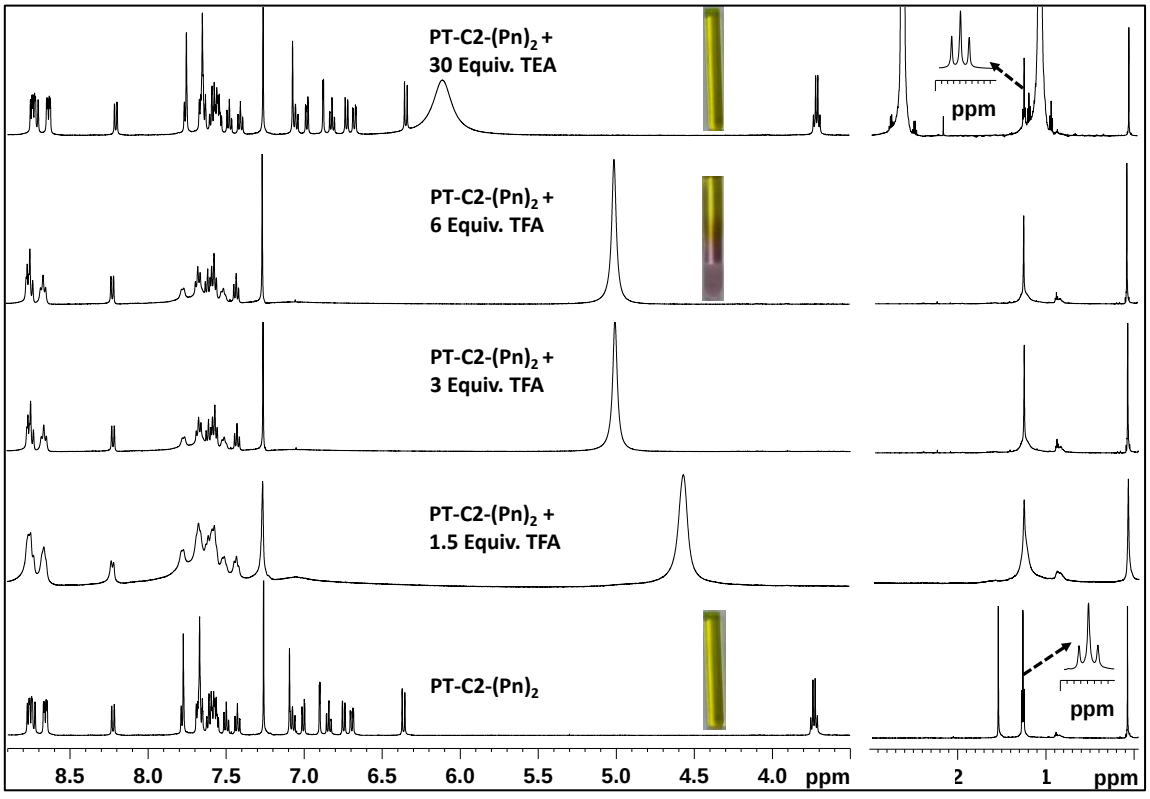

453

454 **Figure S69.** ^1H NMR spectra of PT-C2-$(Pn)_2$ in $CDCl_3$ before and after addition of increased amount TFA followed by excess addition of TEA (top). Insets of
455 each spectrum represent respective photographs taken under normal light.

456

457

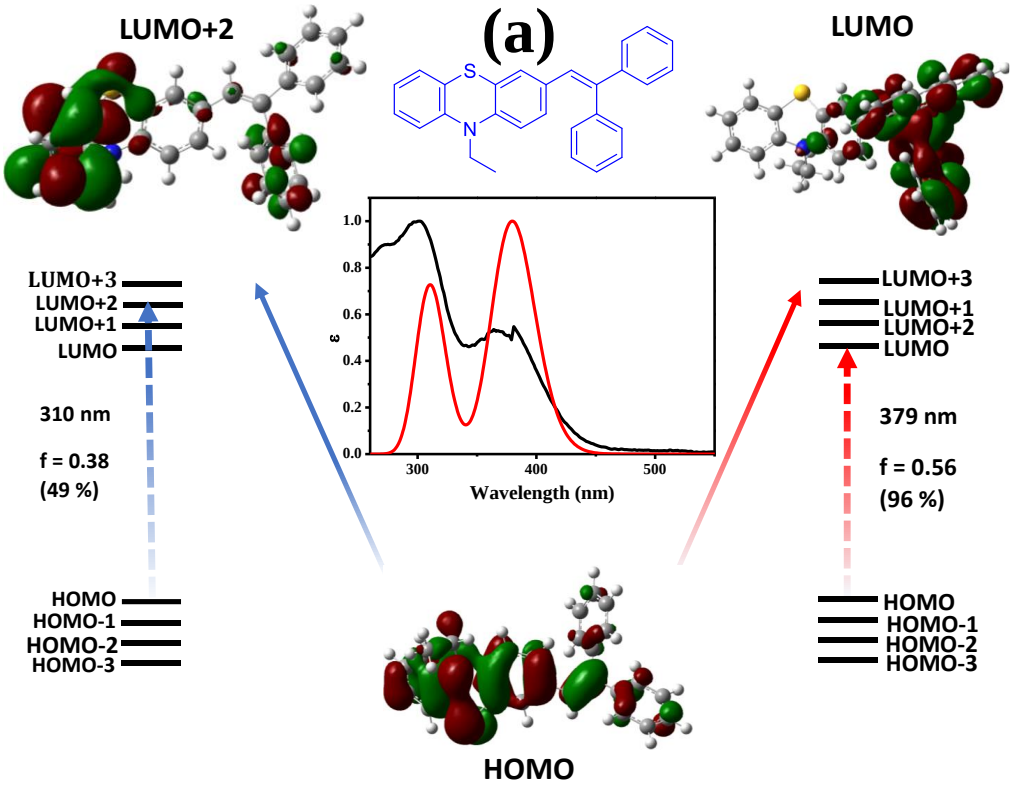

458

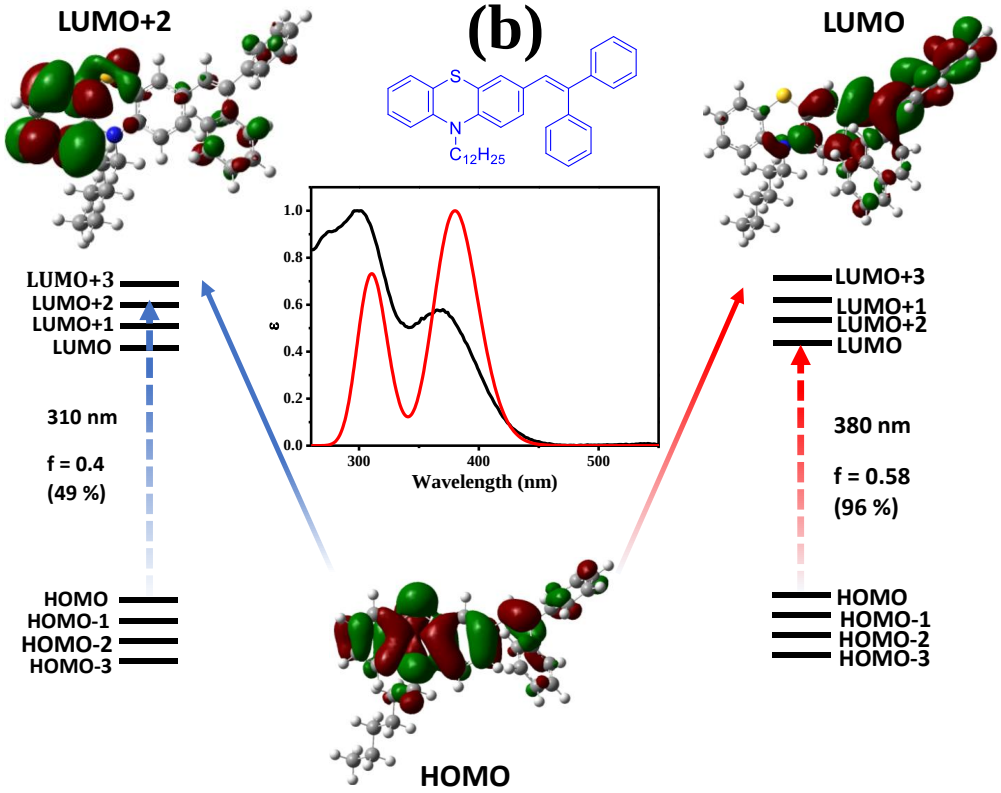

459

460

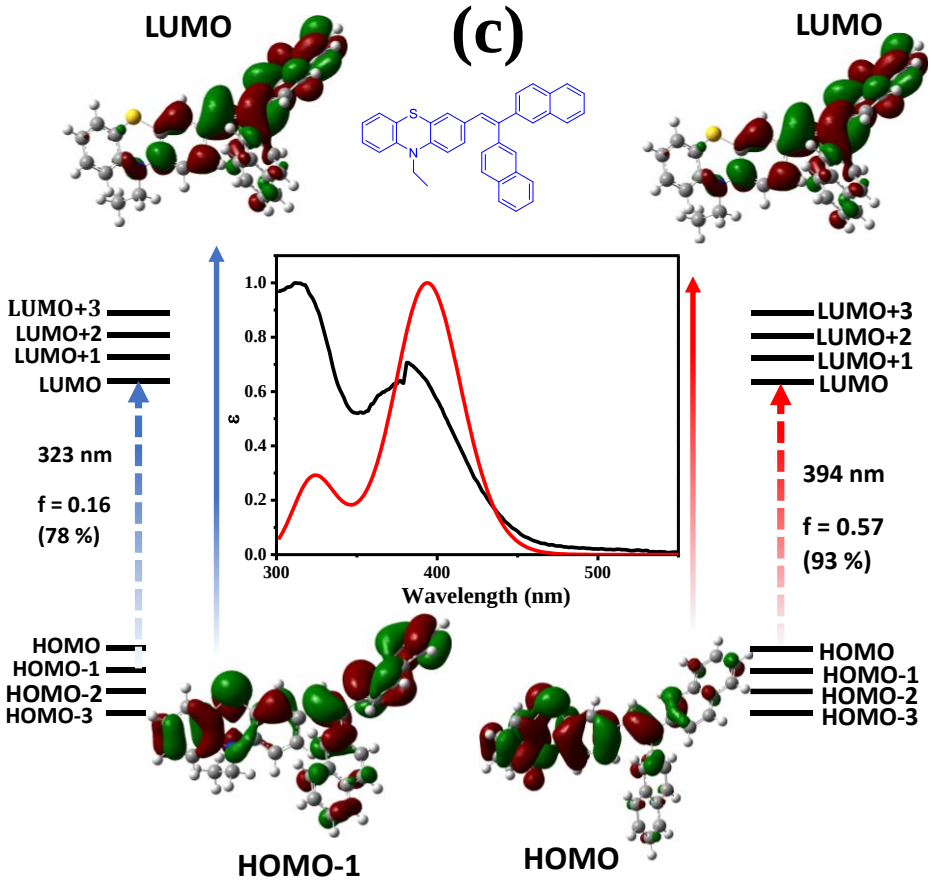
(c)
LUMO
LUMO
LUMO+3
LUMO+2
LUMO+1
LUMO
323 nm
f = 0.16
(78 %)
394 nm
f = 0.57
(93 %)
HOMO
HOMO-1
HOMO-2
HOMO-3
ε
Wavelength (nm)
HOMO-1
HOMO

461

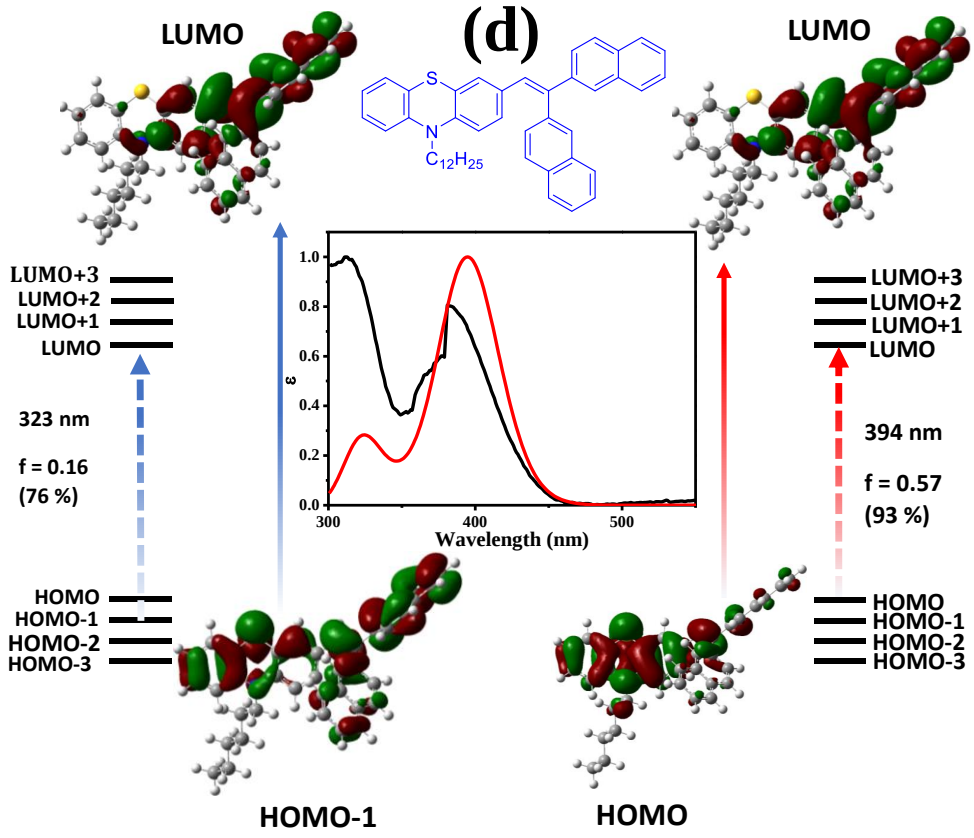
(d)
LUMO
LUMO
LUMO+3
LUMO+2
LUMO+1
LUMO
323 nm
f = 0.16
(76 %)
394 nm
f = 0.57
(93 %)
HOMO
HOMO-1
HOMO-2
HOMO-3
ε
Wavelength (nm)
HOMO-1
HOMO

462

463

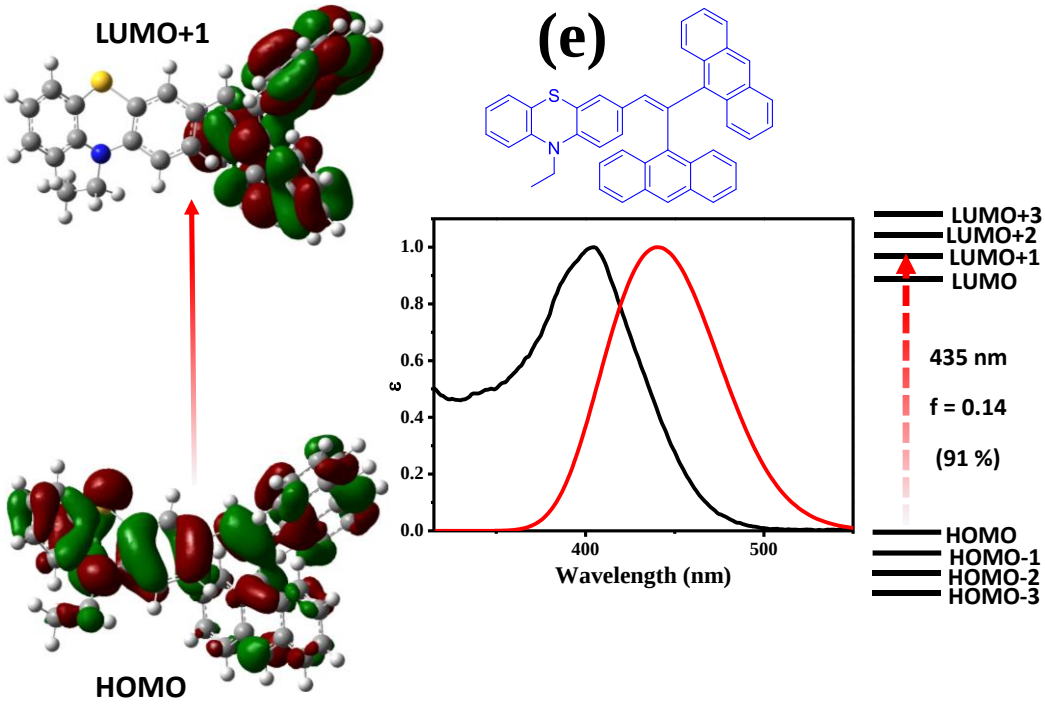

464

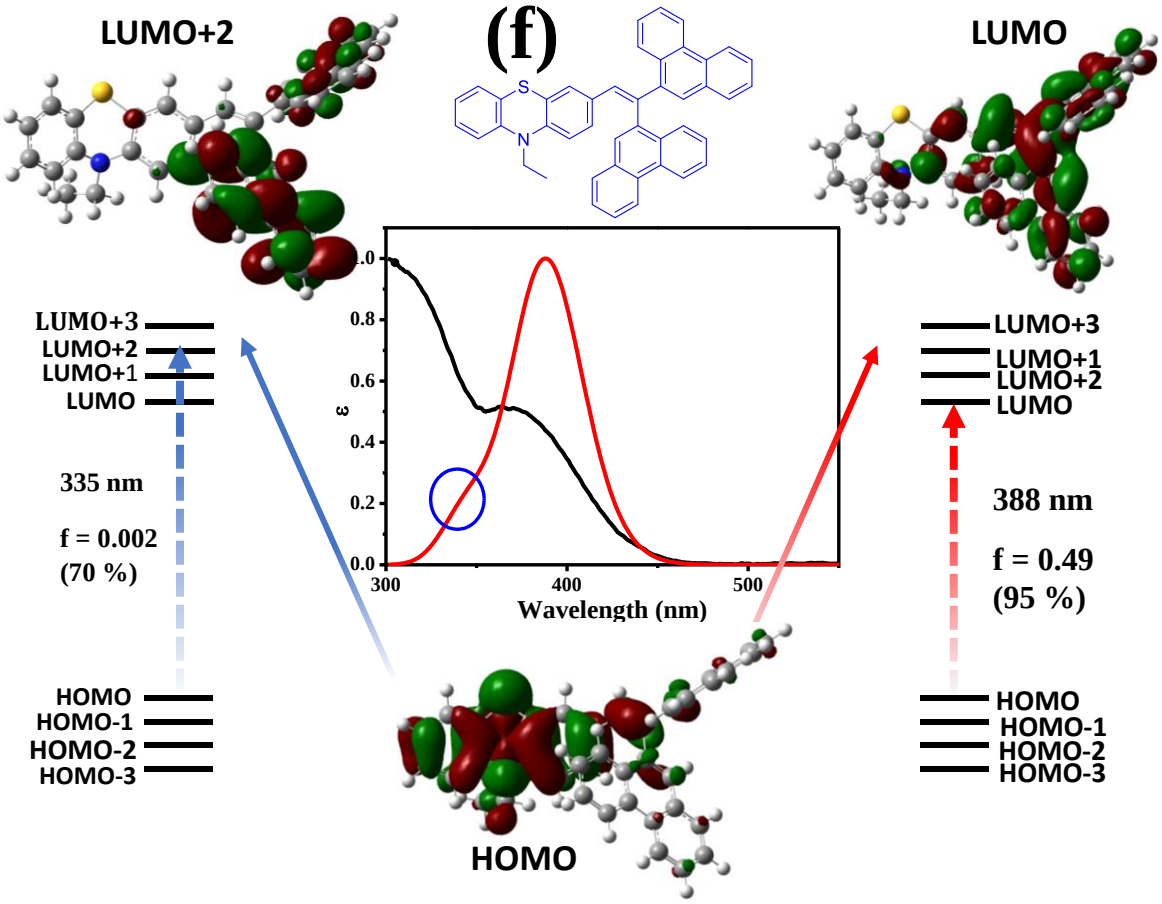

465

466

467

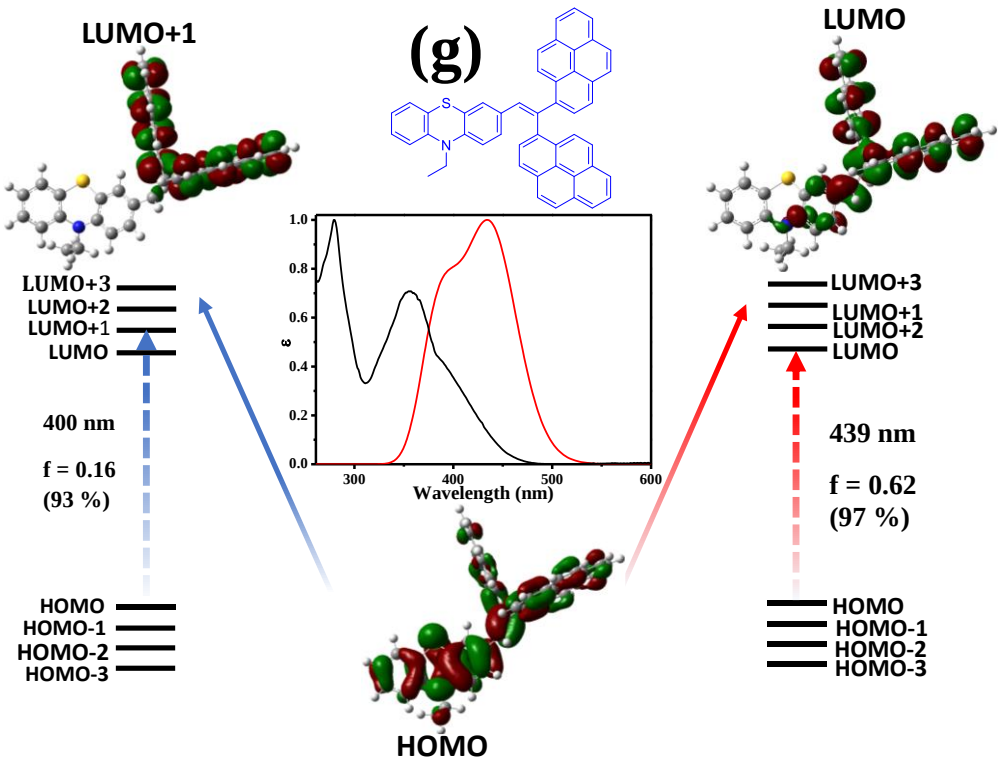

468

469

470 **Figure S70.** Theoretical determined absorption spectra and individual molecular orbital coefficients accountable for CT transition for (a) PT-C2-$(Ph)_2$, (b) PT-
471 C12-$(Ph)_2$, (c) PT-C2-$(Nap)_2$, (d) PT-C12-$(Nap)_2$, (e) PT-C2-$(An)_2$, (f) PT-C2-$(Pn)_2$ and (g) PT-C2-$(Pr)_2$ obtained using td PBE1PBE/6-311+g (d, p) level of theory.

472

473 **Table S6.** Excited-state singlet and triplet energy values of the derivatives, obtained via optimizing the geometries of lowest singlet excited state (S_1) and lowest
474 singlet excited state (T_1) using TDDFT/B3LYP/ 6-311+g (d, p) and unrestricted DFT (UDFT)/B3LYP/ 6-311+g (d, p) respectively in DCM.

Compd.	S (eV)	T (eV)	ΔE_{ST} (eV)
PT-C2-$(Ph)_2$	-41741.96	-41742.84	0.88
PT-C12-$(Ph)_2$	-46022.25	-46023.12	0.87
PT-C2-$(Na)_2$	-50105.74	-50106.51	0.77
PT-C12-$(Na)_2$	-54386.03	-54386.80	0.77
PT-C2-$(An)_2$	-58468.60	-58469.19	0.59
PT-C2-$(Pn)_2$	-58469.06	-58469.83	0.76
PT-C2-$(Pr)_2$	-62618.95	-62619.57	0.63

475

References

1 S. Mallick, S. Maddala, K. Kollimalayan and P. Venkatakrishnan, *J. Org. Chem.*, 2019, **84**, 73–93.

2 W. L. Mendelson and S. Hayden, *Synthetic Communications*, 1996, **26**, 603–610.

3 W. Yu, L. Chen, J. Tao, T. Wang and J. Fu, *Chem. Commun.*, 2019, **55**, 5918–5921.

4 A. M. Hamdy, N. Eleya, H. H. Mohammed, Z. Khaddour, T. Patonay, A. Villinger and P. Langer, *Tetrahedron Letters*, 2013, **54**, 3568–3571.

5 I. Seguy, P. Jolinat, P. Destruel, J. Farenc, R. Mamy, H. Bock, J. Ip and T. P. Nguyen, *Journal of Applied Physics*, 2001, **89**, 5442–5448.